University of Technology

Mechanical Engineering

Department

2017-2018

Chapter Two

Wing Designing and Installation

Dr. Ahmed Shandookh

AIRCRAFT BRANCH

2.1 Introduction: This chapter focuses on the detail design of the wing. The wing may be considered as the most important component of an aircraft, since a fixed-wing aircraft is not able to fly without it. Since the wing geometry and its features are influencing all other aircraft components, we begin the detail design process by wing design. The primary function of the wing is to generate sufficient lift force or simply lift (L). However, the wing has two other productions, namely drag force or drag (D) and nose-down pitching moment (M). While a wing designer is looking to maximize the lift, the other two (drag and pitching moment) must be minimized. In fact, a wing is considered as a lifting surface that lift is produced due to the pressure difference between lower and upper surfaces. Aerodynamics textbooks are a good source to consult for information about mathematical techniques for calculating the pressure distribution over the wing and for determining the flow variables.

During the wing design process, eighteen parameters must be determined. They are as follows:

1. Wing reference (or planform) area (S_W or S_{ref} or S)
2. Number of the wings.
3. Wings position relative to the fuselage (high, mid, or low wing)
4. Cross sectional type effects (airfoil).
5. Incidence (i_w) (or setting angle, α_{set})
6. Aspect ratio (AR)
7. Taper ratio (λ)
8. Tip chord (C_t)
9. Root chord (C_r)
10. Mean Aerodynamic Chord (MAC or C_{mean})
11. Span (b)
12. Twist angle (or washout) (α_t)
13. Sweep angle (Λ)
14. Dihedral angle (Γ)
15. High lifting devices such as flap
16. Horizontal and vertical stabilizer with ailerons and rudders.
17. Other wing accessories
18. Wing lug design.

2.2 Number of Wings:

One of the decisions a designer must make is to select the number of wings. The options are:

1. Monoplane (i.e. one wing)
2. Two wings (i.e. biplane)
3. Three wings

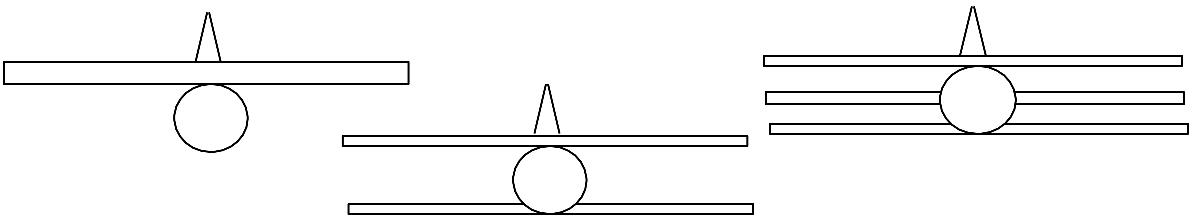

1.Monoplane 2. Biplane 3. Tri-wing

Figure 2.1: Three options in number of wings (front view)

The number of wings higher than three is not practical. Figure 2.1 illustrates front view of three aircraft with various configurations. Nowadays, modern aircraft almost all have monoplane. Currently, there are a few aircraft that employ biplane, but no modern aircraft is found to have three wings. In the past, the major reason to select more than one wing was the manufacturing technology limitations. A single wing usually has a longer wing span compared with two wings (with the same total area). Old manufacturing technology was not able to structurally support a long wing to stay level and rigid. With the advance in the manufacturing technology and new aerospace strong materials; such as advanced light aluminum, and composite materials; this reason is not valid anymore. Another reason was the limitations on the aircraft wing span. Hence a way to reduce the wing span is to increase the number of wings.

Thus, a single wing (that includes both left and right sections) is almost the only practical option in conventional modern aircraft. However, a few other design considerations may still force the modern wing designer to lean toward more than one wing. The most significant one is the aircraft controllability requirements. An aircraft with a shorter wing span delivers higher roll control, since it has a smaller mass moment of inertia about x axis. Therefore, if one is looking to roll faster; one option is to have more than one wing that leads to a shorter wing span. Several maneuverable aircraft in 1940s and 1950s had biplane and even three wings. On the other hand, the disadvantages of an option other than monoplane include higher weight, lower lift, and pilot visibility limits. The recommendation is to begin with a monoplane, and if the design requirements were not satisfied, resort to higher number of wings.

2.3 Wings position relative to the fuselage (high, mid, or low wing):

One of the wing parameters that could be determined at the early stages of wing design process is the wing vertical location relative to the fuselage centerline. This wing parameter will directly influence the design of other aircraft components including aircraft tail design, landing gear design, and center of gravity. In principle, there are four options for the vertical location of the wing. They are:

a. High wing
b. Mid wing
c. Low wing
d. Parasol wing

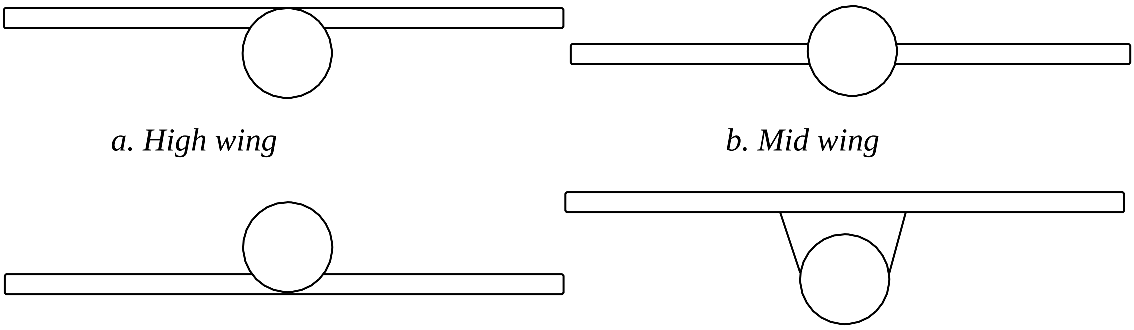

a. High wing *b. Mid wing*

c. Low wing *d. Parasol wing*

Figure 2.2: Options in vertical wing positions

Figure 2.2 shows the schematics of these four options. In this figure, only the front-views of the aircraft fuselage and wing are shown. In general, cargo aircraft and some GA (giant airplane) aircraft have high wing; while most passenger aircraft have low wing. On the other hand, most fighter airplanes and some GA aircraft have mid wing; while hang gliders and most amphibian aircraft have parasol wing. The primary criterion to select the wing location originates from operational requirements, while other requirements such as stability and producibility requirements are the influencing factors in some design cases.

In this section, the advantages and disadvantages of each option is examined. The final selection will be made based on the summations of all advantages and disadvantages when incorporated into design requirements. Since each option has a weight relative to the design requirements, the summation of all weights derives the final choice.

2.3.1 High Wing

The high wing configuration (Figure 2.2-a) has several advantages and disadvantages that make it suitable for some flight operations, but unsuitable for other flight missions. In the following section, these advantages and disadvantages are presented.

a. Advantages:

1. Eases and facilitates the loading and unloading of loads and cargo into and out of cargo aircraft. For instance, truck and other load lifter vehicles can easily move around aircraft and under the wing without anxiety of the hitting and breaking the wing.
2. Facilitates the installation of engine on the wing, since the engine (and propeller) clearance is higher (and safer), compared with low wing configuration.
3. Saves the wing from high temperature exit gasses in this type of aircraft (e.g. Harrier GR9 and BAe Sea Harrier). The reason is that the hot gasses are bouncing back when they hit the ground, so they wash the wing afterward. Even with a high wing, this will severely reduce the lift of the wing structure. Thus, the higher the wing is the farther the wing from hot gasses.
4. Facilitates the installation of strut. This is based on the fact that a strut (rod or tube) can handle higher tensile stress compared with the compression stress. In a high wing, the strut has to withstand tensile stress, while the strut in a low wing must bear the compression stress. Figure 2.2.d shows the sketch of a parasol wing with strut.
5. The aircraft structure is lighter when struts are employed (as item 4 implies).
6. Facilitates the taking off and landing from sea. In a sea-based or an amphibian aircraft, during a take-off operation, water will splash around and will high the aircraft. An engine installed on a high wing will receive less water compared with a low wing. Thus, the possibility of engine shut-off is much less.
7. Facilitates the aircraft control for a hang glider pilot, since the aircraft center of gravity is lower than the wing.
8. Increases the dihedral effect ($C_{l\beta}$). It makes the aircraft laterally more stable. The reason lies in the higher contribution of the fuselage to the wing dihedral effect ($C_{l\beta_w}$).
9. The wing will produce more lift compared with mid and low wing, since two parts of the wing are attached at least on the top part.
10. For the same reason as in item 9, the aircraft will have lower stall speed, since C_{Lmax} will be higher.
11. The pilot has better view in lower-than-horizon. A fighter pilot has a full view under the aircraft.
12. For an engine that is installed under the wing, there is less possibility of sand and debris to enter engine and damage the blades and propellers.

13. There is a lower possibility of human accident to hit the propeller and be pulled to the engine inlet. In few rare accidents, several careless people has died (hit the rotating propeller or pulled into the jet engine inlet).
14. The aerodynamic shape of the fuselage lower section can be smoother.
15. There is more space inside fuselage for cargo, luggage or passenger.
16. The wing drag is producing a nose-up pitching moment, so it is longitudinally destabilizing. This is due to the higher location of wing drag line relative to the aircraft center of gravity ($M_{Dcg} > 0$).

b. Disadvantages:

1. The aircraft tend to have more frontal area (compared with mid wing). This will increase aircraft drag.
2. The ground effect is lower, compared with low wing. During takeoff and landing operations, the ground will influence the wing pressure distribution. The wing lift will be slightly lower than low wing configuration. This will increase the takeoff run slightly. Thus, high wing configuration is not a right option for STOL3 aircraft.
3. Landing gear is longer if connected to the wing. This makes the landing gear heavier and requires more space inside the wing for retraction system. This will further make the wing structure heavier.
4. The pilot has less higher-than-horizon view. The wing above the pilot will obscure part of the sky for a fighter pilot.
5. If landing gear is connected to fuselage and there is not sufficient space for retraction system, an extra space must be provided to house landing gear after retraction. This will increase fuselage frontal area and thus will increase aircraft drag.
6. The wing is producing more induced drag (Di), due to higher lift coefficient.
7. The horizontal tail area of an aircraft with a high wing is about 20% larger than the horizontal tail area with a low wing. This is due to more downwash of a high wing on the tail.
8. A high wing is structurally about 20% heavier than a low wing.
9. The retraction of the landing gear inside the wing is not usually an option, due to the required high length of landing gear.
10. The aircraft lateral control is weaker compared with mid wing and low wing, since the aircraft has more laterally dynamic stability.

Although the high wing has more advantages than disadvantages, all items do not have the same weighing factor. It depends on what design objective is more significant than other objectives in the eyes of the customer. The systems engineering approach delivers an approach to determine the best option for a specific aircraft, using a comparison table.

2.3.2 Low Wing

In this section, advantages and disadvantages of a low wing configuration (Figure 2.2-c) will be presented. Since the reasons for several items are similar with the reasons for a high wing configuration, the reasons are not repeated here. In the majority of cases, the specifications of low wing are compared with a high wing configuration.

a. Advantages:

1. The aircraft take off performance is better; compared with a high wing configuration; due to the ground effect.
2. The pilot has a better higher-than-horizon view, since he/she is above the wing.
3. The retraction system inside the wing is an option along with inside the fuselage.
4. Landing gear is shorter if connected to the wing. This makes the landing gear lighter and requires less space inside the wing for retraction system. This will further make the wing structure lighter.
5. In a light GA aircraft, the pilot can walk on the wing in order to get into the cockpit.
6. The aircraft is lighter compared with a high wing structure.
7. Aircraft frontal area is less.
8. The application of wing strut is usually no longer an option for the wing structure.
9. Item 8 implies that the aircraft structure is lighter since no strut is utilized.
10. Due to item 8, the aircraft drag is lower.
11. The wing has less induced drag.
12. It is more attractive to the eyes of a regular viewer.
13. The aircraft has higher lateral control compared with a high wing configuration, since the aircraft has less lateral static stability, due to the fuselage contribution to the wing dihedral effect ($C_{l\beta_w}$).
14. The wing has less downwash on the tail, so the tail is more effective.
15. The tail is lighter; compared with a high wing configuration.
16. The wing drag is producing a nose-down pitching moment, so a low wing is longitudinally stabilizing. This is due to the lower position of the wing drag line relative to the aircraft center of gravity ($M_{Dcg} < 0$).

b. Disadvantages:

1. The wing generates less lift; compared with a high wing configuration; since the wing has two separate sections.
2. With the same token to item 1, the aircraft will have higher stall speed; compared with a high wing configuration; due to a lower C_{Lmax}.
3. Due to item 2, the take-off run is longer.
4. The aircraft has lower airworthiness due to a higher stall speed.
5. Due to item 1, wing is producing less induced drag.
6. The wing has less contribution to the aircraft dihedral effect; thus the aircraft is laterally dynamically less stable.
7. Due to item 4, the aircraft is laterally more controllable, and thus more maneuverable.
8. The aircraft has a lower landing performance, since it needs more landing run.
9. The pilot has a lower lower-than-horizon view. The wing below the pilot will obscure part of the sky for a fighter pilot.

Although the low wing has more advantages than disadvantages, all items do not have the same weighing factors. It depends on what design objective is more significant than other objectives in the eyes of the customer. The systems engineering approach delivers an approach to determine the best option for a specific aircraft.

2.3.3 Mid Wing

In general, features of the mid-wing configuration (Figure 2.2-b) stand somewhat between features of high-wing configuration and features of low-wing configuration. The major difference lies in the necessity to cut the wing spar in two halves in order to save the space inside the fuselage. However, another alternative is not to cut the wing spar and letting it to pass through the fuselage; which leads to an occupied space of the fuselage. Both alternatives carry a few disadvantages. Other than those features that can be easily derived from two previous sections, some new features of a mid-wing configuration are as follows:

1. The aircraft structure is heavier, due to the necessity of reinforcing wing root at the intersection with the fuselage.
2. The mid wing is more expensive compared with high and low-wing configurations.
3. The mid wing is more attractive compared with two other configurations.
4. The mid wing is aerodynamically streamliner compared with two other configurations.
5. The strut is usually not used to reinforce the wing structure.

6. The pilot can get into the cockpit using the wing as a step in a small GA aircraft.
7. The mid-wing has less interference drag than low-wing and high-wing.

2.3.4 Parasol Wing:

This wing configuration is usually employed in hang gliders plus amphibian aircraft. In several areas, the features are similar to a high wing configuration. The reader is referred to above items for more details and the reader is expected to be able to derive conclusion by comparing various configurations. Since the wing is utilizing longer struts, it is heavier and has more drag, compared with a high wing configuration.

2.4 Cross Sectional Type Effects on Wing Selection:

There are two ways to determine the wing airfoil section:

1. Airfoil design
2. Airfoil selection

The design of the airfoil is a complex and time-consuming process and needs expertise in fundamentals of aerodynamics at graduate level. Since the airfoil needs to be verified by testing it in a wind tunnel, it is expensive too. Large aircraft production companies such as Boeing and Airbus have sufficient human expert (aerodynamicists) and budget to design their own airfoil for every aircraft, but small aircraft companies, experimental aircraft producers and homebuilt manufacturers do not afford to design their airfoils. Instead they select the best airfoils among the current available airfoils that are found in several books or websites.

With the advent of high speed and powerful computers, the design of airfoil is not as hard as thirty years ago. There is currently a couple of aerodynamic software packages (CFD) in the market that can be used to design airfoil for variety of needs. Not only aircraft designers need to design their airfoils, but their other many areas that airfoil needs to be design for their products.

If you have enough time, budget and manpower; and decide to design an airfoil for your aircraft, you are referred to the references that are listed at the end of the aircraft design textbooks. But remember the airfoil design is a design project for itself and needs to be integrated into the aircraft design process properly. But if you are a junior aircraft designer with limited resources, you are recommended to select the airfoil from the available airfoil database.

Any aerodynamics textbook introduces several theories to analyze flow around an airfoil. The application of potential-flow theory together with boundary-layer theory to airfoil design and analysis was accomplished many years ago. Since then, potential-flow and boundary layer theories have been steadily improved. With the advent of computers, these theories have been used increasingly to complement wind-tunnel tests. Today, computing costs are so low that a complete potential-flow and boundary-layer analysis of an airfoil costs considerably less than one percent of the equivalent wind-tunnel test. Accordingly, the tendency today is toward more and more commonly applicable computer codes. These codes reduce the amount of required wind-tunnel testing and allow airfoils to be tailored to each specific application.

A regular flight operation consists of take-off, climb, cruise, turn, maneuver, descent, approach and landing. Basically, the airfoil's optimum function is in cruise, that an aircraft spends much of its flight time in this flight phase. At a cruising flight, lift (L) is equal to aircraft weight (W), and drag (D) is equal to engine thrust (T). Thus, the wing must produce sufficient lift coefficient, while drag coefficient must be minimum. Both of these coefficients are mainly coming from airfoil section. Thus, two governing equations for a cruising flight are:

$$L = W = \frac{1}{2}\rho V^2 S C_L = mg \qquad 2.1$$

$$D = T = \frac{1}{2}\rho V^2 S C_D = ngT_{max} \quad \text{where n: variable (0.6~0.9)} \qquad 2.2$$

2.4.1 General Features of an Airfoil

Any section of the wing cut by a plane parallel to the aircraft xz plane is called an airfoil. It is usually looks like a positive cambered section that the thicker part is in front of the airfoil. An airfoil-shaped body moved through the air will vary the static pressure on the top surface and on the bottom surface of the airfoil. A typical airfoil section is shown in figure 2.3, where several geometric parameters are illustrated. If the mean camber line in a straight line, the airfoil is referred to as symmetric airfoil, otherwise it is called cambered airfoil.

The camber of airfoil is usually positive. In a positive cambered airfoil, the upper surface static pressure in less than ambient pressure, while the lower surface static pressure is higher than ambient pressure. This is due higher airspeed at upper surface and lower speed at lower surface of the airfoil (see figure 2.4 and 2.5). As the airfoil angle of attack increases, the pressure difference between upper and lower surfaces will be higher

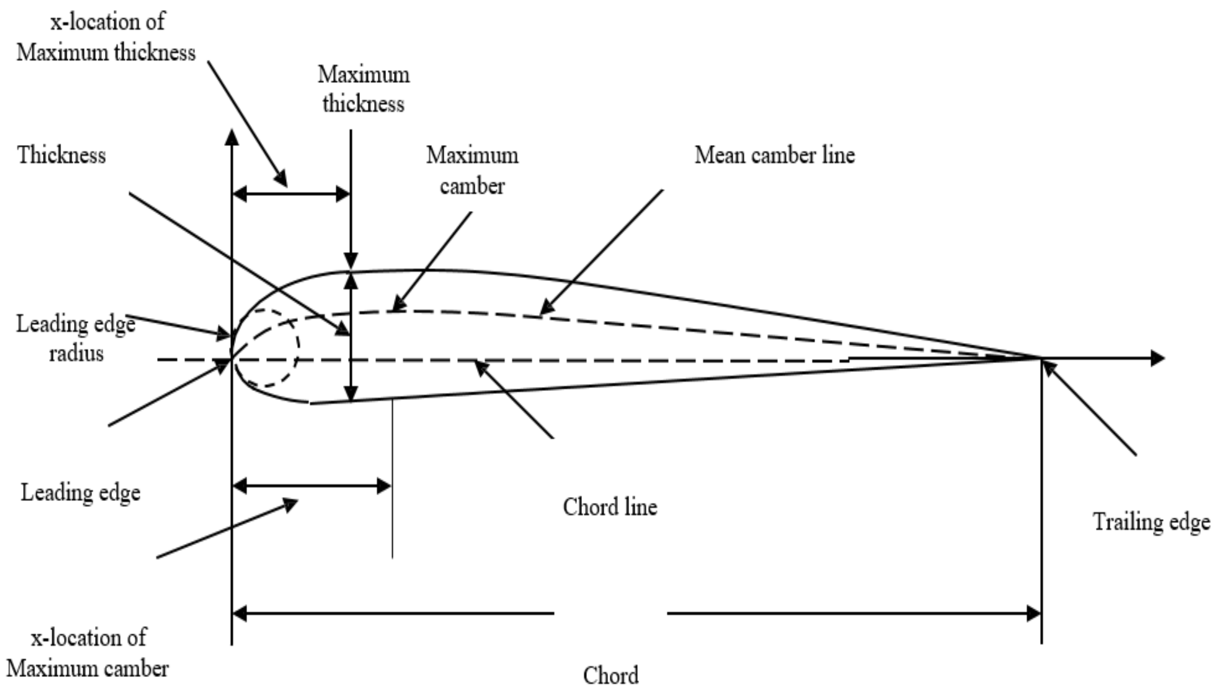

Figure 2.2: Airfoil geometric parameters

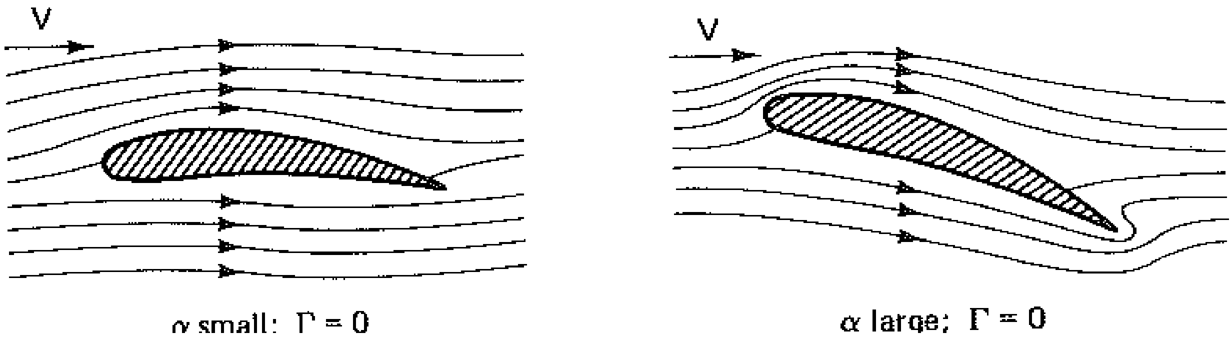

a. **Small angle of attack** **b. Large angle of attack**

Figure 2.3: Flow around an airfoil

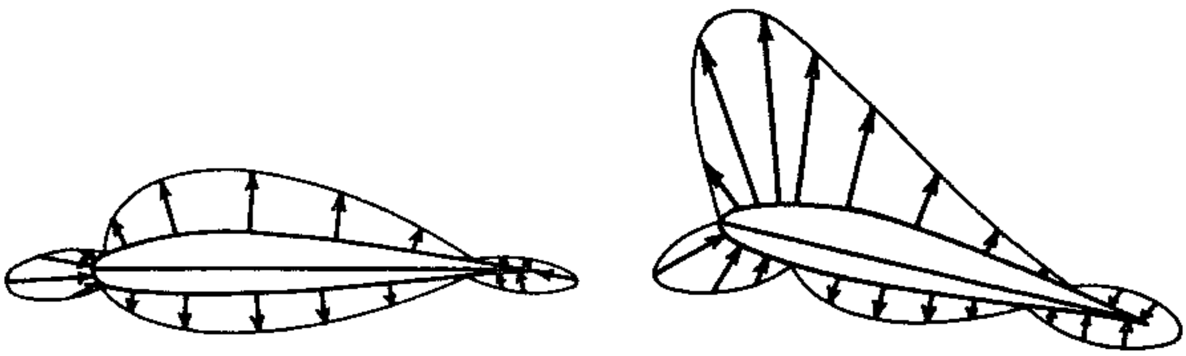

a. **Small angle of attack** **b. Large angle of attack**

Figure 2.4: Angle of attack effects on pressure distribution around an airfoil

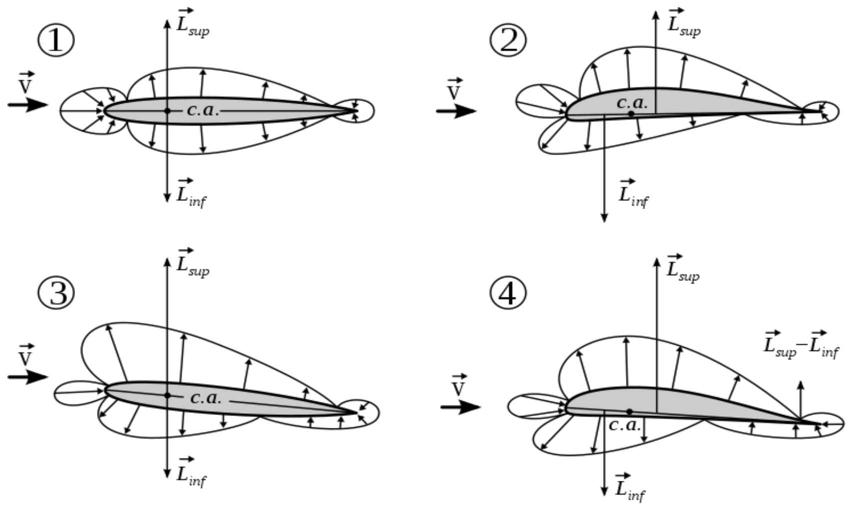

Figure 2.5: Airfoil shape effects on pressure distribution around it

2.4.2 Characteristic Graphs of an Airfoil

In the process of wing airfoil selection, we do not look at airfoil geometry only, or its pressure distribution. Instead, we examine the airfoil operational outputs that are more informative to satisfy design requirements. There are several graphs that illustrate the characteristics of each airfoil when compared to other airfoils in the wing airfoil selection process. These are mainly the variations of non-dimensional lift, drag, and pitching moment relative with angle of attack. Two aerodynamic forces and one aerodynamic pitching moment are usually non- dimensional by dividing them to appropriate parameters as follows.

$$C_L = \frac{L}{{}^1/_2(\rho V^2(S\times 1))} \qquad 2.3$$

$$C_D = \frac{D}{{}^1/_2(\rho V^2(S\times 1))} \qquad 2.4$$

$$C_M = \frac{M}{{}^1/_2(\rho V^2(S\times 1)S)} \qquad 2.5$$

where L, D, and M are lift, drag, and pitching moment of a two-dimensional airfoil. The area (C x1) is assumed to be the airfoil chord times the unit span (b = 1).

Thus, we evaluate the performance and characteristics of an airfoil by looking at the following graphs.

1. The variations of lift coefficient versus angle of attack
2. The variations of pitching moment coefficient about quarter chord versus angle of attack
3. The variations of pitching moment coefficient about aerodynamic center versus lift coefficient
4. The variations of drag coefficient versus lift coefficient
5. The variations of lift-to-drag ratio versus angle of attack

These graphs have several critical features that are essential to the airfoil selection process. Let’s first have a review on these graphs.

1. The graph of lift coefficient (C_l) versus angle of attack (α)

Figure 2.6 shows the typical variations of lift coefficient versus angle of attack for a positive cambered airfoil. Seven significant features of this graph are: stall angle (α_s), maximum lift coefficient (C_{lmax}), zero lift angle of attack (α_o), ideal lift coefficient (C_{li}) and angle of attack corresponding to ideal lift coefficient (α_{Cli}), lift coefficient at zero angle of attack (C_{lo}), and lift curve slope ($C_{l\alpha}$). These are critical to identify the performance of an airfoil.

a. The stall angle (α_s) is the angle of attack at which the airfoil stalls; i.e. the lift coefficient will no longer increase with increasing angle of attack. The maximum lift coefficient that corresponds to stall angle is the maximum angle of attack. The stall angle is directly related to the flight safety, since the aircraft will lose the balance of forces in a cruising flight. If the stall is not controlled properly; the aircraft may enter a spin and eventually crash. In general, the higher the stall angle, the safer is the aircraft, thus a high stall angle is sought in airfoil selection. The typical stall angles for majority of airfoils are between 12 to 16 degrees. This means that the pilot is not allowed to increase the angle of attack more than about 16 degrees. Therefore, the airfoil which has the higher stall angle is more desirable.

b. The maximum lift coefficient (C_{lmax}) is the maximum capacity of an airfoil to produce non-dimensional lift; i.e. the capacity of an aircraft to lift a load (i.e. aircraft weight). The maximum lift coefficient is usually occurring at the stall angle. The stall speed (V_S) is inversely a function of maximum lift coefficient, thus the higher C_{lmax} leads in the lower V_S. Thus, the higher C_{lmax} results in a safer flight. Therefore, the higher maximum lift coefficient is desired in an airfoil selection process.

c. The zero lift angle of attack (α_o) is the airfoil angle of attack at which the lift coefficient is zero. A typical number for α_o is around -2 degrees when no high lift device is employed. However, when a high lift device is employed; such as -40 degrees of flap down; the α_o increases to about -12 degrees. The design objective is to have a higher α_o (more negative), since it leaves the capacity to have more lift at zero angle of attack. This is essential for a cruising flight, since the fuselage center line is aimed to be level (i.e. zero fuselage angle of attack) for variety of flight reasons such as comfort of passengers.

d. The ideal lift coefficient (C_{li}) is the lift coefficient at which the drag coefficient does not vary significantly with the slight variations of angle of attack. The ideal lift coefficient is usually corresponding to the minimum drag coefficient. This is very critical in airfoil selection, since the lower drag coefficient means the lower flight cost. Thus, the design objective is to cruise at flight situation such that the cruise lift coefficient is as close as possible to the ideal lift coefficient. The value of this C_{li} will be clear when the graph of variation of drag coefficient versus lift coefficient is discussed. The typical value of ideal lift coefficient for GA aircraft is about 0.1 to 0.4, and for a supersonic aircraft is about 0.01 to 0.05.

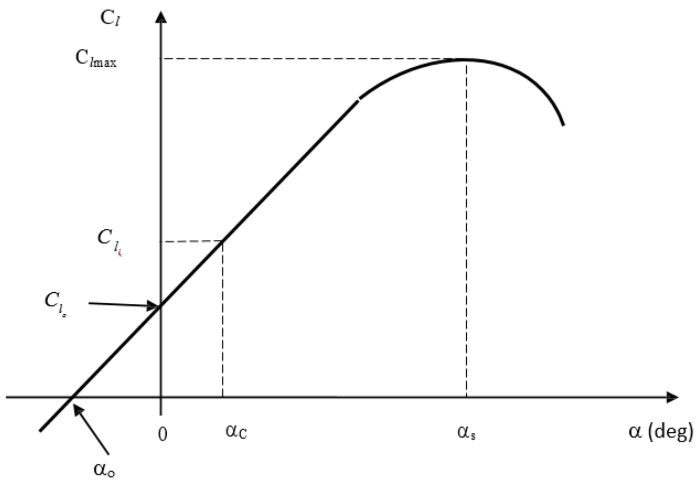

Figure 2.6: The variations of lift coefficient versus angle of attack

- **e.** The angle of attack corresponding to ideal lift coefficient (α_{Cli}) is self-explanatory. The wing setting angle is often selected to be the same as this angle, since it will result in a minimum drag. On the other hand, the minimum drag is corresponding to the minimum engine thrust, which means the minimum flight cost. This will be discussed in more details, when wing setting angle is discussed. The typical value of α_{Cli} is around 2 to 5 degrees. Thus, such an angle will be an optimum candidate for the cruising angle of attack.
- **f.** The lift coefficient at zero angle of attack (C_{lo}) is the lift coefficient when angle of attack is zero. From design point of view, the more (C_{lo}) is better, since it implies we can produce a positive lift even at zero angle of attack. Thus, the more (C_{lo}) is the better.
- **g.** The lift curve slope ($C_{l\alpha}$) is another important performance feature of an airfoil. The lift curve slope is the slope of variation of lift coefficient with respect to the change in the angle of attack, and its unit is 1/deg or 1/rad. Since the main function of an airfoil is to produce lift, the higher the slope, the better the airfoil. The typical value of lift curve slope of a 2D airfoil is around 2π (or 6.28) per radian (about 0.1 per degrees). It implies that for each 1 degree of change in the airfoil angle of attack, the lift coefficient will be increased by 0.1. The lift curve slope (1/rad) may be found by the following empirical equation

$$C_{l_\alpha} = dC_l/d\alpha = 1.8\pi\left(1 + 0.8(t_{max}/c)\right) \qquad 2.6$$

where t_{max}/c is the maximum thickness-to-chord ratio of the airfoil

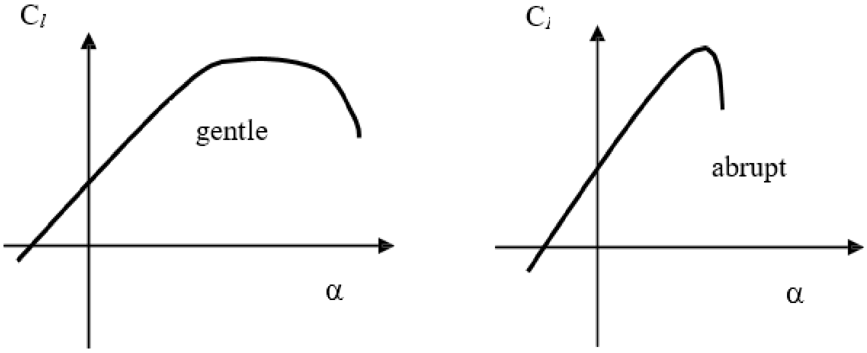

Figure 2.7: Stall characteristics

h. Another airfoil characteristic is the shape of the lift curve at and beyond the stall angle of attack (stall behavior). An airfoil with a gentle drop in lift after the stall, rather than an abrupt or sharp rapid lift loss, leads to a safer stall from which the pilot can more easily recover (see figure 2.7). Although the sudden airfoil stall behavior does not necessarily imply sudden wing stall behavior, a careful wing design can significantly modify the airfoil tendency to rapid stall. In general, airfoils with thickness or camber, in which the separation is associated with the adverse gradient on the aft portion rather than the nose pressure peak, have a more gradual loss of lift. Unfortunately, the best airfoils in this regard tend to have lower maximum lift coefficient.

As it is observed, there are several parameters to judge about the acceptability of an airfoil. In the next section, the technique to select the best airfoil based on these performance characteristics will be introduced.

2. The variations of pitching moment coefficient versus angle of attack

Figure 2.8 shows the typical variations of pitching moment coefficient about quarter chord versus angle of attack for a positive cambered airfoil. The slope of this graph is usually negative and it is in the region of negative C_m for typical range angle of attacks. The negative slope is desirable, since it stabilizes the flight, if the angle of attack is disturbed by a gust. The negative C_m is sometimes referred to as nose-down pitching moment. This is due to its negative direction about y-axis which means the aircraft nose will be pitched down by such moment.

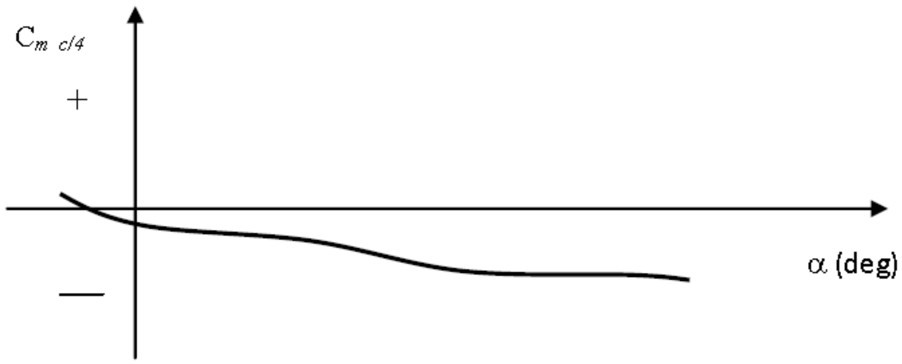

Figure 2.8: The variations of pitching moment coefficient versus angle of attack

Figure 2.9 also illustrates the typical variations of pitching moment coefficient about aerodynamic center versus lift coefficient for a positive cambered airfoil. The magnitude of C_m is constant (recall the definition of aerodynamic center) for a typical ranges of lift coefficient. The typical magnitude is usually about -0.02 to -0.05. However; when "C_m" is transferred from "ac" to another point (such as c/4), it will not be constant anymore. The design objective is to have the C_m close to zero as much as possible. The reason is that the aircraft must be in equilibrium in cruising flight. This pitching moment must be nullified by another component of the aircraft, such as tail. Thus, the higher C_m (more negative) results in a larger tail, which means the heavier aircraft. Therefore, the airfoil which has the lower C_m is more desirable. It is interesting to note that the pitching moment coefficient for a symmetrical airfoil section is zero.

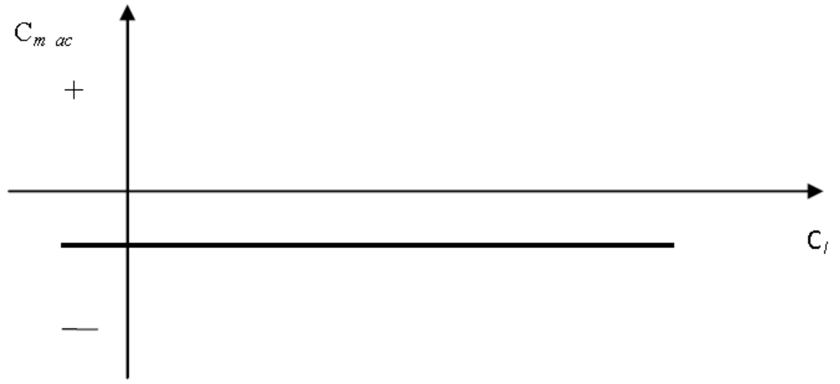

Figure 2.9: The variations of pitching moment coefficient versus lift coefficient

3. The variations of drag coefficient as a function of lift coefficient

Figure 2.10 shows the typical variations of drag coefficient as a function of lift coefficient for a positive cambered airfoil. The lowest point of this graph is called minimum drag coefficient ($C_{d\min}$). The corresponding lift coefficient to the minimum drag coefficient is called $C_{l\min}$. As the drag is directly related to the cost of flight, the $C_{d\min}$ is of great importance in airfoil design or airfoil selection. A typical value for $C_{d\min}$ is about 0.003 to 0.006. Therefore, the airfoil which has the lower $C_{d\min}$ is more desirable.

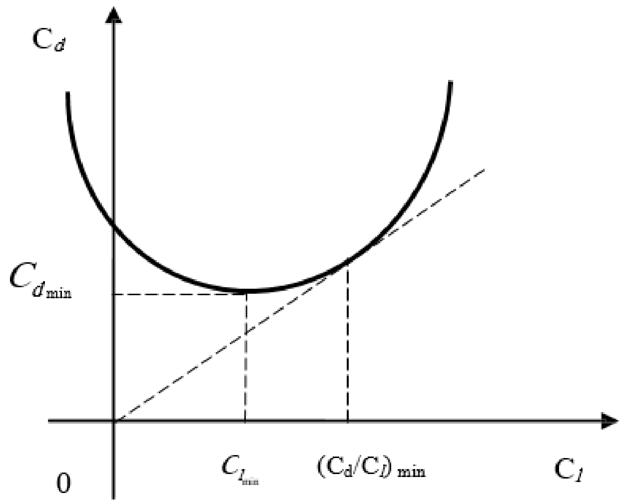

Figure 2.10: The typical variations of drag coefficient versus lift coefficient

A line drawn through the origin and tangent to the graph locates a point that denotes to the minimum slope. This point is also of great importance, since it indicates the flight situation that maximum C_l-to-C_d ratio is generated, since $(C_d/C_l)_{min} = (C_l/C_d)_{max}$. This is an important output of an airfoil, and it is referred to as the maximum lift-to-drag ratio. In addition of requirement of lowest C_{dmin}, the highest $(C_l/C_d)_{max}$ is also desired. These two objectives may not happen at the same time in one airfoil, but based on aircraft mission and weight of each design requirement, one of them gets more attention. The variation of drag coefficient as a function of lift coefficient (figure 2.10) may be mathematically modeled by the following second order equation:

$$C_D = C_{D_{min}} + K\left(C_l - C_{l_{min}}\right)^2 \qquad 2.7$$

where K is called section drag factor. The parameter K can be determined by selecting a point on the graph (C_{l1} and C_{d1}) and plugging in the equation 2.7.

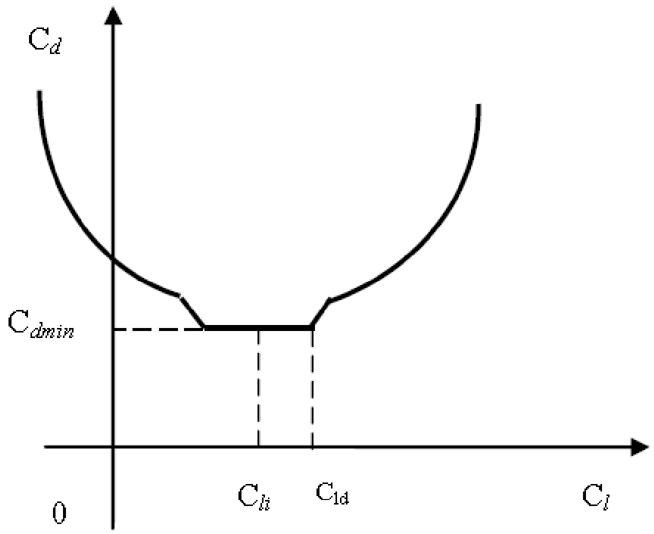

Figure 2.11: The variations of C_l versus C_d for a laminar airfoil

Figure 2.11 shows the typical variations of drag coefficient as a function of lift coefficient for a laminar airfoil; such as in 6-series NACA airfoils. This graph has a unique feature which is the bucket, due to the bucket shape of the lower portion of the graph. The unique aspect of the bucket is that the C_{dmin} will not vary for a limited range of C_l. this is very significant, since it implies that the pilot can stay at the lowest drag point while changing the angle of attack. This situation matches with the cruising flight, since the aircraft weight is reducing as the fuel is burned. Hence, the pilot can bring aircraft nose down (decrease the angle of attack) with being worried about an increase in the aircraft drag. Therefore, it is possible to keep the engine throttle low during cruising flight. The middle point of the bucket is called ideal lift coefficient (C_{li}), while the highest Cl in the bucket region is referred to as design lift coefficient (C_{ld}). These two points are among the list of significant criteria to select/design an airfoil. Remember that the design lift coefficient occurs at the point whose C_d/C_l is minimum or C_l/C_d is maximum. For some flight operations (such as cruising flight), flying at the point where lift coefficient is equivalent with (C_{li}) is the goal, while for some other flight operations (such as loiter), the objective is to fly at the point where lift coefficient is equivalent with (C_{ld}). This airfoil lift coefficient is a function of aircraft cruise lift coefficient (C_{Li}) as discussed in chapter one.

4. **The variations of lift-to-drag ratio (C_l/C_d) as a function of angle of attack**

The last interesting graph that is utilized in the process of airfoil selection is the variations of lift-to-drag ratio (C_l/C_d) as a function of angle of attack. Figure 2.12 illustrates the typical variations of lift-to-drag ratio versus angle of attack. As it is noted, this graph has one maximum point where the value of the lift-to-drag ratio is the highest at this point. The angle of attack corresponding to this point is an optimum candidate for a loitering flight (α_l).

The application of these four graphs and twelve parameters in the airfoil selection process will be introduced in the later sections.

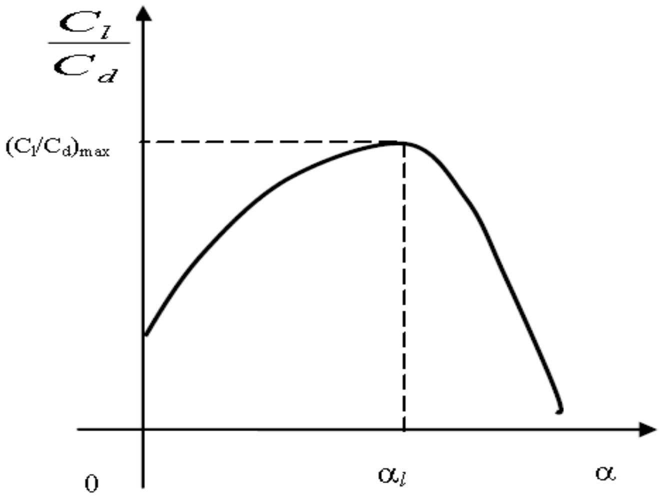

Figure 2.12 The typical variations of lift-to-drag ratio versus angle of attack

2.5 Wing Incidence (i_w) (or setting angle, α_{set}):

The wing incidence (i_w) is the angle between fuselage center line and the wing chord line at root (see figure 2.13). It is sometimes referred to as the wing setting angle (α_{set}). The fuselage center line lies in the plane of symmetry and is usually defined parallel to the cabin floor. This angle could be selected to be variable during a flight operation, or be constant throughout all flight operations. If it is selected to vary during flight, there is no need to determine wing setting angle for the purpose of the aircraft manufacture. However, in this case, the mechanism to vary the wing incidence during flight phases must be designed. Thus, the required wing incidence for every flight phase must be calculated. The variable wing incidence is not recommended, since there is a huge safety and operational concerns. To allow for the wing to have a variable setting angle, there must be a single shaft around which the wing is rotated by pilot control. Such a mechanism is not 100% reliable for aviation purposes, due to fatigue, weight, and stress concentration concerns. In the history of aviation, there is only one aircraft (Vought f8u Crusader) whose wing had variable incidence. A flying wing; such as Northrop Grumman B-2 Spirit has no wing incidence, since there is no fuselage, however the wing angle of attack must be determined for operational purposes.

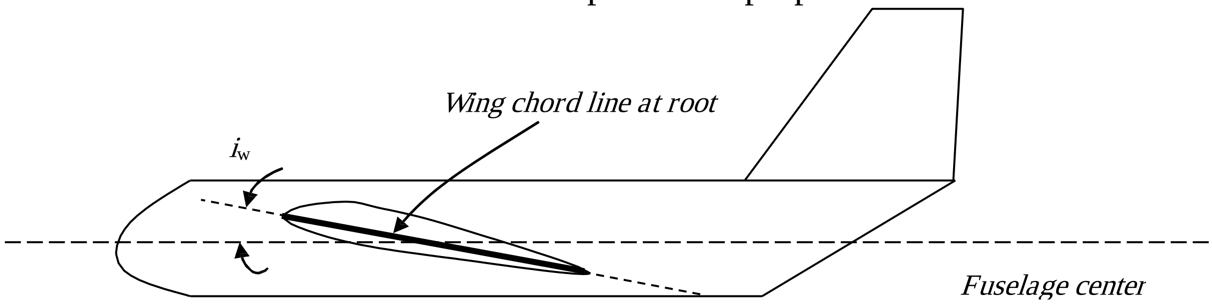

Figure 2.13: Wing setting (incidence) angle

A second, very convenient option is to have a constant wing setting angle. The wing can be attached to the fuselage via welding, screw, or other manufacturing technique at the specified setting angle. This is much safer compared with variable setting angle. For this option, the designer must determine the angle at which the wing is attached to the fuselage. The wing incidence must satisfy the following design requirements:

1. The wing must be able to generate the desired lift coefficient during cruising flight.
2. The wing must produce minimum drag during cruising flight.
3. The wing setting angle must be such that the wing angle of attack could be safely varied (in fact increased) during take-off operation.
4. The wing setting angle must be such that the fuselage generates minimum drag during cruising flight (i.e. the fuselage angle of attack must be zero in cruise).

These design requirements naturally match with the wing airfoil angle of attack corresponding to the airfoil ideal lift coefficient (see figure 2.14). Therefore, as soon as the wing ideal lift coefficient is determined, a reference to C_l-α graph demonstrates the wing setting angle.

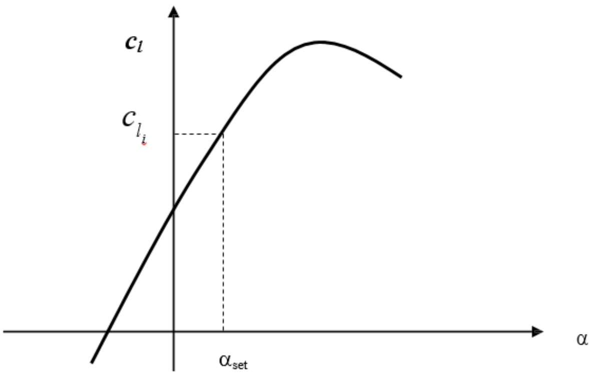

Figure 2.14 Wing setting angle corresponds with ideal lift coefficient

The typical number for wing incidence for majority of aircraft is between 0 to 4 degrees. As a general guidance, the wing setting angle in supersonic fighters, is between 0 to 1 degrees; in GA aircraft, between 2 to 4 degrees; and in jet transport aircraft is between 3 to 5 degrees. It is very hard to have the exact same incidence on both left and right-wing sections. Due to this fact, when there is an inboard stall, the aircraft will roll. The wing outboard stall is unacceptable; if a transport aircraft is at approach, and an outboard stall occurs, it is a disaster. The reason is that the ailerons are not effective to apply roll control.

Table 2.1 illustrates the wing incidence for several aircraft.

No	Aircraft	Type	Wing incidence	Cruising speed (knot)
1	Airbus 310	Jet transport	5^{o} 30'	Mach 0.8
2	Fokker 50	Prop-driven transport	3^{o} 30'	282
3	Sukhoi Su-27	Jet fighter	0^{o}	Mach 2.35
4	Embraer FMB-120 Brasilia	Prop-driven transport	2^{o}	272
5	Embraer Tucano	Turbo-Prop Trainer	1^{o} 25'	222
6	Antonov An-26	Turbo-prop Transport	3^{o}	235
7	BAe Jetstream 31	Turbo-prop Business	3^{o}	282
8	BAe Harrier	V/STOL close support	1^{o} 45'	570
9	Lockheed P-3C Orion	Prop-driven transport	3^{o}	328
10	Rockwell/DASA X-31A	Jet combat research	0^{o}	1485
11	ATR 42	Prop-driven transport	2^{o}	265
12	Beech Super King Air B200	Turbo-prop Transport	3^{o} 48'	289
13	SAAB 340B	Turbo-prop Transport	2^{o}	250
14	AVRO RJ	Jet Transport	3^{o} 6'	412
15	McDonnell MD-11	Jet Transport	5^{o} 51’	Mach 0.87
16	F-15J Eagle	Fighter	0	> Mach 2.2

The wing setting angle may be modified as the design process progresses. For instance, a fuselage with large unsweep over the rear portion to accept aft cargo doors may have their minimum drag at a small positive angle of attack. In such cases, the wing incidence will be reduced accordingly. Another, les fundamental, consideration is that stopping performance during landing operation to get as much weight on the braked wheels as possible. Thus, there is a benefit to reduce the wing incidence slightly to the extent that the change is not felt significantly in the cabin. Reducing the nose gear length will do the same thing. This technique is limited in passenger aircraft because a level cabin floor is desirable on the ground. But, for fighter aircraft, the level floor is not a design consideration.

2.6 Aspect ratio (AR)

Aspect ratio (AR) is defined as the ratio between the wing span; b and the wing Mean Aerodynamic Chord (MAC or $\bar{C}$).

$$AR = \frac{b}{\bar{C}} \qquad 2.8$$

The wing planform area with a rectangular or straight tapered shape is defined as the span times the mean aerodynamic chord:

$$S = b.\bar{C} \qquad 2.9$$

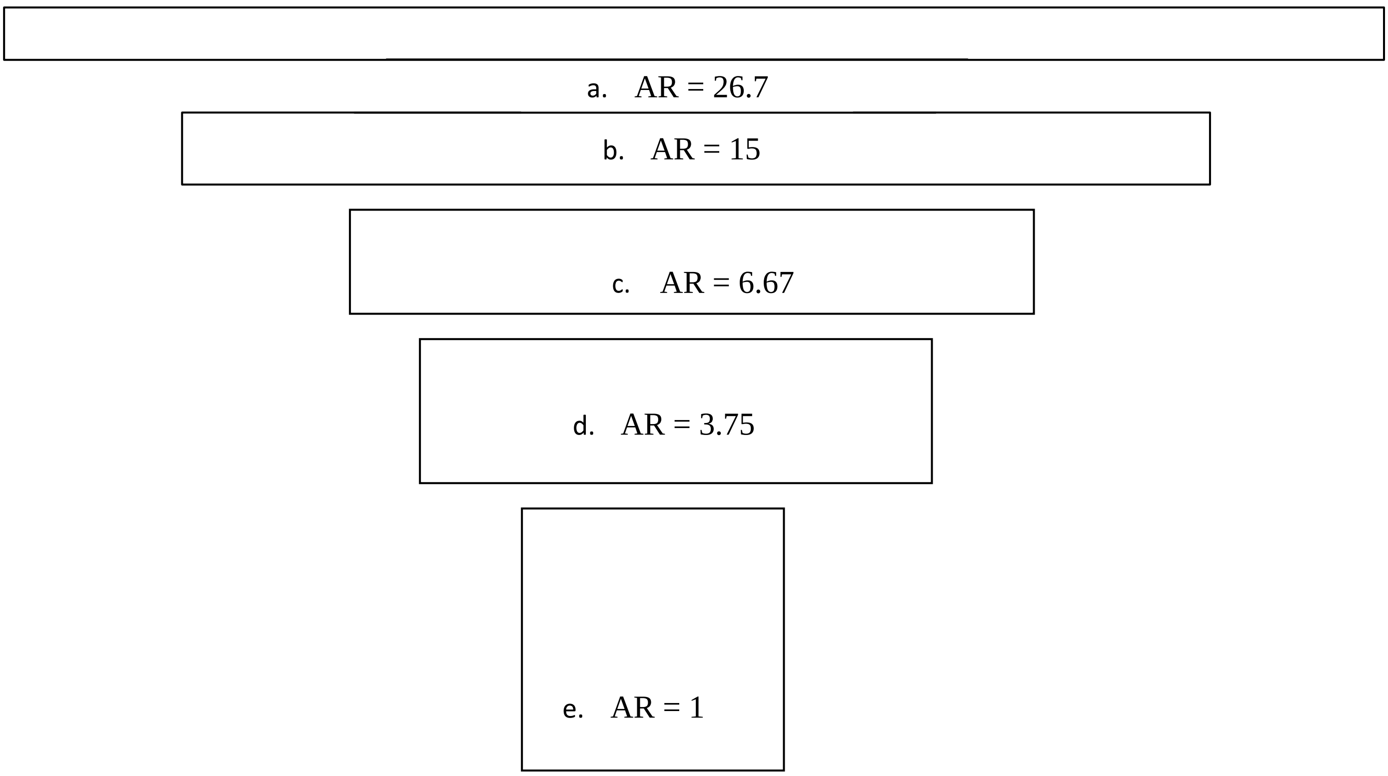

Figure 2.15: Several rectangular wings with the same planform area but different aspect ratio AR

Thus, the aspect ratio shall be redefined as:

$$AR = \frac{bb}{\bar{C}.b} = \frac{b^2}{S} \qquad 2.10$$

This equation is not to be used for the wing with geometry other than rectangle; such as triangle, trapezoid or ellipse; except when the span is redefined. Example 2.1 clarifies this point. At this point, only wing planform area is known. The designer has infinite options to select the wing geometry. For instance, consider an aircraft whose wing reference area has been determined to be 30 m^2. A few design options are as follows:

1. A rectangular wing with a 30 m span and a 1 m chord (AR =30)
2. A rectangular wing with a 20 m span and a 1.5 m chord (AR =13.333)
3. A rectangular wing with a 15 m span and a 2 m chord (AR = 7.5)
4. A rectangular wing with a 10 m span and a 3 m chord (AR = 3.333)
5. A rectangular wing with a 7.5 m span and a 4 m chord (AR = 1.875)
6. A rectangular wing with a 6 m span and a 5 m chord (AR = 1.2)
7. A rectangular wing with a 3 m span and a 10 m chord (AR = 0.3)
8. A triangular (Delta) wing with a 20 m span and a 3 m root chord (AR = 13.33; please note that the wing has two sections (left and right))
9. A triangular (Delta) wing with a 10 m span and a 6 m root chord (AR = 3.33)

There are other options too; but since we have not discussed the parameter of taper ratio; we will not address them at this moment. Figure 2.15 depicts several rectangular wings with different aspect ratio. These wings have the same planform area, but their spans and chords are different. In terms of lift equation (equation 2.1), all are expected to generate the same lift, provided they have the same lift coefficient. However, the wing lift coefficient is not a function of wing area; rather, it is a function of non-dimensional aerodynamic characteristics of the wing such as airfoil and aspect ratio.

The question for a wing designer is how to select the aspect ratio, or which wing geometry is the best. To address this question, we need to discuss the effects of aspect ratio on various flight features such as aircraft performance, stability, control, cost, and manufacturability.

1. From aerodynamic points of view, as the AR is increased, the aerodynamic features of a three-dimensional wing (such as $C_{L\alpha}$, α_o, α_s, C_{Lmax}, C_{Dmin}) are getting closer to its two- dimensional airfoil section (such as $C_{l\alpha}$, α_o, α_s, C_{lmax}, C_{dmin}). This is due to reduction of the influence of wing tip vortex. The flow near the wing tips tends to curl around the tip, being forced from the high-pressure region just underneath the tips to the low-pressure region on top. As a result, on the top surface of the wing, there is generally a spanwise component of flow from the tip toward the wing root, causing the streamlines over the top surface to bend toward the root. Similarly, on the bottom surface of the wing,

there is generally a spanwise component of flow from the root toward the wing tip, causing the streamlines over the bottom surface to bend toward the tip.

2. Due to the first item, as the AR is increased, the wing lift curve slope ($C_{L\alpha}$) is increased toward the maximum theoretical limit of 2π1/rad (see figure 2.16). The relationship between 3d wing lift curve slope ($C_{L\alpha}$) and 2d airfoil lift curve slope ($C_{l\alpha}$) is as follows:

$$C_{L\alpha} = \frac{dC_L}{d\alpha} = \frac{C_{L\alpha}}{1+\frac{C_{L\alpha}}{\pi.AR}} \qquad 2.11$$

For this reason, a high AR (longer) wing is desired.

3. As the AR is increased, the wing stall angle (α_s) is decreased toward the airfoil stall angle. Since the wing effective angle of attack is increased (see figure 2.16). For this reason, the horizontal tail is required to have an aspect ratio lower than wing aspect ratio to allow for a higher tail stall angle. This will result in the tail to stall after wing has stalled, and allow for a safe recovery. For the same reason, a canard is desired to have an aspect ratio to be more than the wing aspect ratio. For this reason, a high AR (longer) wing is desired.

4. Due to the third item, as the AR is increased, the wing maximum lift coefficient (C_{Lmax}) is increased toward the airfoil maximum lift coefficient (C_{lmax}). This is due to the fact that the wing effective angle of attack is increased (see figure 2.16). For this reason, a high AR (longer) wing is desired.

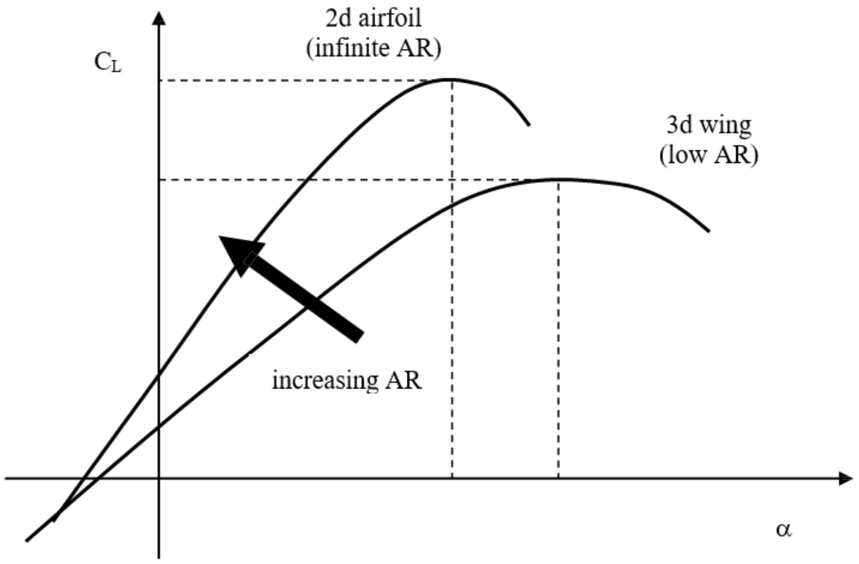

Figure 2.16 The effect of AR on C_L versus angle of attack graph

5. As the AR is increased, the wing will be heavier. The reason is the requirement for structural stiffness. As the wing gets longer, the wing weight (W_w) bending moment (M) gets larger (since $M = \frac{W_w}{2}\frac{b}{2}$), and wing root will have a higher

stress. Thus, the wing root must be stronger to hold the long wing. This requires a heavier wing. The more weight of the wing translates to more cost. For this reason, a low AR (shorter) wing is desired.

6. As the $\sqrt{AR}$ is increased, the aircraft maximum lift-to-drag ratio is increased. Since:

$$\left(\frac{L}{D}\right)_{max} = \frac{1}{2\sqrt{KC_{Do}}} \qquad \text{where } k = \frac{1}{\pi.e.AR} \qquad 2.12$$

where K is the wing induced drag factor, e is the Oswald span efficiency factor, and C_{Do} is the aircraft zero-lift drag coefficient. For this reason, a high AR (longer) wing is desired. This is one of the reasons that the gliders have large aspect ratio and long wing. For this reason, a high AR (longer) wing is desired.

7. As the AR is increased, the wing induced drag is decreased, since the induced drag (C_{Di}) is inversely proportional to aspect ratio. For this reason, a low AR (shorter) wing is desired.

$$C_{Di} = \frac{C_L^2}{\pi.e.AR} \qquad 2.13$$

8. As the AR is increased, the effect of wing tip vortex on the horizontal tail is decreased. As explained in item 1, the tendency for the flow to leak around the wing tips establishes a circulation which trails downstream of the wing; i.e. a trailing vortex is created at each wing tip. This downward component is called downwash. If the tail is in the region of downwash, the tail effective angle of attack is reduced by downwash. This will influence the longitudinal stability and longitudinal control of the aircraft.
9. As the AR increases, the aileron arm will be increased, since the aileron are installed outboard of the wing. This means that the aircraft has more lateral control.
10. As the AR increases, the aircraft mass moment of inertia around x-axis will be increased. This means that it takes longer to roll. In another word, this will reduce the maneuverability of aircraft in roll. For instance, the Bomber aircraft Boeing B-52; that has a very long span; takes several seconds to roll at low speed, whilst the fighter aircraft F-16 Falcon takes a fraction of a second to roll. For this reason, a low AR (shorter) wing is desired for a maneuverable aircraft. The tactical supersonic missiles have a low AR of around 1 to enable them to roll and maneuver as fast as possible.
11. If the fuel tank is supposed to be inside wing, it is desirable to have a low aspect ratio wing. This helps to have a more concentrated fuel system. For this reason, a low AR (shorter) wing is desired.
12. As the aspect ratio is increased, the wing stiffness around y-axis is decreased. This means that the tendency of the wing tips to drop during a take-off is increased, while the tendency to rise during high speed flight is increased. In practice, the manufacture of a very high aspect ratio wing with sufficient structural strength is difficult. For example, the transport aircraft Boeing 747 with AR of 7.7 and wingspan of 59.6 m whose wing tips drop about 1 foot

while the aircraft in on the ground prior to take-off. The wingtip drop is not desirable, especially for a take-off maneuver, since the wing tip clearance is of great importance for safety. For this reason, a low AR (shorter) wing is desired. A shorter wing is easier to build compared with a long wing. For the manufacturability reason, a low AR (shorter) wing is desired.

Table 2.2: Typical values of wing aspect ratio

No	Aircraft type	Aspect ratio
1	Hang glider	4-8
2	Glider (sailplane)	20-40
3	Homebuilt	4-7
4	General Aviation	5-9
5	Jet trainer	4-8
6	Low subsonic transport	6-9
7	High subsonic transport	8-12
8	Supersonic fighter	2-4
9	Tactical missile	0.3-1
10	Hypersonic aircraft	1-3

13. A shorter wing needs lower cost to build compared with a long wing. For the cost reason, a low AR (a shorter wing) is desired.
14. As the AR is increased, the occurrence of the aileron reversal is more expected, since the wing will be more flexible. The aileron reversal is not a desirable phenomenon for a maneuverable aircraft. For this reason, a low AR (shorter) wing is desired.
15. In general, a wing with rectangular shape and high AR is gust sensitive.

As noted, aspect ratio has several influences over the aircraft features. For some design requirements, a low aspect ratio wing is favorable, while for other design requirements, a high aspect ratio wing is desirable. The exact value of the AR will be determined through a thorough investigation and lots of calculation over aircraft performance, stability, control, manufacturability, and cost.

A systems engineering technique via using a weighted parametric table must be employed to determine the exact value of the aspect ratio. Table 2.2 illustrates the typical values of aspect ratio for different aircraft type. Table 2.3 illustrates the aspect ratio for several aircraft. As noted, the aspect ratio ranges from 2.2 for fighter aircraft Eurofighter 2000 to 32.9 for high altitude long endurance (HALE) aircraft Socata. The fighter aircraft MiG-29 with a low aspect ratio wing, and Sailplane Schleicher ASK-18 with a high AR wing respectively.

Table 2.3: Aspect ratio and taper ratio for several aircraft

No	Aircraft	Type	Engine	V_{max} (knot)	S (m^2)	AR	λ
1	Cessna 172	GA	Piston	121	16.2	7.52	0.67
2	Air Tractor AT-402B	Agricultural	Turboprop	174	27.3	8.9	1
3	Piper Comanche	GA	Piston	170	16.5	7.3	0.46
4	McDonnell DC-9	Transport	Turbofan	Mach 0.84	86.8	8.56	0.25
5	Lockheed L-1011	Transport	Turbofan	Mach 0.86	321	7.16	0.29
6	Boeing 747-400	Transport	Turbofan	Mach 0.92	525	6.96	0.3
7	Tucano	Trainer	Turboprop	Mach 0.4	19.2	6.4	0.465
8	Airbus 310	Transport	Turbofan	Mach 0.9	219	8.8	0.26
9	Jetstream 41	Regional Airliner	Turboprop	295	32.59	10.3	0.365
10	Lockheed F-16 Falcon	Fighter	Turbofan	> Mach 2	27.87	3.2	0.3
11	SAAB 39 Gripen	Fighter	Turbofan	> Mach 2	27	2.6	0.25
12	Grumman B-2 Spirit	Bomber	Turbofan	550	465.5	5.92	0.24
13	Schweizer SA 2-38A	Surveillance	Piston	157	21	18.2	0.4
14	Grob G 850 Strato 2C	Surveillance	Piston	280	145	22	0.25
15	Stemme S10	Motor glider	Piston	97	18.7	28.2	0.26
16	Socata HALE	Surveillance	Turboprop	162	70	32.9	0.6
17	Voyager	Circle the globe	Piston	106	30.1	38	0.25
18	Eurofighter 2000	Fighter	Turbofan	Mach 2	50	2.2	0.19
19	Dassault Mirage 2000	Fighter	Turbofan	Mach 2.2	41	2	0.08

2.7 Taper ratio (λ)

Taper ratio (λ) is defined as the ratio between the tip chord (C_t) and the root chord (C_r). This definition is applied to the wing, as well as the horizontal tail, and the vertical tail. Root chord and tip chord are illustrated in figure 2.17.

$$\lambda = \frac{C_t}{C_r} \qquad 2.14$$

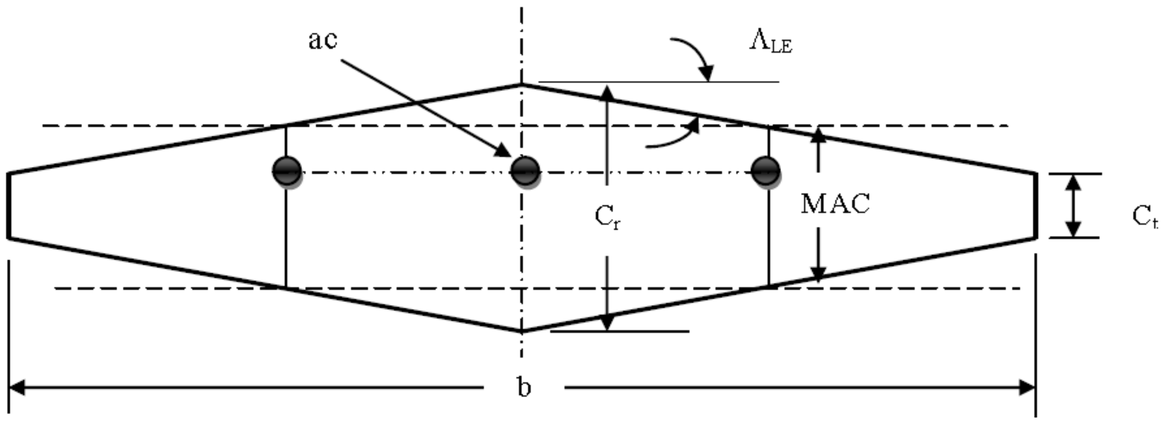

Figure 2.17: Mean Aerodynamic Chord and Aerodynamic Center in a straight wing

The geometric result of taper is a smaller tip chord. In general, the taper ratio varies between zero and one.

$$0 \leq \lambda \leq 1$$

Where three major planform geometries relating to taper ratio are rectangular, trapezoidal and delta shape (see Figure 2.18).
In general, a rectangular wing planform is aerodynamically inefficient, while it has a few advantages, such as performance, cost and ease of manufacture. A wing with a rectangular planform has a larger downwash angle at the tip than at the root. Therefore, the effective angle of attack at the tip is reduced compared with that at the root. Thus, the wing tip will tend to stall later than the root. The spanwise lift distribution is far from elliptical; where it is highly desirable to minimize the induced drag. Hence, one of the reasons to taper the planform is to reduce the induced drag.

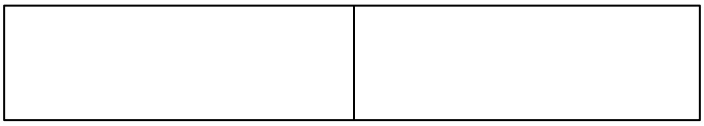

a. Rectangle (λ =1)

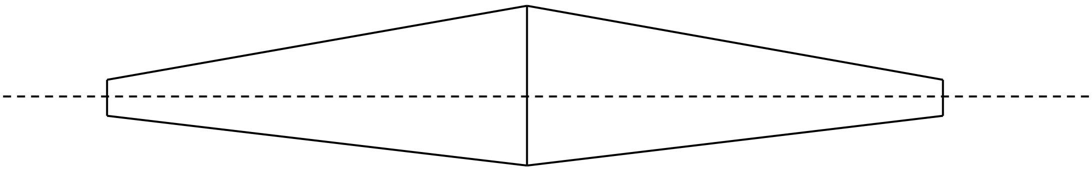

b. Trapezoid $0 < \lambda < 1$ (straight tapered)

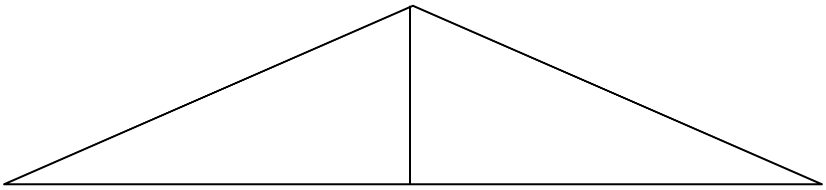

c. Triangle (delta) $\lambda = 0$

Figure 2.18: Wings with various taper ratio

In addition, since the tip chord is smaller than root chord, the tip Reynolds number will be lower, as well as a lower tip induced downwash angle. Both effects will lower the angle of attack at which stall occurs. This will result in the tip may stall before the root. This is undesirable from the viewpoint of lateral stability and lateral control. On the other hand, a rectangular wing planform is structurally inefficient, since there is a lot of area outboard, which supports very little lift. Wing taper will help resolve this problem as well. The effect of wing taper can be summarized as follows:

1. The wing taper will change the wing **lift distribution**. This is assumed as an advantage of the taper, since it is a technical tool to improve the lift distribution. One of the wing design objective is to generate the lift such that the spanwise lift distribution be elliptical. Based on this item, the exact

value for taper ratio will be determined by lift distribution requirement.

2. The wing taper will increase the **cost** of the wing manufacture, since the wing ribs will have different shapes. Unlike a rectangular planform that all ribs are similar; each rib will have different size. If the cost is of major issue (such as for homebuilt aircraft), do not taper the wing.
3. The taper will reduce the wing **weight**, since the center of gravity of each wing section (left and right) will move toward fuselage center line. This results in a lower bending moment at the wing root. This is an advantage of the taper. Thus, to reduce the weight of the wing, more taper (toward 0) is desired.
4. Due to item 3, the wing mass moment of inertia about x-axis (longitudinal axis) will be decreased. Consequently, this will improve the aircraft **lateral control**. In this regard, the best taper is to have a delta wing (λ= 0).
5. The taper will influence the aircraft static **lateral stability** ($C_{l\beta}$), since the taper usually generates a sweep angle (either on the leading edge or on quarter chord line). The effect of the weep angle on the aircraft stability will be discussed in section later.

As noted, taper ratio has mixed influences over the aircraft features. The aspect ratio of a conventional aircraft is a compromise between conflicting aerodynamic, structural, performance, stability, cost, and manufacturability requirements. For some design requirements (e.g. cost, manufacturability), no taper ratio wing is favorable; while for other design requirements (such as stability, performance, and safety), a tapered wing is desirable. The first estimate of the taper ratio will be determined by lift distribution calculations, as introduced in the next section. The exact value of the taper ratio will be finalized through a thorough investigation and lots of calculations over aircraft performance, stability, control, manufacturability, and cost. A systems engineering technique by using a weighted parametric table must be employed to determine the exact value of the taper ratio. Table 2.3 illustrates the taper ratio for several aircraft. The typical effect of taper ratio on the lift distribution is sketched in figure 2.19.

In the normal flight range, the resultant aerodynamic forces acting on any lifting surface (e.g. lift, tail) can be represented as a lift and drag acting at the Aerodynamic Center (ac), together with a pitching moment which is independent of angle of attack. Methods for determining planform aerodynamic center locations may be found in most aerodynamic textbooks. Until compressibility effects begin to play a role, it is experienced that the planform aerodynamic center ranges from 25 percent to about 30 percent of Mean Aerodynamic Chord (MAC or $\bar{C}$). In the transonic and supersonic speed range, the ac tends to move aft, such that at transonic speeds, the ac moves close to the 50 percent chord point on the MAC. The aerodynamic center lies in the plane of symmetry of the wing. However, in determining MAC, it is convenient to work with the half wing. For a general planform, the location of length of the MAC can be determined using the following integral:

$$\bar{C} = \frac{2}{S}\int_0^{b/2} C^2(y)\,dy \qquad 2.15$$

where c is the local chord and y is the aircraft lateral axis. For a constant-taper and constant- sweep angle (trapezoidal) planform, (see the geometry of figure 2.17), Mean Aerodynamic Chord is determined as follows:

$$\bar{C} = \frac{2}{3}C_r\left(\frac{1+\lambda+\lambda^2}{1+\lambda}\right) \qquad 2.16$$

Table 2.3 illustrates the aspect ratio for several jet and prop-driven aircraft.

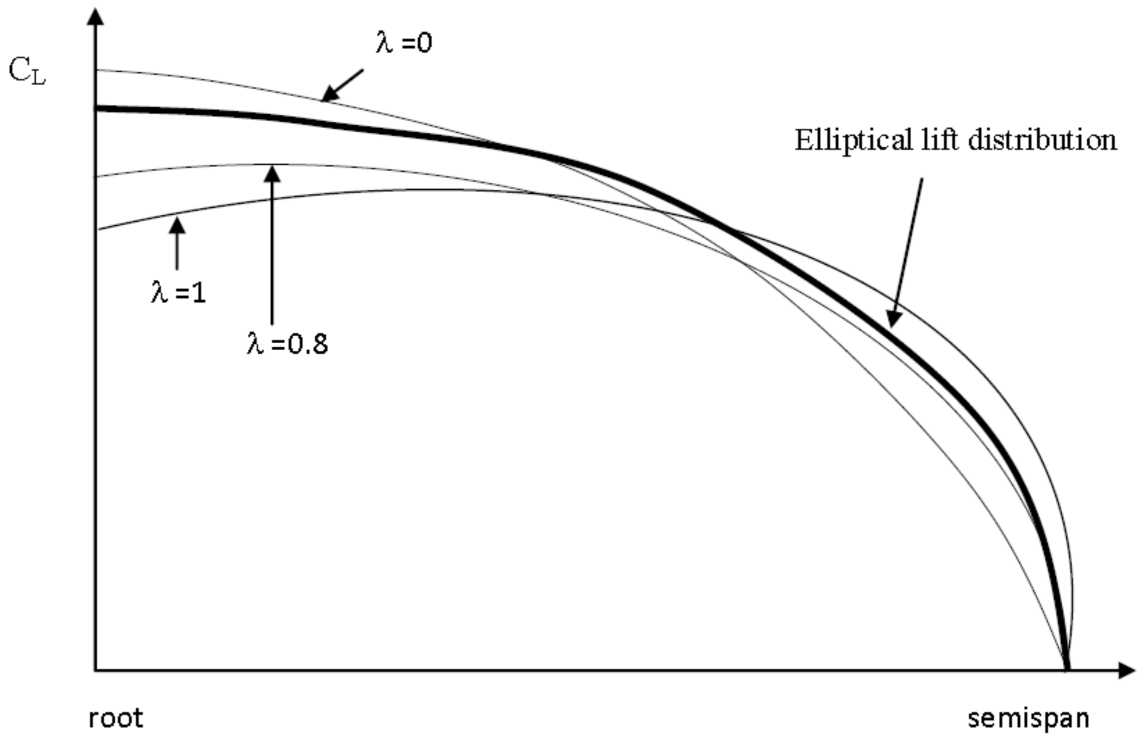

Figure 2.19: The typical effect of taper ratio on the lift distribution

2.8 The Significance of Lift and Load Distributions

The distribution of wing non-dimensional lift (i.e. lift coefficient; C_L) per unit span along the wing is referred to as *lift distribution*. Each unit area of the wing along the span is producing a specific amount of lift. The total lift is equal to the summation of these individual lifts. The lift distribution goes to zero at the tips, because there is a pressure equalization from the bottom to the top of the wing precisely at y = -b/2 and +b/2. Hence no lift is generated at these two points. In addition, the variation of "lift coefficient times sectional chord ($C \cdot C_L$)" along span is referred to as the "*load* *distribution"*. Both lift distribution and load distribution are of great importance in the wing design process. The major application of lift distribution is in aerodynamic calculation, while the primary application of the load distribution is in wing structural design as well as controllability analysis.

In the past (1930s), it was thought that for an elliptic lift distribution, the chord must vary elliptically along the span. The direct result of such logic was that the wing planform must be elliptical. For this reason, several aircraft wing planforms such as *Super-Marine Spitfire*, a famous British World War II fighter were made elliptic. But, today, we know that there are various parameters that make the lift distribution elliptic, thus, there is no need for the wing planform to be planform. The type of both lift distribution and load distribution are very important in wing design; and will influence the aircraft performance, airworthiness, stability, control, and cost. Ideally both lift distribution and load distribution are preferred to be elliptical. For the above-mentioned reasons, the elliptical lift distribution and the elliptical load distribution are ideal and are the design objectives in the wing design process. An elliptical lift distribution is sketched in figure 2.20, where a front view of the wing is illustrated. The horizontal axis in figure 2.20 is y/s where y is the location is y-axis, and s denotes the semi-span (s = b/2). In this figure, no high lift device (e.g. flap) is deflected and the effect of the fuselage is ignored. The elliptical lift distribution and elliptical load distribution have the following desirable properties:

1. If the wing tends to stall (C_{Lmax}), the wing root is stalled before the wing tip ($C_{Lroot} = C_{Lmax}$ while $C_{Ltip} < C_{Lmax}$). In a conventional aircraft, the flaps are located inboard, while the ailerons are installed outboard of the wing. In such a situation, ailerons are active, since the flow over the wing outboard section is healthy. This is of greater importance for spin recovery (which often happens after stall); since the aileron (in addition to rudder) application are very critical to stop the autorotation. Thus, the elliptical lift distribution provision guarantees the flight safety in the event of stall (see figure 2.21).

2. The bending moment at the wing root is a function of load distribution. If the load distribution is concentrated near to the root, the bending moment is considerably less that when it is concentrated near the tip. The center of an elliptical load distribution is closer to the wing root; thus, it leads to a lower bending moment, which results in a less bending stress and a less stress

concentration at wing root (see figure 2.22). This means a lighter wing spar and lighter wing structure that is always one of the design requirements. The load distribution is a function of the lift distribution.

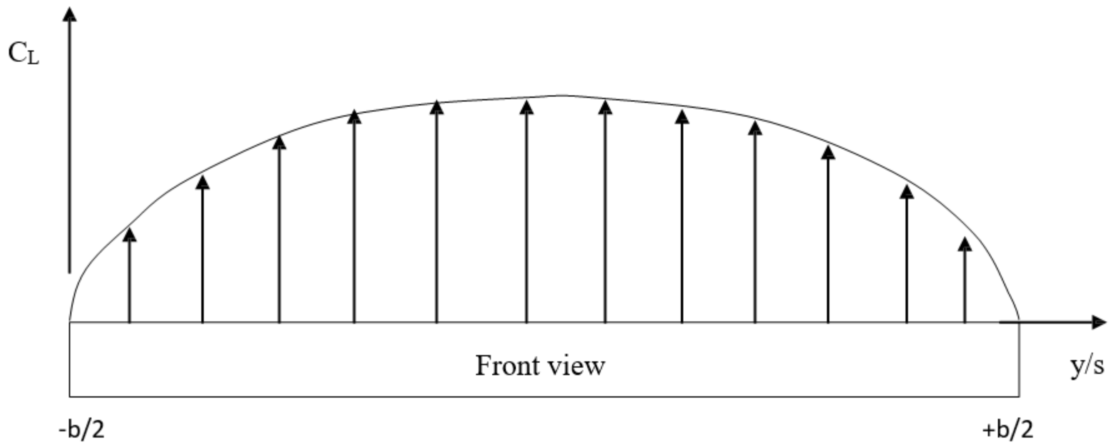

Figure 2.20: Elliptical lift distribution over the wing

3. The center of gravity of each wing section (left or right) for an elliptical load distribution is closer to the fuselage center line. This means a lower wing mass moment of inertia about x- axis which is an advantage in the lateral control. Basically, an aircraft rolls faster when the aircraft mass moment of inertia is smaller.
4. The downwash is constant over the span for an elliptical lift distribution. This will influence the horizontal tail effective angle of attack.
5. For an elliptical lift distribution, the induced angle of attack is also constant along the span.
6. The variation of lift over the span for an elliptical lift distribution is steady (gradually increasing from tip (zero) to the root (maximum)). This will simplify the wing spar(s) design.

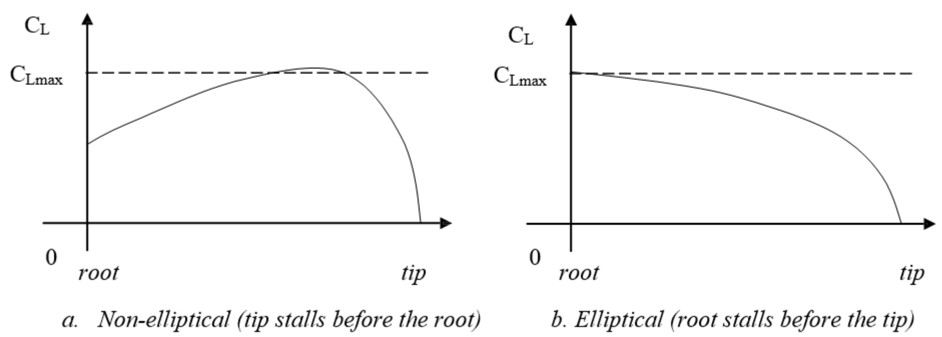

Figure 2.21: Lift distribution over a half wing

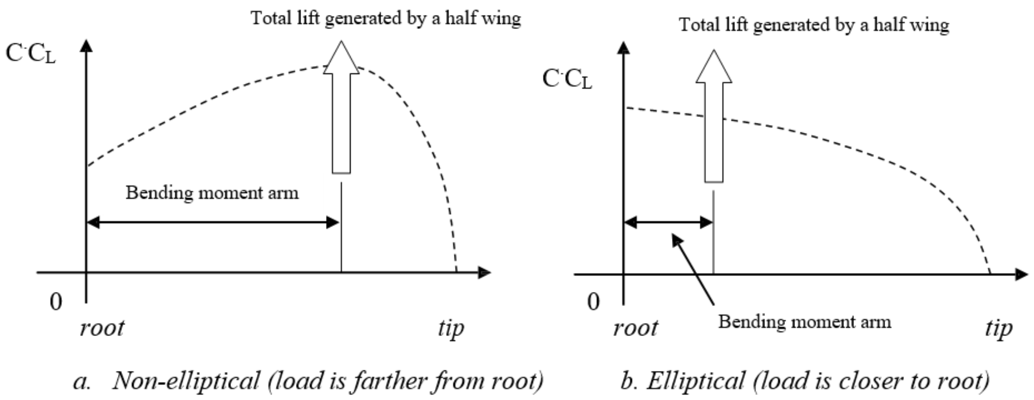

Figure 2.22: Load distribution over a half wing

The reader may have noticed that if the contribution of the fuselage is added to the wing lift distribution, the distribution may not be elliptical; due to negligible fuselage lift contribution. This is true, and more realistic, since in a conventional aircraft, the wing is attached to the fuselage. What we examined here in this section is an ideal case, and the students may modify the lift distribution by considering the fuselage contribution. Figure 2.23 depicts the fuselage contribution to a low wing configuration. Similar case may be made for the effect of flap of lift distribution when deflected. Figure 2.24 illustrates the flap contribution to the wing lift distribution. In principle, the goal in the wing design is to obtain an elliptical wing distribution without considering the contributions of fuselage, flap, or other components.

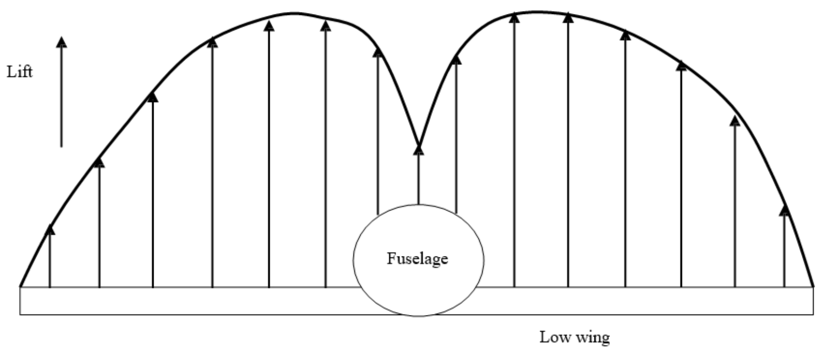

Figure 2.23: The fuselage contribution to the lift distribution of a low wing configuration

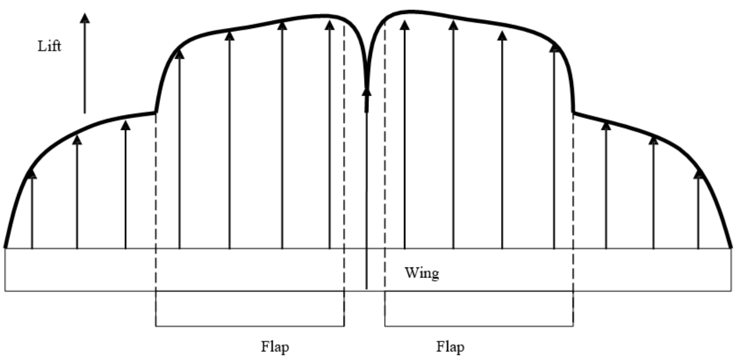

Figure 2.24: The flap contribution to the lift distribution

2.9 Sweep Angle

Consider the top view of an aircraft. The angle between a constant percentage chord line along the semi-span of the wing and the lateral axis perpendicular to the aircraft centerline (y-axis) is called leading edge sweep (Λ_{LE}). The angle between the wing leading edge and the y-axis of the aircraft is called leading edge sweep (Λ_{LE}). Similarly, the angle between the wing trailing edge and the longitudinal axis (y-axis) of the aircraft is called trailing edge sweep (Λ_{TE}). In the same fashion, the angle between the wing quarter chord line and the y-axis of the aircraft is called quarter chord sweep ($\Lambda_{C/4}$). And finally, the angle between the wing 50 percent chord line and the y-axis of the aircraft is 50 percent chord sweep ($\Lambda_{C/2}$).

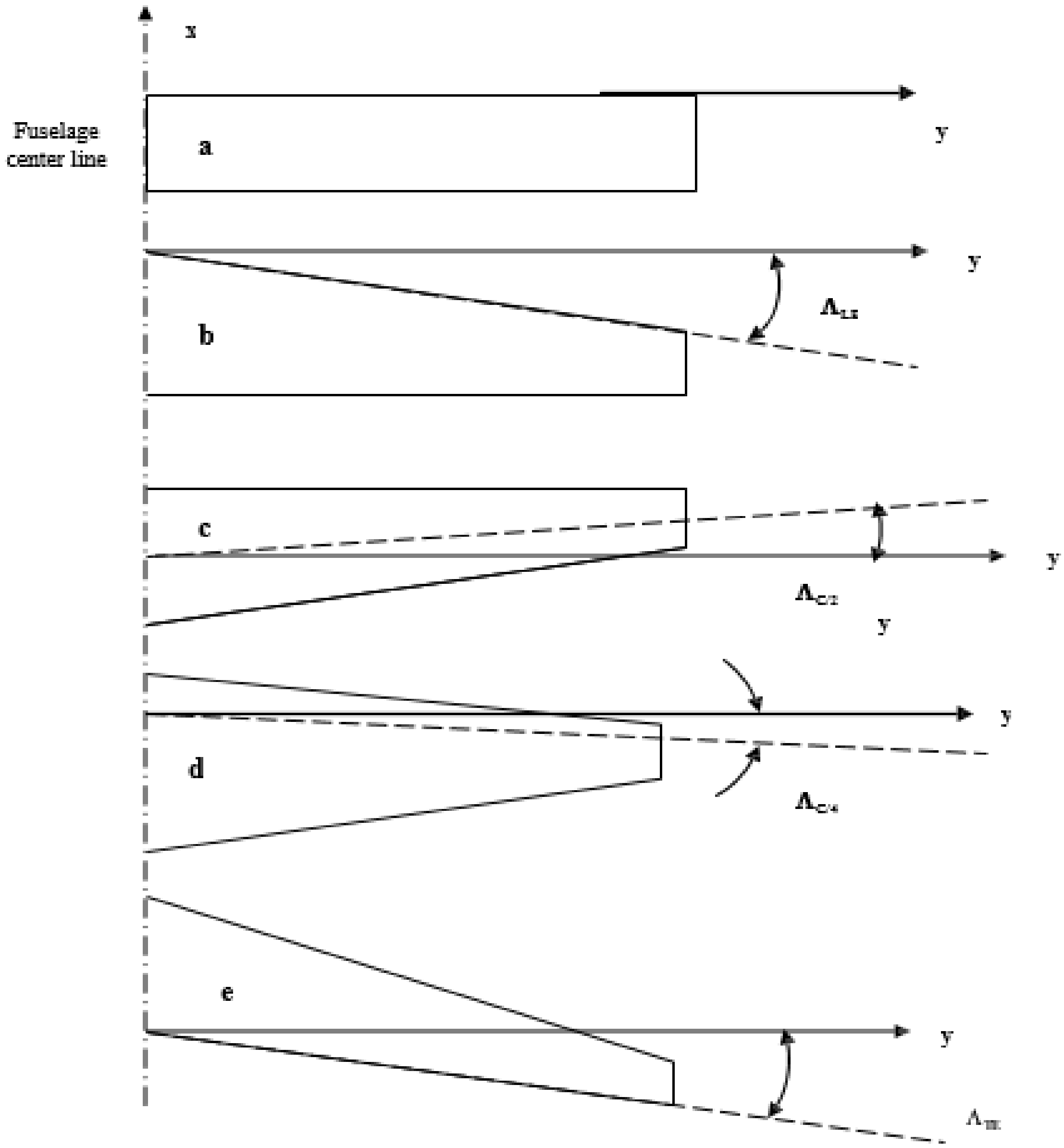

Figure 2.25: Five wings with different sweep angles

If the angle is greater than zero (i.e. wing is inclined toward tail), it is called aft (afterword) sweep or simply sweep; otherwise it is referred to as forward sweep. Figure 2.25 shows five wings with various sweep angles. Figure 2.25a illustrates a wing without sweep, while figures 2.25b through 2.25d show four swept wings. The leading-edge sweep is depicted in the wing of figure 2.25b, while trailing edge sweep is shown in the wing of figure 2.25e. In addition, the quarter chord sweep is illustrated in the wing of figure 2.25d, and the 50 percent chord sweep is illustrated in the wing of figure 2.25c. Most high-speed airplanes designed since the middle 1940s – such as North American F-86 Saber - have swept wings. On sweptback tapered wing, typical of almost all high-speed aircraft, the leading edge has more sweep than the trailing edge.

With reference to the definition of sweep angle, a particular wing may have aft leading- edge sweep, while it has forward trailing edge sweep. Among four types of sweep angles, the quarter chord sweep and leading-edge sweep are the most important ones. The subsonic lift due angle of attack normally acts at the quarter chord. In addition, the crest is usually close to the quarter chord. The discussion in this section regarding the characteristics (advantages and disadvantages) of sweep angle is mostly about leading edge sweep angle, unless otherwise stated. Basically, a wing is being swept for the following five design goals:

1. Improving the wing aerodynamic features (lift, drag, pitching moment) at transonic, supersonic and hypersonic speeds by delaying the compressibility effects.
2. Adjusting the aircraft center of gravity.
3. Improving static lateral stability.
4. Impacting longitudinal and directional stability.
5. Increasing pilot view (especially for fighter pilots).

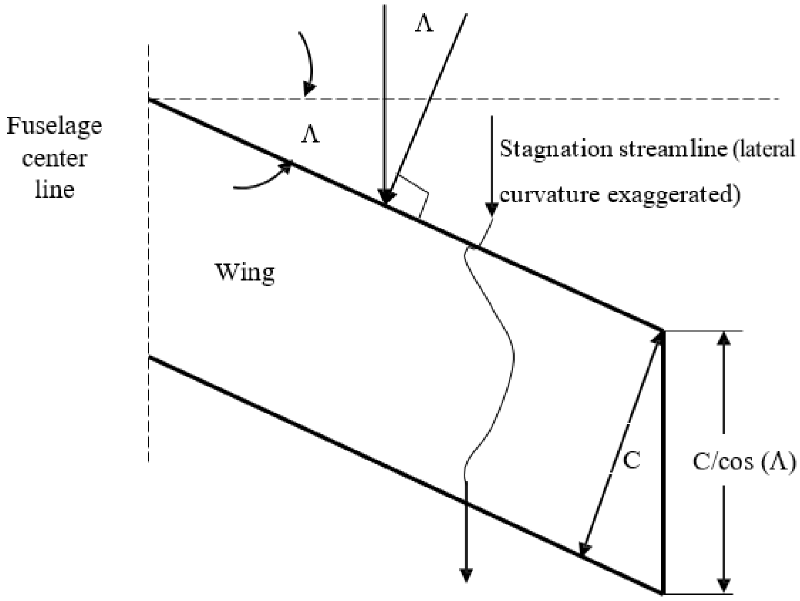

Figure 2.26: The effective of the sweep angle of the normal Mach number

These items will be described in more details in this section. For more information, the reader needs to refer to technical textbooks that are listed at the end of this chapter. The practical influence of the sweep angle on various flight features are as follows:

1. The sweep angle, in practice, tends to increase the distance between leading edge and trailing edge. Accordingly, the pressure distribution will vary.
2. The effective chord length of a swept wing is longer (see Figure 2.26) by a factor of 1/cos (Λ). This makes the effective thickness-to-chord ratio thinner, since the thickness remains constant.
3. Item 2 can be also translated into the reduction of Mach number (M_n) normal to the wing leading edge to M cos (Λ). Hence, by sweeping the wing, the flow behaves as if the airfoil section is thinner, with a consequent increase in the critical Mach number of the wing. For this reason, a classic design feature used to increase M_{cr} is to sweep the wing.
4. The effect of the swept wing is to curve the streamline flow over the wing as shown in figure 2.26. The curvature is due to the deceleration and acceleration of flow in the plane perpendicular to the quarter chord line. Near the wing tip the flow around the tip from the lower surface to the upper surface obviously alters the effect of sweep. The effect is to unsweep the spanwise constant-pressure lines; isobar. To compensate, the wing tip may be given additional structural sweep.
5. The wing aerodynamic center (ac) is moved aft by the wing aft sweep at about few percent. The aft movement of the ac with increase in sweptback angle occurs because the effect of the downwash pattern associated with a swept wing is to raise the lift coefficient on the outer wing panel relative to the inboard lift coefficient. Since sweep movers the outer panel aft relative to the inner portion of the wing, the effect on the center of lift is an aft ward movement. The effect of wing sweep on ac position is shown in figure 2.27 for aspect ratios of 7 and 10 and for taper ratios of 0.25 and 0.5.

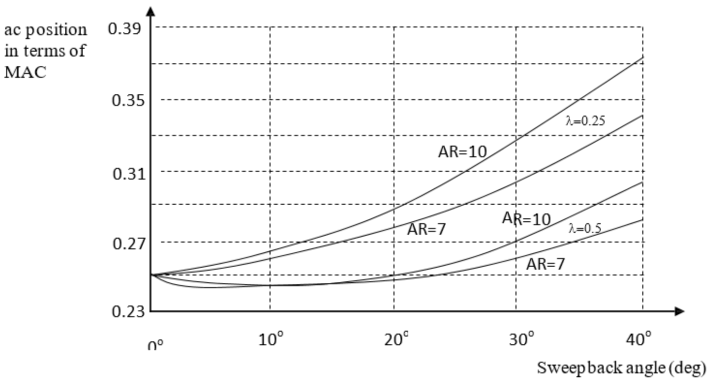

Figure 2.27: Effect of wing sweepback on ac position for several combinations of AR and λ

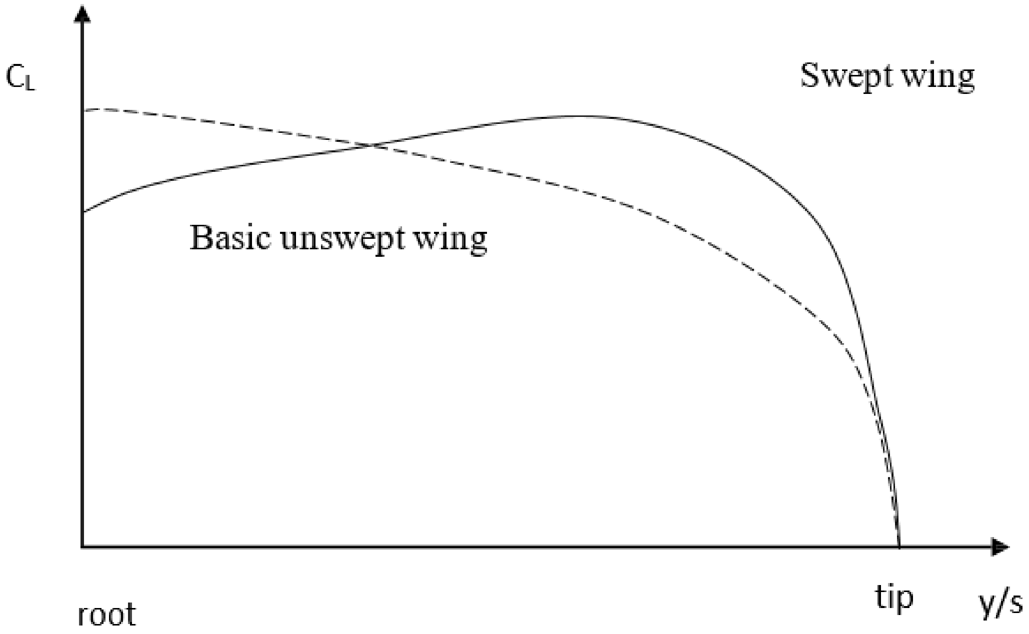

Figure 2.28: Typical effect of sweep angle on lift distribution

6. The effective dynamic pressure is reduced, although not by as much as in cruise.
7. The sweep angle tends to change the lift distribution as sketched in figure 2.28. The reason becomes clear by looking at the explanations in item 5. As the sweep angle is increased, the Oswald efficiency factor (e) will decrease (Equation 2.15). The Oswald span efficiency for a straight wing and swept wing are given respectively by equation 2.17a and 2.17b.

$$e = 1.78(1 - 0.045AR^{0.68}) - 0.64 \qquad 2.17a$$

$$e = 1.78(1 - 0.045AR^{0.68})[cos(\Lambda_{LE})]^{0.15} - 3.1 \qquad 2.17b$$

Equation 2.17a is for a straight wing and Equation 2.17b is for a swept wing where sweep angle is more than 30 degrees. When the Oswald span efficiency is equal to 1, it indicates that the lift distribution is elliptical, otherwise it is non-elliptic. Equation 2.17 is not valid for low aspect ratio wings (AR less than 6).
8. The wing maximum lift coefficient can actually increase with increasing sweep angle. However, the maximum useful lift coefficient actually decreases with increasing sweep angle, due to loss of control in pitch up situation. Whether or not pitch up occurs depends not only on the combination of sweep angle and aspect ratio, but also an airfoil type, twist angle, and taper ratio. Thus, the sweep angle tends to increase stall speed (Vs). The maximum lift coefficient of the basic wing without high lift device is governed by the following semi-empirical relationship:

$$C_{Lmax_{(\Lambda\neq 0)}} = C_{lmax}[0.86 - 0.002(\Lambda)] \qquad 2.18$$

where sweep angle (Λ) is in degrees and C_{lmax} denotes the maximum lift coefficient for the outer panel airfoil section.
9. Wing sweep tends to reduce the wing lift curve slope ($C_{L\alpha}$). A modified equation based on Prandtl-Glauert approximation is introduced as follows:

$$C_{L\alpha} = \frac{2\pi AR}{2+\sqrt{AR^2(1+tan^2\Lambda-M^2)+4}} \qquad 2.19$$

Where M is free stream Mach number.

10. The aircraft pitching moment will be increased, provided the aircraft cg is forward of aircraft ac. The reason is that wing aerodynamic center is moving aft with increase in sweep angle.
11. An aft swept wing tends to have tip stall because of the tendency toward outboard, spanwise flow. This causes the boundary layer to thicken as it approaches the tips. For the similar reason, a swept forward wing would tend toward root stall. This tends to have an influence opposite to that of wing twist.
12. On most aft swept wing aircraft, the wing tips are located behind the aircraft center of gravity. Therefore, any loss of lift at the wing tips causes the wing center of pressure to move forward. This in turn will cause the aircraft nose to pitch up. This pitch up tendency can cause the aircraft angle of attack to increase even further. This may result in a loss of aircraft longitudinal control. For the similar reason, a forward swept wing aircraft would exhibit a pitch down tendency in a similar situation.
13. Tip stall on a swept wing is very serious. If the outboard section of a swept wing stalls, the lift loss is behind the wing aerodynamic center. The inboard portion of the wing ahead of the aerodynamic center maintains its lift and produces a strong pitch-up moment, tending to throw the aircraft deeper into the stall. Combined with the effect of tip stall on the pitching moment produced by the tail, this effect is very dangerous and must be avoided by options such as wing twist.
14. A swept wing produces a negative rolling moment because of a difference in velocity components normal to the leading edge between the left and right-wing sections. The rolling moment due to aft sweep is proportional to the sine of twice the leading- edge sweep angle.

    $$C_{l\beta} \propto sin(2\Lambda_{LE}) \qquad 2.20$$

    This makes the dihedral effect ($C_{l\beta}$) more negative and it means that a swept wing has an inherent dihedral effect. Hence, a swept wing may not need a dihedral or Anhedral to satisfy lateral-directional stability requirements. Thus, the sweep angle tends to reinforce the dihedral effect. It is interesting to note that making the dihedral effect ($C_{l\beta}$) more negative will make an aircraft more spirally stable. At the same time, the Dutch-roll damping ratio tends to decrease. This presents a design conflict which must be resolved through some compromise.

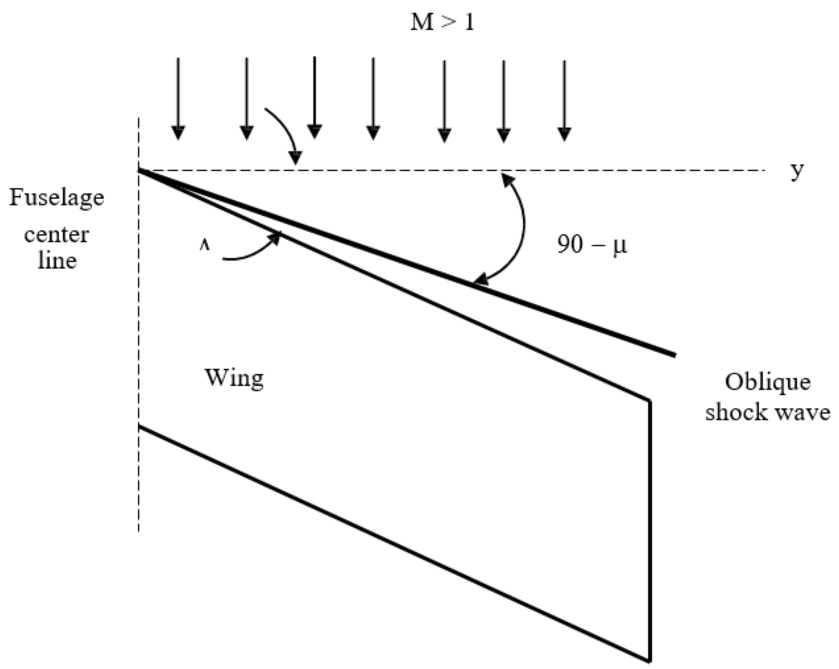

Figure 2.29 The sweep angle and Mach angle in supersonic flight

15. In supersonic flight, the sweep angle tends to reduce the shock wave drag. The drag generated by the oblique shock wave is referred to as wave drag, which is inherently related to the loss of total pressure and increase of entropy across the oblique shock waves created by the wing. For this purpose, the sweep angle must be greater (see figure 2.29) than Mach angle, μ:

$$\mu = \sin^{-1}\left(\frac{1}{M}\right) \qquad 2.21$$

$$\Lambda = 1.2 \times (90 - \mu) \qquad 2.22$$

where M is the aircraft cruising Mach number. A 20 percent higher sweep angle will guarantee the low wave drag at supersonic speeds.

16. A wing with high wing loading (W/S) and high quarter-chord sweep ($\Lambda_{C/4}$) exhibits a good ride in turbulence.
At hypersonic speeds (e.g. Space Shuttle), if the oblique shock wave is very close to the wing leading edge; due to a low sweep angle; it generates very high temperature due to aerodynamic heating (about 1650 ^{o}C) such that the wing leading edge surface may be melted. Thus, the sweep angle must be such that wing leading edge surface survive very high temperature. This ensures that the wing is located inside Mach cone.

17. With the application of the sweep angle, the wing effective span (b_{eff}) will be shorter than original theoretical span. This results in a lower wing mass moment of inertia about x-axis, which increases the lateral controllability of the aircraft. Hence, the higher the sweep angle, allows for better maneuverability.

2.9.1 Sweep angle selection guideline: As noted, sweep angle has several advantages and disadvantages such that can only be decided through a compromise. The following guidelines help the students to select the initial value and to update the value throughout the design iterative process.

a. Low subsonic aircraft: If the aircraft maximum speed is less than Mach 0.3 (the borderline to include the compressibility effect), no sweep angle is recommended for the wing, since its advantages negates all the improvement it produced. For instance, by using 5 degrees of sweep angle, you may have reduced the aircraft drag by say 2 percent. But you have increased the cost by say 15 percent as well as adding complexity to the wing manufacturing. Thus, a straight wing is recommended.

b. High subsonic and supersonic aircraft: The initial value can be determined through equation 2.22 as a function of aircraft cruising speed. However, the final value will be finalized after a series of calculations and analysis on aerodynamics, performance, stability, control, structure, as well as cost, and manufacturability. Remember, if the wing is tapered, it must have a sweep angle anyway.

Table 2.4: Sweep angles for several low and high-speed aircraft

No	Aircraft	Type	First flight	Max speed (Mach, knot)	Λ_{LE} (deg)
1	Cessna 172	Single piston engine GA	1955	121 knot	0
2	Tucano	Turboprop trainer	1983	247 knot	4
3	AIRTECH	Turboprop Transport	1981	228 knot	3^{o} 51' 36''
4	ATR 42	Turboprop Transport	1984	265 knot	3^{o} 6'
5	Jetstream 31	Turboprop business	1967	Mach 0.4	5^{o} 34'
6	Beech Starship	Turboprop business	1991	Mach 0.78	20
7	DC-9 series 10	Jet Passenger	1965	Mach 0.84	24
8	Falcon 900B	Business Jet	1986	Mach 0.87	24^{o} 30'
9	Gulfstream V	Business Jet	1996	Mach 0.9	27
10	Boeing 777	Jet Transport	1994	Mach 0.87	31.6
11	B-2A Spirit	Strategic Bomber	1989	Mach 0.95	33
12	MD-11	Jet Transport	2001	Mach 0.945	35
13	Boeing 747	Jet Transport	1969	Mach 0.92	37^{o} 30'
14	Airbus 340	Jet Transport	1991	Mach 0.9	30
15	F-16	Fighter	1974	> Mach 2	40
16	F/A-18	Fighter	1992	> Mach 1.8	28
17	Mig-31	Fighter	1991	Mach 2.83	40
18	Su-34	Fighter	1996	Mach 2.35	42
19	Eurofighter Typhoon	Fighter	1986	Mach 2	53
20	Mirage 2000	Fighter	1975	Mach 2.2	58
21	Concorde	Supersonic Jet Transport	1969	Mach 2.2	75 inboard 32 outboard
22	Space Shuttle	Spacecraft (flies in air during return mission)	1981	Mach 21	81 inboard 44 outboard

Table 2.4 shows sweep angles of several aircraft along with their maximum speeds. As noted, as the maximum speed is increased, so do the sweep angle.
The following practical comments; including a few drawbacks; will help the student's designer to make the right decision on the wing sweep angle:

1. **Variable sweep:** If the aircraft needs to have different sweep angles at various flight conditions, an ideal option is to select the variable sweep wing. This is an ideal objective from few design aspects, but on the other hand, it generates design problems. The example is a fighter aircraft that spends the vast majority of its flight time at subsonic speeds, using its supersonic capability for short ‘supersonic dashes”, depending on its mission.

   A variable-sweep wing is a wing that may be swept back and then returned to its original position during flight. It allows the wing's geometry to be modified in flight. Typically, a swept wing is more suitable for high speeds (e.g. cruise), while an unswept wing is suitable for lower speeds (e.g. take- off and landing), allowing the aircraft to carry more fuel and payload, as well as improving field performance. A variable-sweep wing allows a pilot to select the exact wing configuration for the intended speed. The variable-sweep wing is most useful for those aircraft that are expected to function at both low and high speed, thus it has been used primarily in fighters.

   A number of successful designs (with variable-sweep); such as Bell X-5, Grumman F-14 Tomcat, General Dynamics F-111, Rockwell supersonic Bomber B-1B, Mikoyan Mig-23, Panavia Tornado, and Sukhoi Su-27; were introduced from the 1940s through the 1970s. However, the recent advances in flight control technology and structural materials have allowed designers to closely tailor the aerodynamics and structure of aircraft, removing the need for variable geometry to achieve the required performance. Aerodynamically, the exact sweep angle will generate the lowest possible drag while produce the highest possible lift and control. The drawback is the loose structural integrity as well as the sweep angle control mechanism problem (manual or automatic). The last variable-sweep wing military aircraft to date was the Soviet Tu-160 "Blackjack", which first flew in 1980.

2. **Wing-fuselage interference:**

It is at the wing root that the straight fuselage sides more seriously degrade the sweep effect by interfering with the curved flow of Figure 2.24. Wing airfoils are often modified near the root to change the basic pressure distribution to compensate for the distortion to the swept wing flow. Since the fuselage effect is to increase the effective airfoil camber, the modification is to reduce the root airfoil camber and in some cases to use negative camber. The influence of the fuselage then changes the altered root airfoil pressure back to the desired positive camber pressure distribution existing farther out along the wing span. This same swept wing root compensation can be achieved by adjusting the fuselage shape to match the natural swept wing streamlines. This imposes serious manufacturing burdens and passenger cabin arrangement problems. Thus, the airfoil approach is more preferred for transport aircraft. Instead, the employment of large fillet or even fuselage shape variation is appropriate for fighter aircraft.

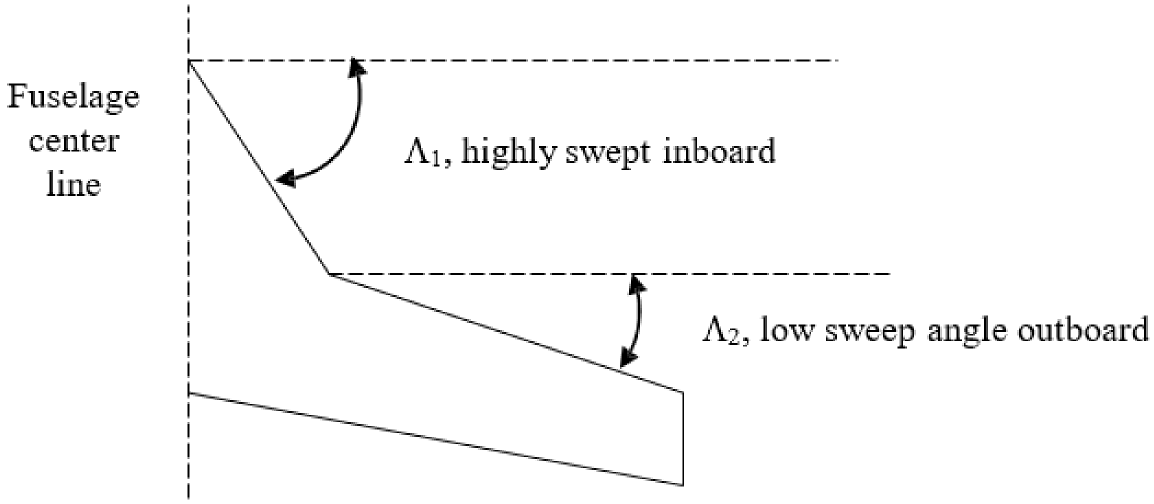

Figure 2.30: Top view of a wing with two sweep angels

3. **Non-constant sweep:** In some cases, one sweep angle cannot satisfy all design requirements. For instance, a very high sweep angle wing satisfies the high-speed cruise requirements, however, at low subsonic speed, the aircraft is not satisfactorily controllable or laterally stable. One solution is to divide the wing sections into inboard plane, and outboard plane; each having different sweep angles (see figure 2.30). The supersonic transport aircraft Concorde and Space Shuttle have such feature.

4. **Control surfaces:** The sweep angel will influence the performance of high lift device (such as flap) as well as control surfaces (such as ailerons). In practice, since both high lift device and control surface have to have sweep angles (with slightly different values); their lifting forces will be spoiled. Consequently, the high lift device's contribution to generate lift at low speed will be reduced. With the same logic, it can be shown that the aileron will also produce less lateral control. To compensate for these shortcomings, both control surface and high lift device must have slightly larger areas.

5. **Spar:** When the wing has a sweep angle, the wing spar can no longer be one piece, since two wing sections (left and right) have opposite sweep angles. This is assumed to be a disadvantage of sweep angle, since the wing structural integrity will be negatively influenced. This adds to the complexity of the wing manufacturing as well.

6. **Effective span (b_{eff}) and Effective Aspect Ratio (AR_{eff}):** With the presence of the sweep angle, the wing span (b) will have slightly different meaning, so the new parameter of effective span (b_{eff}) is introduced. When the 50 percent chord line sweep angle is not zero, the wing span will be greater than wing effective span. Wing span in a straight wing is basically defined as the distance between two

wing tips parallel to aircraft the lateral axis (y-axis). However, in a swept wing, wing span is defined as twice the distance between one wing tip to fuselage center line parallel to 50 percent sweep chord line. Thus, the effective wing span in a swept wing is defined as the distance between wing tips parallel to aircraft lateral axis (y- axis). Figure 2.31 depicts the difference between span and effective span. This indicates that wing sweep angle alters the wing span to effective span which is smaller.

$$\mathbf{AR_{eff}} = \frac{b_{eff}^2}{S} \qquad 2.23$$

The technique to determine effective span is based on the laws of triangle. The application of the technique is illustrated in the examples 2.1 and 2.2.

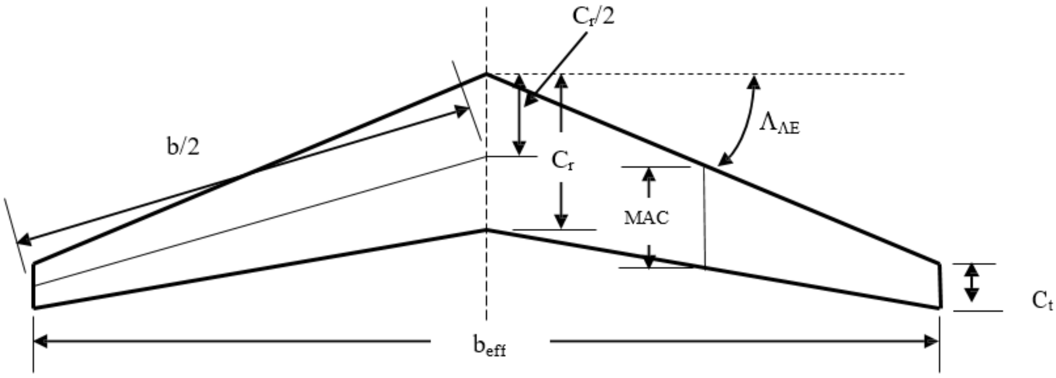

Figure 2.31 Effective wing span in a swept wing

Example 2.1

An aircraft has a wing area of S = 20 m^2, aspect ratio AR = 8, and taper ratio of λ= 0.6. It is required that the 50 percent chord line sweep angle be zero. Determine tip chord, root chord, mean aerodynamic chord, and span, as well as leading edge sweep, trailing edge sweep and quarter chord sweep angles.

Solution:

To determine the unknown variables, we first employ the following equations:

$$AR = \frac{b^2}{S} \rightarrow b = \sqrt{S.AR} = \sqrt{20 \times 8} \rightarrow b = 12.65\ m$$

$$AR = \frac{b}{\bar{C}} \rightarrow \bar{C} = \frac{b}{AR} = \frac{12.65}{8} \rightarrow \bar{C} = 1.58\ m$$

$$\bar{C} = \frac{2}{3} C_r \left(\frac{1 + \lambda + \lambda^2}{1 + \lambda} \right) \rightarrow 1.58 = \frac{2}{3} C_r \left(\frac{1 + 0.6 + 0.6^2}{0.6} \right) \rightarrow C_r = 1.936\ m$$

$$\lambda = \frac{C_t}{C_r} \rightarrow 0.6 = \frac{C_t}{1.936} \rightarrow C_t = 1.161\ m$$

Since the 50 percent chord line sweep angle is zero ($\Lambda_{C/2} = 0$), the leading edge, trailing edge, and quarter chord sweep angel are determined using the triangle law in triangle ABC (see figure 2.32) as follows:

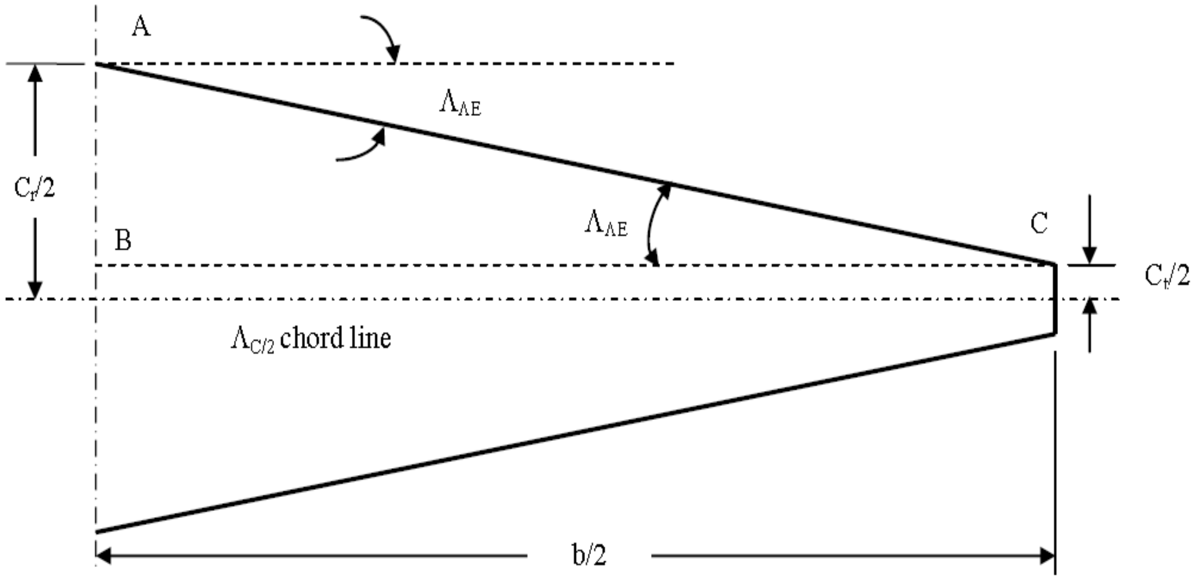

Figure 2.32: The wing of Example 5.3(λ and angles are exaggerated)

$$\tan(\Lambda_{LE}) = \frac{AB}{BC} \rightarrow \Lambda_{LE} = \tan^{-1}\left(\frac{\frac{C_r}{2} - \frac{C_t}{2}}{b/2}\right) = \tan^{-1}\left(\frac{\frac{1.936}{2} - \frac{1.161}{2}}{12.65/2}\right)$$

$$\rightarrow \Lambda_{LE} = 3.5\,\mathrm{deg}\ \ (sweep\ back)$$

The wing is straight; thus the trailing edge sweep angle would be:

$$\Lambda_{LE} = -3.5\,\mathrm{deg}\ \ (sweep\ forward)$$

The quarter chord sweep angle is determined using tangent law in a similar triangle as follows:

$$\Lambda_{C/4} = \tan^{-1}\left(\frac{\frac{C_r - C_t}{4}}{b/2}\right) = \tan^{-1}\left(\frac{\frac{1.936 - 1.161}{4}}{12.65/2}\right) \rightarrow \Lambda_{C/4} = 1.753\ deg$$

(Sweep back)

It is interesting to note that, although the wing is straight ($\Lambda_{C/2} = 0$), but the leading edge, trailing edge and quarter chord line all are swept.

Example 2.2

An aircraft has a wing area of S = 20 m^2, aspect ratio AR = 8, and taper ratio of λ = 0.6. It is required that the 50 percent chord line sweep angle be 30 degrees. Determine tip chord, root chord, mean aerodynamic chord, span, and effective span, as well as leading edge sweep, trailing edge sweep and quarter chord sweep angles.

Solution:

To determine the unknown variables, we first employ the following equations:

$$AR = \frac{b^2}{S} \rightarrow b = \sqrt{S.AR} = \sqrt{20 \times 8} \rightarrow b = 12.65\, m$$

$$AR = \frac{b}{\bar{C}} \rightarrow \bar{C} = \frac{b}{AR} = \frac{12.65}{8} \rightarrow \bar{C} = 1.58\, m$$

$$\bar{C} = \frac{2}{3} C_r \left(\frac{1+\lambda+\lambda^2}{1+\lambda}\right) \rightarrow 1.58 = \frac{2}{3} C_r \left(\frac{1+0.6+0.6^2}{0.6}\right) \rightarrow C_r = 1.936\, m$$

$$\lambda = \frac{C_t}{C_r} \rightarrow 0.6 = \frac{C_t}{1.936} \rightarrow C_t = 1.161\, m$$

Since the 50 percent chord line sweep angle is 30 degrees ($\Lambda_{C/2}$ = 30 deg), the leading edge, trailing edge, and quarter chord sweep angel are determined using the triangle law (see figure 2.33). But we first need to calculate a few parameters. In the right triangle CIF that includes 50 percent chord sweep angle ($\Lambda_{C/2}$), we can write:

$$\sin(\Lambda_{C/2}) = \frac{FI}{b/2} \rightarrow FI = \frac{12.65}{2}\sin(30) \rightarrow FI = 3.1625\, m$$

$$(CI)^2 + (FI)^2 = (CF)^2 \rightarrow (CI) = \sqrt{(CF)^2 - (FI)^2} \rightarrow \frac{b_{eff}}{2}$$

$$= \sqrt{\left(\frac{12.65}{2}\right)^2 - 3.1625^2} \rightarrow b_{eff} = 10.955\, m$$

Hence, the effective span is less than regular span. Consequently, the effective aspect ratio is reduced to:

$$AR_{eff} = \frac{b_{eff}^2}{S} = \frac{10.955}{20} \rightarrow AR_{eff} = 6$$

It is noted that the AR has been reduced from 8 to 6. The distance IH is:

$$IH = FI - \frac{C_t}{2} = 3.1625 - \frac{1.161}{2} = 2.582\, m$$

In the right triangle AKH that includes leading edge sweep angle (ΛLE), we have:

$$\tan(\Lambda_{LE}) = \frac{KH}{AK} = \frac{KI + IH}{b_{eff}/_2} = \frac{\frac{C_r}{2} + 2.582}{10.955/2} = 0.648 \rightarrow (\Lambda_{LE}) = 33\,\text{deg}(aft\ sweep)$$

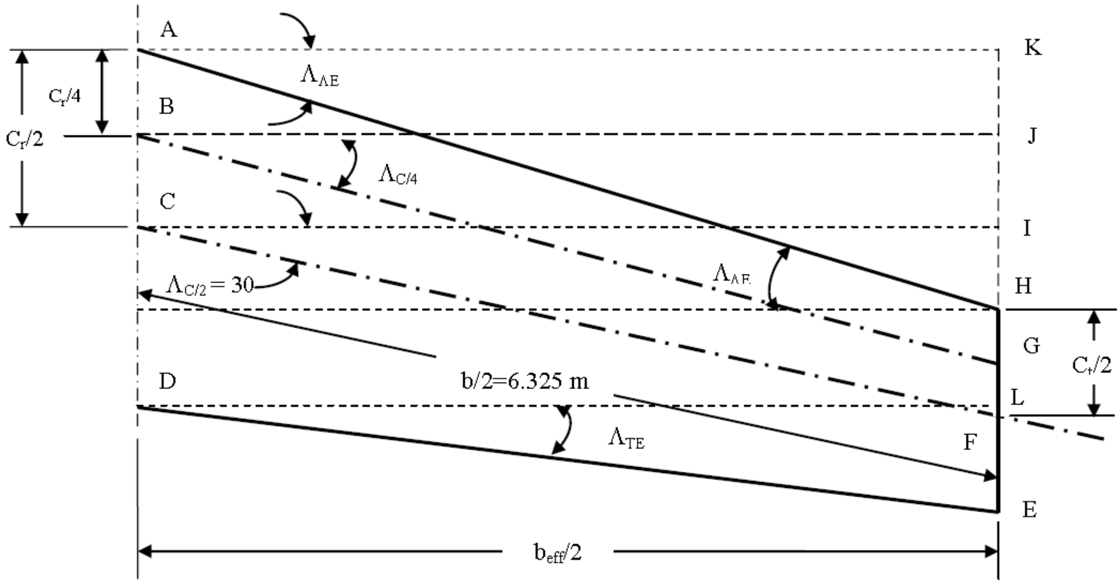

Figure 2.33 The top view of the right wing of Example 2.2

In the right triangle GJB that includes quarter chord sweep angle ($\Lambda_{C/4}$), we have:

$$\tan(\Lambda_{C/4}) = \frac{GJ}{BJ} = \frac{GH + JH}{b_{eff}/_2} = \frac{\frac{C_t}{4} + KH - KJ}{b_{eff}/2} = \frac{\frac{C_t}{4} + (KI + IH) - KJ}{b_{eff}/2}$$

$$= \frac{\frac{C_t}{4} + \left(\frac{C_r}{2} + 2.582\right) - \frac{C_r}{4}}{b_{eff}/2} = \frac{\frac{1.161}{4} + \left(\frac{1.936}{2} + 2.582\right) - \frac{1.936}{4}}{10.955/2} = 0.613$$

$$\rightarrow (\Lambda_{LE}) = 31.5\,\text{deg}\ (aft\ sweep)$$

This reveals that both leading edge sweep and quarter chord sweep angles are greater than 50 percent chord line sweep angle. Finally, in the right triangle DLE that includes trailing edge sweep angle (Λ_{TE}), we have:

$$\tan(\Lambda_{TE}) = \frac{EL}{LD} = \frac{EK + KL}{b_{eff}/_2} = \frac{EK - C_r}{b_{eff}/2} = \frac{\frac{C_t}{2} + (KI + IH) - C_r}{b_{eff}/2}$$

$$= \frac{\frac{C_t}{2} + \left(\frac{C_r}{2} + 2.582\right) - C_r}{b_{eff}/2} = \frac{\frac{1.161}{4} + \left(\frac{1.936}{2} + 2.582\right) - 1.936}{10.955/2} = 0.401$$

$$\rightarrow (\Lambda_{TE}) = 21.85\,\text{deg}\ (aft\ sweep)$$

The trailing edge sweep angel is considerably less than 50 percent chord line sweep angle.

2.10 Wings Twist Angle:

If the wing tip is at a lower incidence than the wing root, the wing is said to have negative twist or simply twist (α_t) or washout. On the other hand, if the wing tip is at a higher incidence than the wing root, the wing is said to have positive twist or wash-in. The twist is usually negative; which means the wing tip angle of attack is lower than root angle of attack as sketched in figure 2.34a. This indicates that wing angle of attack is reduced along the span. The wings on a number of modern aircraft have different airfoil sections along the span, with different values of zero lift angle of attack; this is called aerodynamic twist. The wing tip airfoil section is often thinner than root airfoil section as sketched in figure 2.34b. Sometimes, the tip and root airfoil sections have the same thickness-to-chord ratio, but the root airfoil section has higher zero-lift angle of attack (i.e. more negative) than tip airfoil section.

When the tip incidence and root incidence are not the same, the twist is referred to as *geometric twist*. However, if the tip airfoil section and root airfoil section are not the same, the twist is referred to as *aerodynamic twist*. Both types of twist have advantages and disadvantages by which the designer must establish a selection that satisfies the design requirement. The application of twist is a selection as a decision making, but the amount of twist is determined via calculations. In this section, both items will be discussed.

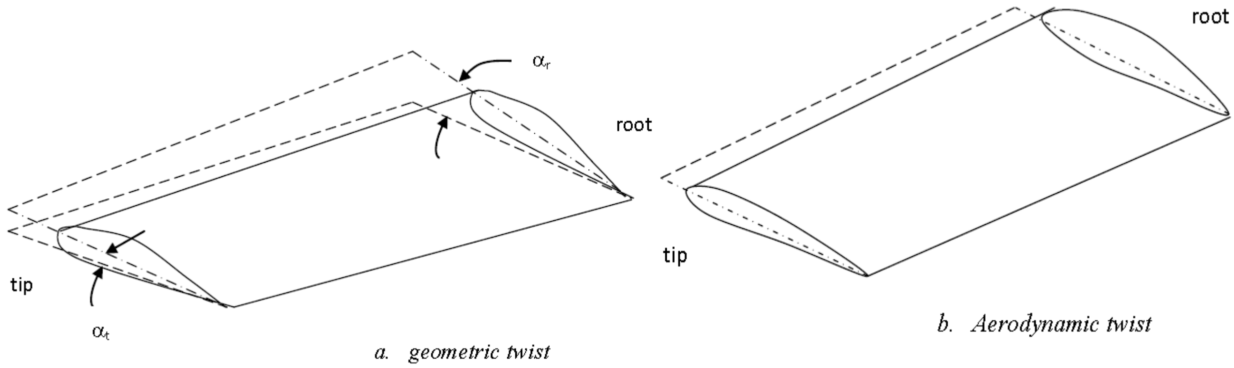

Figure 2.34: Wing twist

In practice, the application of aerodynamic twist is more convenient than the geometric twist. The reason is that in aerodynamic twist, a part of the wing has different ribs than another part, while all parts of the wing have the same incidence. The difficulty in the application of geometric twist arises from manufacturing point of view. Every portion of the wing has a unique incidence, since the angle of attack must be decreased (usually linearly) from wing setting angle; i_w (at the root) to a new value at the tip. This technique is applied by twisting the main wing spar, through which wing (rib) twist is automatically applied. The alternative solution is to divide each section of the wing (left and right) into two portions; inboard portion and outboard portion. Then, the inboard portion has the incidence equal to wing setting angle, while the outboard portion has the value such that the twist is produced. If situation allows, both geometric and aerodynamic twist may be employed. There are two major goals for the employing the twist in wing design process:

1. Avoiding tip stall before root stall.
2. Modification of lift distribution to an elliptical one.

In addition to two above-mentioned desired goals, there is another one unwanted output in twist:

3. Reduction in lift

When the wing root enters the stall before the wing tip, the pilot is able to utilize the aileron to control the aircraft, since the fair low at outboard section has not yet been stalled. This provision improves the safety of the aircraft in the advent of wing stall. The significance of the elliptical lift distribution has been described in section 2.7. The major drawback in twist is the loss of lift, since the twist is usually negative. As the angle of attack of a wing section is decreased, lift coefficient will be decreased too. The criterion and the limit for the wing twist is that the twist angle must not be such high that it results in a negative lift in the outer wing portions. Since any section has a zero-lift angle of attack (α_o), the criterion is formulated as follows:

$$|\alpha_t| + i_w \geq |\alpha_o| \qquad 2.24$$

When a portion of the outboard of the wing generates a negative lift, the overall lift is decreased. This is not desirable and must be avoided in the twist angle determination process. The typical value for the geometric twist is between -1 to - 4 degrees (i.e. negative twist). The exact value of the twist angle must be determined such that the tip stalls after root as well as the lift distribution be elliptic. Figure 2.35 illustrates the typical effect of a (negative) twist angle on the lift distribution. Table 2.4 shows twist angles for several aircraft. As noted, several aircraft such as Cessna 208, Beech 1900D, Beechjet 400A, AVRO RJ100, and Lockheed C-130 Hercules have both geometric and aerodynamic twists.

Figure 2.35: The typical effect of a (negative) twist angle on the lift distribution

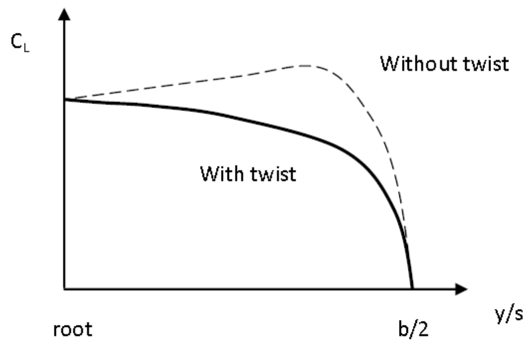

Table 2.4: Twist angles for several aircraft

a. Geometric twist

No	Aircraft	MTOW (lb)	Wing incidence at root (i_w) (deg)	Wing angle at tip (deg)	Twist (deg)
1	Fokker 50	20,800	+3.5	+1.5	-2
2	Cessna 310	4,600	+2.5	-0.5	-3
3	Cessna Citation I	11,850	+2.5	-0.5	-3
4	Beech King Air	11,800	+4.8	0	-4.8
5	Beech T-1A Jaw Hawk	16,100	+3	-3.3	-6.3
6	Beech T-34C	4,300	+4	+1	-3
7	Cessna Station Air 6	3,600	+1.5	-1.5	-3
8	Gulfstream IV	73,000	+3.5	-2	-5.5
9	Northrop-Grumman E-2C Hawkeye	55,000	+4	+1	-3
10	Piper Cheyenne	11,200	+1.5	-1	-2.5
11	Beech Super King	12,500	+ 3^o 48'	-1^o 7'	4.55'
12	Beech starship	14,900	+3	-5	-3.5
13	Cessna 208	8000	$+2^o$ 37'	-3^o 6'	-5^o 31'
14	Beech 1900D	16,950	$+3^o$ 29'	-1^o 4'	-4^o 25'
15	Beech jet 400A	16,100	+3	-3^o 30'	-6^o 30'
16	AVRO RJ100	101,500	$+3^o$ 6'	0	-3^o 6'
17	Lockheed C-130 Hercules	155,000	+3	0	-3
18	Pilatus PC-9	4,960	+1	-1	-2
19	Piper PA-28-161 Warrior	2,440	+2	-1	-3

b. Aerodynamic twist

No	Aircraft	MTOW (lb)	Root airfoil section	Tip airfoil section	$\Delta t/C$ (%)
1	Cessna 208	8000	NACA 23017.424	NACA 23012	5
2	Beech 1900D	16,950	NACA 23018	NACA 23012	6
3	Beech jet 400A	16,100	t/C = 13.2%	t/C = 11.3%	1.9
4	AVRO RJ100	101,500	t/C = 15.3%	t/C = 12.2%	3.1
5	Lockheed C-130 Hercules	155,000	NACA 64A318	NACA 64A412	6
6	Gulfstream IV-SP	74,600	t/C = 10%	t/C = 8.6%	1.4
7	Boeing 767	412,000	t/C = 15.1%	t/C = 10.3%	4.8
8	Harrier II	31,000	t/C = 11.5%	t/C = 7.5%	4
9	BAE Sea Harrier	26,200	t/C = 10%	t/C = 5%	5
10	Kawasaki T-4	12,544	t/C = 10.3%	t/C = 7.3%	3

2.11 Wings Dihedral Angle:

When you look at the front view of an aircraft, the angle between the chord-line plane of a wing with the “xy” plane is referred to as the wing dihedral (Γ). The chord line plane of the wing is an imaginary plane that is generated by connecting all chord lines across span. If the wing tip is higher than the xy plane, the angle is called positive dihedral or simply dihedral, but when the wing tip is lower than the xy plane, the angle is called negative dihedral or Anhedral (see figure 2.36). For the purpose of aircraft symmetricity, both right and left sections of a wing must have the same dihedral angle. There are several advantages and disadvantages for dihedral angle. In this section, these characteristics are introduced, followed by the design recommendations to determine the dihedral angle.

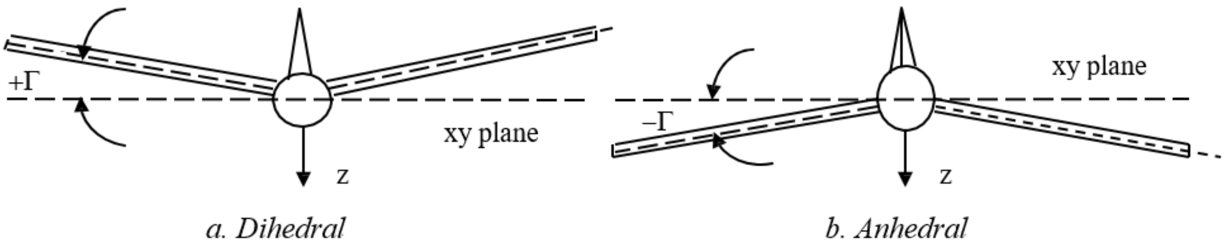

Figure 2.36. Dihedral, Anhedral (aircraft front view)

The primary reason of applying the wing dihedral is to improve the lateral stability of the aircraft. The lateral stability is mainly a tendency of an aircraft to return to original trim level-wing flight condition if disturbed by a gust and rolls around the x axis. In some references, it is called *dihedral stability*, since a wing dihedral angle provides the necessary restoring rolling moment. The lateral static stability in primarily represented by a stability derivative called aircraft dihedral effect ($C_{l\beta} = \frac{dC_l}{d\beta}$) that is the change in aircraft rolling moment coefficient due to a change in aircraft sideslip angle (β).

Observe a level-wing aircraft that has experienced a disturbance (see figure 2.37) which has produced an undesired rolling moment (e.g. a gust under one side of the wing). When the aircraft rolls, one side of the wing (say left) goes up, while other side (say right) goes down. This is called a positive roll. The right-wing section that has dropped has temporally lost a few percentage of its lift. Consequently, the aircraft will accelerate and slip down toward the right wing which produces a sideslip angle (β). This is equivalent to a wing approaching from the right of the aircraft, the sideslip angle is positive. In response, a laterally statically stable aircraft must produce a negative rolling moment to return to the original wing-level situation. This is technically translated into a negative dihedral effect ($C_{l\beta} < 0$).

The role of the wing dihedral angle is to induce a positive increase in angle of attack ($\Delta\alpha$). This function of the wing dihedral angle is done by producing a normal velocity ($V_n = V\Gamma$).

$$\Delta\alpha \approx V\Gamma / U \approx U\beta\Gamma / U \approx \beta\Gamma \qquad 2.25$$

where U is the airspeed component along x-axis, and V is the airspeed component along y-axis. It is this increment in angle of attack which produces a corresponding increment in lift. This in turn results is a negative rolling moment contribution. It is interesting that the left-wing section experiences exactly the opposite effect which also results in a negative rolling moment. Therefore, the rolling moment due to sideslip due to geometric wing dihedral is proportional to the dihedral angle. Basically, a positive wing geometric dihedral causes the rolling moment due to sideslip derivative $C_{l\beta}$; to be negative. Aircraft must have a certain minimum amount of negative rolling moment due to sideslip; dihedral effect. This is needed to prevent excessive spiral instability. Too much dihedral effect tends to lower Dutch roll damping. More negative $C_{l\beta}$ means more spiral stability, but at the same time, less dutch-roll stability.

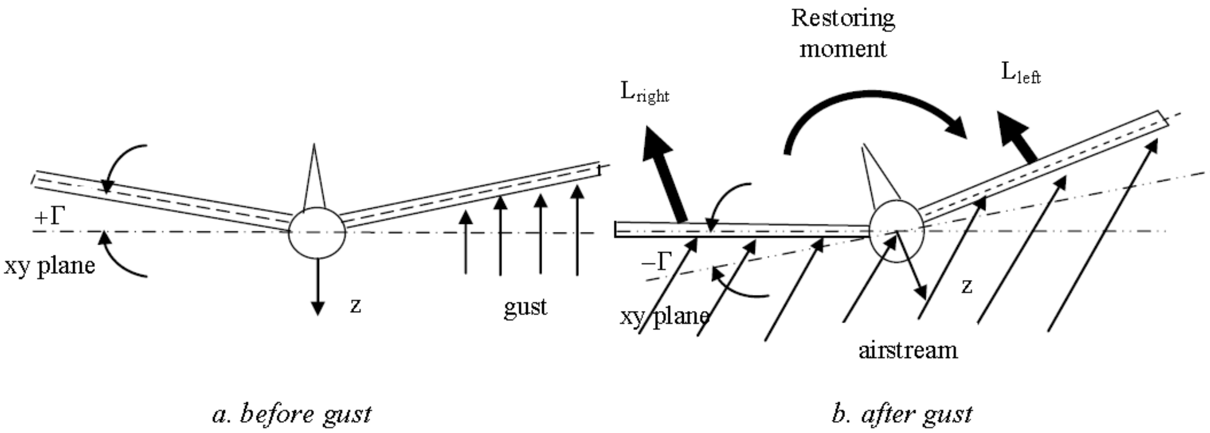

Figure 2.37: The effect of dihedral angle on a disturbance in roll (aircraft front view)

The Anhedral has exactly the opposite function. In another word, the Anhedral is laterally destabilizing. The reason for using Anhedral in some configuration is to balance between the roles of wing parameters (such as sweep angle and wing vertical position) in lateral stability. The reason is that, the more laterally stable aircraft means the less rolling controllable aircraft. In the wing design, one must be careful to determine the wing parameters such that satisfy both stability and controllability requirements. Since the primary reason for the wing dihedral angle is the lateral stability, but wing sweep angles and wing vertical position are driven by not only lateral stability, but also performance requirements, and operational requirements.

For instance, a cargo aircraft has usually a high wing to satisfy the loading and unloading operational requirements. The high wing contribution to lateral stability is highly positive, that means the aircraft is laterally stable more than necessary. In order to make the aircraft less laterally stable, one of the designer’s option is to add an Anhedral to the wing. This decision does not alter the operational characteristics of the aircraft, but improve the rolling controllability of the aircraft. In general, high wing aircraft have inherent dihedral effect while low wing aircraft tend to be deficient in inherent dihedral effect; $C_{l\beta}$. For this reason, low wing aircraft tend to have considerably greater dihedral angle than high wing aircraft. On the other hand, swept wing aircraft tend to have too much dihedral effect; $C_{l\beta}$ due to sweep angle. This can be offset in high wing aircraft by giving the wing negative dihedral (i.e. Anhedral). The balance between lateral stability and roll control is a major criterion for the determination of dihedral angle.

Another effect of wing dihedral effect is to alter the ground and water clearance, since aircraft wings, nacelles and propellers must have a minimum amount of ground and water clearance. It is clear that dihedral would increase ground and water clearance, while Anhedral would decrease ground and water clearance. In aircraft with high aspect ratio and highly elastic wings (such as record breaker Voyager) the elastic deformation of the wing in flight generates extra dihedral angle. This must be considered in the wing design of such aircraft.

When the dihedral angle is applied on a wing, the wing effective planform area (S_{eff}) is reduced. This in turn will reduce the lift generated by the wing without dihedral, which is undesirable. If you need to apply the dihedral angle to a wing, consider the lowest value for the dihedral to minimize the lift reduction. The effective wing planform area as a function of dihedral angle is determined as follows:

$$S_{eff} = S_{ref}\cos(\Gamma) \qquad 2.26$$

Table 2.5 illustrates dihedral (and Anhedral) angles for several aircraft along with their wing vertical position. As noted, the typical dihedral angle is a value between -15 to +10 degrees. Table 2.6 shows typical values of dihedral angle for swept or unswept wings of various wing vertical positions. This table is a recommended reference for the starting point. You can select an initial value for the dihedral angle from this table. However, the exact value of the dihedral angle is determined during the stability and control analysis of whole aircraft. When other aircraft components (e.g. fuselage, tail) are designed, evaluate the lateral stability of the whole aircraft.

Table 2.5: Dihedral (or Anhedral) angles for several aircraft

No	Aircraft	Type	Wing position	Dihedral (deg)
1	Pilatus PC-9	Turboprop Trainer	Low-wing	7 (outboard)
2	MD-11	Jet Transport	Low-wing	6
3	Cessna 750 Citation X	Business Jet	Low-wing	3
4	Kawasaki T-4	Jet Trainer	High-wing	-7
5	Boeing 767	Jet Transport	Low-wing	4^{o} 15'
6	Falcon 900 B	Business Jet Transport	Low-wing	0^{o} 30'
7	C-130 Hercules	Turboprop Cargo	High-wing	2^{o} 30'
8	Antonov An-74	Jet STOL Transport	Parasol-wing	-10
9	Cessna 208	Piston Engine GA	High-wing	3
10	Boeing 747	Jet Transport	Low-wing	7
11	Airbus 310	Jet Transport	Low-wing	11^{o} 8'

12	F-16 Fighting Falcon	Fighter	Mid-wing	0
13	BAE Sea Harrier	V/STOL Fighter	High-wing	-12
14	MD/BAe Harrier II	V/STOL Close Support	High-wing	-14.6
15	F-15J Eagle	Fighter	High-wing	-2.4
16	Fairchild SA227	Turboprop Commuter	Low-wing	4.7
17	Fokker 50	Turboprop Transport	High-wing	3.5
18	AVRO RJ	Jet Transport	High-wing	-3
19	MIG-29	Fighter	Mid-wing	-2

The suggested value for aircraft dihedral effect ($C_{l\beta}$) to have an acceptable lateral controllability and lateral stability is a value between -0.1 to +0.4 1/rad. Then you can adjust the dihedral angle to satisfy all design requirements. If one dihedral angle for whole wing does not satisfy all design requirements, you may divide the wing into inboard and outboard sections; each with different dihedral angle. For instance, you may apply dihedral angle to the outboard plane, in order to keep the wing level in the inboard plane.

Table 2.6: Typical values of dihedral angle for various wing configurations

No	Wing	Low wing	Mid-wing	High wing	Parasol wing
1	Unswept	5 to 10	3 to 6	-4 to -10	-5 to -12
2	Low subsonic swept	2 to 5	-3 to +3	-3 to -6	-4 to -8
3	High subsonic swept	3 to 8	-4 to +2	-5 to -10	-6 to -12
4	Supersonic swept	0 to -3	1 to -4	0 to -5	NA
5	Hypersonic swept	1 to 0	0 to -1	-1 to -2	NA

2.12 High Lift Device:

2.12.1. The Functions of High Lift Device

One of the design goals in wing design is to maximize the capability of the wing in the generation of the lift. This design objective is technically shown as maximum lift coefficient (C_{Lmax}). In a trimmed cruising flight, the lift is equal to weight. When the aircraft generates its maximum lift coefficient, the airspeed is referred to as stall speed.

$$L = W = \frac{1}{2}\rho V_s^2 S C_{Lmax} = mg \qquad 2.27$$

Two design objectives among the list of objectives are:
1. maximizing the payload weight,
2. minimizing the stall speed (Vs).

As the equation 2.27 indicates, increasing the C_{Lmax} tends to increase the payload weight (W) and decrease the stall speed. The lower stall speed is desirable since a safe take-off and landing requires a lower stall speed. On the other hand, the higher payload weight will increase the efficiency of the aircraft and reduce the cost of flight. A higher C_{Lmax} allows the aircraft to have

a smaller wing area that results in a lighter wing. Hence, in a wing design, the designer must find way to maximize the C_{Lmax}. In order to increase the lift coefficient, the only in-flight method is to temporarily vary (increase) the wing camber. This will happen only when the high lift device is deflected downward. In 1970's the maximum lift coefficient at take-off was 2.8; while the record currently belongs to Airbus A-320 with a magnitude of 3.2.
The primary applications of high lift devices are during take-off and landing operations. Since the airspeed is very low compared with cruising speed, the wing must produce more lift coefficient. The aircraft speed during take-off and landing is slightly greater than stall speed. Airworthiness standards specify the relationship between take-off speed and landing speed with stall speed. As a general rule, we have:

$$V_{TO} = k.V_s \qquad 2.28$$

where k is about 1.1 for fighter aircraft, and about 1.2 for jet transports and GA aircraft.
The application of the high lift device tends to change the airfoil section's and wing's camber (in fact the camber will be positively increased). This in turn will change the pressure distribution along the wing chord as sketched in figure 2.38. In this figure, C_P denotes the pressure coefficient. In contrast, the leading edge high lift device tends to improve the boundary layer energy of the wing. Some type of high lift device has been used on almost every aircraft designed since the early 1930s. High lift devices are the means to obtain the sufficient increase in C_{Lmax}. At the airfoil level, a high lift device deflection tends to cause the following six changes in the airfoil features:

1. Lift coefficient (C_l) is increased,
2. Maximum lift coefficient (C_{lmax}) is increased,
3. Zero-lift angle of attack (α_o) in changed,
4. Stall angle (α_s) is changed,
5. Pitching moment coefficient is changed.
6. Drag coefficient is increased.
7. Lift curve slope is increased.

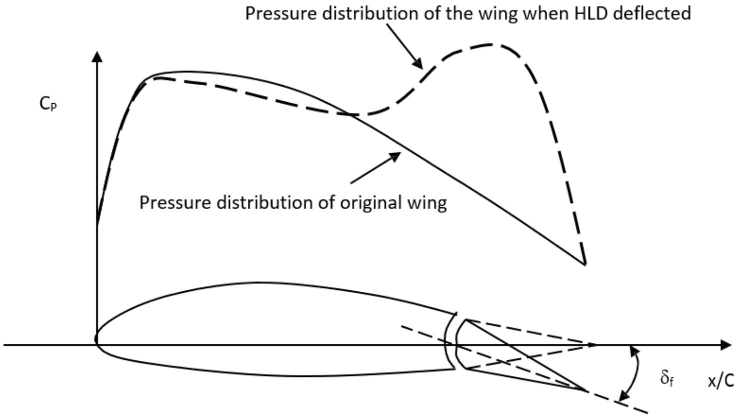

Figure 2.38: Example of pressure distribution with the application of a high lift device

These effects are illustrated in figure 2.39. Along with three desirable advantages (first two items) to the application of high lift devices; there are a few negative side-effects (the last five items) as well. A plain flap tends to decrease stall angle, while a slotted flap and leading- edge slat tend to increase the stall angle. In addition, among all types of flaps, the Fowler flap and leading-edge slat tend to increase the lift curve slope ($C_{L\alpha}$). On the other hand, leading edge flap tend to increase (shift to the right) the zero-lift angle of attack (α_o).

A reduction in stall angle is undesirable, since the wing may stall at a lower angle of attack. During the take-off and landing operation, a high angle of attack is required to successfully take-off and land. The high angle of attack will also tend to reduce the take-off run and landing run that is desirable in the airport at which have a limited runway length. An increase in pitching moment coefficient requires higher horizontal tail area to balance the aircraft. An increase in drag coefficient decreases the acceleration during take-off and landing. Although the application of high lift device generates three undesirable side effects, but the advantages outweigh the disadvantages.
If the natural value of C_{Lmax} for an aircraft is not high enough for safe take-off and landing, it can be temporarily increased by mechanical high lift devices. Thus, employing the same airfoil section; one is able to increase C_{Lmax} temporarily as needed without actually pitching the aircraft. Two flight operations at which the C_{Lmax} needs to be increased are take-off and landing. Table 2.7 shows the maximum lift coefficient for several aircraft at take-off and landing configurations.

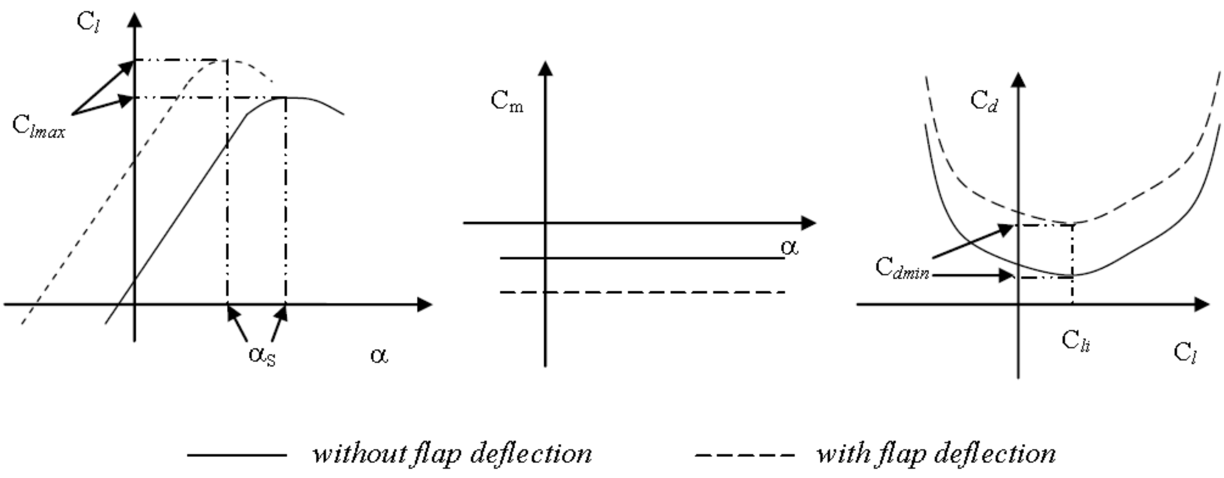

Figure 2.39: Typical effects of high lift device on wing airfoil section features

In a cruising flight, there is no need to utilize the maximum lift coefficient since the speed is high. These mechanical devices are referred to as High Lift

Devices (HLD). High Lift Devices are parts of wings to increase the lift when deflected down. They are located at inboard section of the wing and usually employed during take-off and landing.

Table 2.7: Maximum lift coefficient for several aircraft

C_{Lmax}	Cessna 172	Piper Cherokee	Short Skyvan 3	Gulfstream II	DC-9	Boeing 727	Airbus 300	Learjet 25
Take-Off	1.5	1.3	2.07	1.4	1.9	2.35	2.7	1.37
Landing	2.1	1.74	2.71	1.8	2.4	2.75	3	1.37

2.12.2. High Lift Device Classification

Two main groups of high lift devices are:
1. leading edge high lift device (LEHLD), and
2. trailing edge high lift devices (TEHLD or flap).

There are many types of wing trailing edge flaps that the most common of them are split flap, plain flap, single-slotted flap, double-slotted flap, triple-slotted flap, and fowler flap as illustrated in figure 2.40a. They are all deflected downward to increase the camber of the wing, so C_{Lmax} will be increased. The most common of leading edge devices are leading edge flap, leading edge slat, and Kruger flap as shown by in figure 2.40b. A common problem with the application of high lift devices is how to deal with the gap between high lift device and the main wing. This gap can be either sealed or left untouched. In both cases, there are undesirable side effects. If the gap left open, the airflow from downside escapes to the upper surface which in turn degrades the pressure distribution. On the other hand, if the gap is sealed by a means such diaphragm, it may be blocked by ice during flight into colder humid air. In both cases, it needs special attention as an operational problem. In the following, the technical features of various high lift devices are discussed.

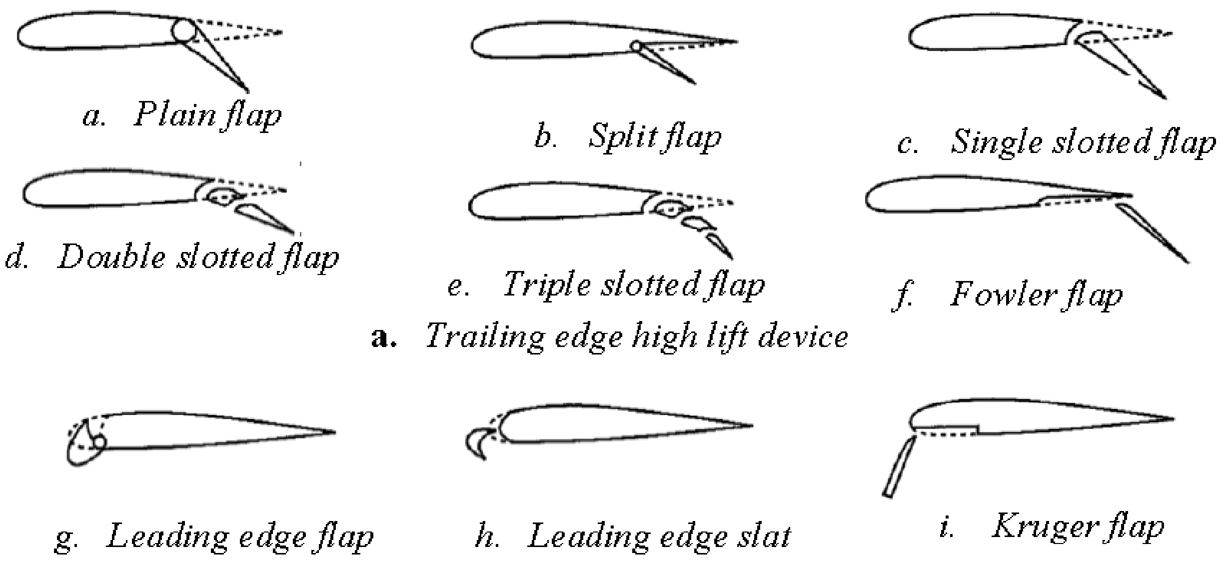

b. *Leading edge high lift device*

Figure 2.40 Various types of high lift devices

1. The *plain flap* (figure 2.40-a) is the simplest and earliest type of high lift device. It is an airfoil shape that is hinged at the wing trailing edge such that it can be rotated downward and upward. However, the downward deflection is considered only. A plain flap increases the lift simply by mechanically increasing the effective camber of the wing section. In terms of cost, a plain flap is the cheapest high lift device. In terms of manufacturing, the plain flap is the easiest one to build. Most home build aircraft and many General Aviation aircraft are employing the plain flap. The increment in lift coefficient for a plain flap at 60^o degrees of deflection (full extension) is about 0.9. If it is deflected at a lower rate, the C_L increment will be lower. Some old GA aircraft such as Piper 23 Aztec D has a plain flap. It is interesting to know that the modern fighters such aircraft F-15E Eagle and MIG-29 also employ plain flaps.

2. In the *split flap* (figure 2.40-b), only the bottom surface of the flap is hinged so that it can be rotated downward. The split flap performs almost the same function as a plain flap. However, the split flap produces more drag and less change in the pitching moment compared to a plain flap. The split flap was invented by Orville Wright in 1920, and it was employed, because of its simplicity, on many of the 1930s and 1950s aircraft. However, because of the higher drag associated with split flap, they are rarely used on modern aircraft.

3. The *single slotted flap* (figure 2.40-c) is very similar to a plain flap, except it has two modifications. First, the leading edges of these two trailing edge flaps are different. The leading edge of a single slotted flap is carefully designed such that it modifies and stabilizes the boundary layer over the top surface of the wing. A low pressure is created on the leading edge that allows a new boundary layer to form over the flap which in turn causes the flow to remain attached to very high flap deflection. The second modification is to allow the flap move rearward during the deflection (i.e. the slot). The aft movement of single slotted flap actually increases the effective chord of the wing which in turn increases the effective wing planform area. The larger wing planform area naturally generated more lift.
Thus, a single slotted flap generates considerably higher lift than a plain and split flap. The main disadvantage is the higher cost and the higher degree of complexity in the manufacturing process associated with the single slotted flap. Single slotted flap is in common use on modern light, general aviation aircraft. In general, the stall angle is increased by the application of the slotted flap. Several modern GA light aircraft such as Beech Bonanza F33A and several turboprop transport aircraft such as Beech 1900D and Saab 2000 has deployed single slotted flap.

4. The *double slotted flap* is similar to a single slotted flap, except it has two slots; I.e. the flap is divided into two segments, each with a slot as sketched in figure 2.40-d. A flap with two slots almost doubles the advantages of a single slotted flap. This benefit is achieved at the cost of increased mechanical complexity and higher cost. Most modern turboprop transport aircraft such as ATR-42; and several jet aircraft such as trainer Kawasaki T-4 employ the double slotted flap. The jet transport aircraft Boeing 767 has single slotted outboard flap and double slotted inboard flap. It is a common practice to deflect the first segment (slot) of the flap during a take-off operation, but employs full deflection (both segments) during landing. The reason is that more lift coefficient is needed during a landing that a take-off.

5. A *triple slotted flap* (figure 2.40-e) is an extension to a double slotted flap; i.e. has three slots. This flap is mechanically the most complex; and costly most expensive flap in design and operation. However, a triple slotted flap produces the highest increment in lift coefficient. It is mainly used in heavy weight transport aircraft which have high wing loading. The jet transport aircraft Boeing 747 has employed the triple slotted flap.

6. A *Fowler flap* (figure 2.40-f) has a special mechanism such that when deployed, not only deflects downward, but also translates or tracks to the trailing edge of the wing. The second feature increases the exposed wing area; which means a further increase in lift. Because of this benefit, the concept of the Fowler flap may be combined with the double slotted and triple slotted flaps. For instance, jet transport aircraft Boeing B-747 has utilized triple slotted Fowler flap. In general, the wing lift curve slope is slightly increased by the application of the Fowler flap. Maritime patrol aircraft Lockheed Orion P-3 with 4 turboprop engines has a Fowler engine.

7. A *leading edge flap (or droop)* in illustrated in figure 2.40-g. This flap is similar to trailing edge plain flap, except it is installed at the leading edge of the wing. Hence, the leading-edge pivots downward, increasing the effective camber. A feature of the leading-edge flap is that the gap between the flap and main wing body is sealed with no slot. In general, the wing zero-lift angle of attack is shifted to the right by the application of leading edge flap. Since the leading-edge flap has a lower chord compared with the trailing edge flaps, it generates a lower increment in lift coefficient (ΔC_L is about 0.3).

8. The *leading-edge slat* (see figure 2.40-h) is a small, highly cambered section, located slightly forward of the leading edge the wing body. When deflected, a slat is basically a flap at the leading edge, but with an unsealed gap between the flap and the leading edge. In addition to the primary airflow over the wing, there is a secondary flow that takes place through the gap between the slat and the wing leading edge. The function of a leading-edge slat is primarily to modify the pressure distribution over the top surface of the wing. The slat itself, being highly cambered, experiences a much lower pressure over its top surface; but the flow interaction results in a higher pressure over the top surface of the main wing body. Thus, it delays flow separation over the wing and mitigates to some extent the

otherwise strong adverse pressure gradient that would exist over the main wing section.
By such process, the lift coefficient is increased with no significant increase in drag. Since the leading-edge slat has a lower chord compared with the trailing edge flaps, it generates a lower increment in lift coefficient (ΔC_L is about 0.2). Several modern jet aircraft such as two seat fighter aircraft Dassault Rafale, Eurofighter 2000, Bombardier BD 701 Global Express, McDonnell Douglas MD-88, and Airbus A-330 have leading edge slat. In general, the wing lift curve slope is slightly increased by the application of leading edge slat.

Table 2.8. Lift coefficient increment by various types of high lift devices (when deflected 60 degrees)

No	High lift device	ΔC_L
1	Plain flap	0.7-0.9
2	Split flap	0.7-0.9
3	Fowler flap	1-1.3
4	Slotted flap	1.3 C_f/C
5	Double slotted flap	1.6 C_f/C
6	Triple slotted flap	1.9 C_f/C
7	Leading edge flap	0.2-0.3
8	Leading edge slat	0.3-0.4
9	Kruger flap	0.3-0.4

9. A *Kruger flap* is demonstrated in figure 2.40-i. This leading edge high lift device is essentially a leading-edge slat which is thinner, and which lies flush with the bottom surface of the wing when not deflected. Therefore, it is suitable for use with thinner wing sections. The most effective method used on all large transport aircraft is the leading-edge slat. A variant on the leading-edge slat is a variable camber slotted Kruger flap used on the Boeing 747. Aerodynamically, this is a slat, but mechanically it is a Kruger flap.
As a general comparison, table 2.8 shows the typical values of maximum wing lift coefficient for various types of high lift devices. In this table, the symbol C_f/C denotes the ratio between the chord of high lift device to the chord of the main wing body as shown in figure 2.41. Table 2.9 demonstrates various features for high lift devices of several aircraft.

2.12.3. Design Technique:

In designing the high lift device for a wing, the following items must be determined:
1. High lift device location along the span
2. The type of high lift device (among the list in figure 2.40)
3. High lift device chord (C_f)
4. High lift device span (b_f)

5. High lift device maximum deflection (down) (δ_{fmax})
The last three parameters are sketched in figure 2.41. The first and second item must be selected through an evaluation and analysis technique considering all advantages and disadvantages of each option regarding design requirements. However, the last three parameters must be determined through a series of calculations. In the following, the design technique for high lift device to determine the above five items will be presented.

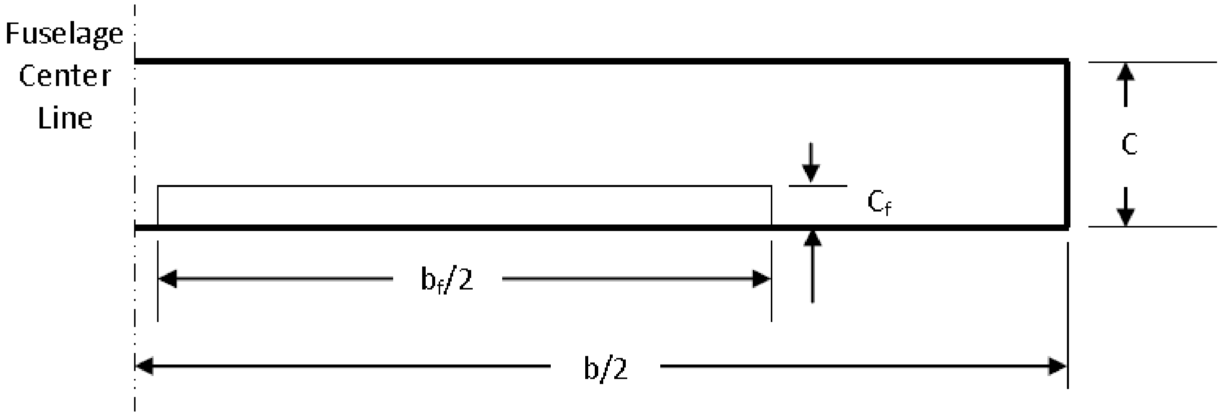

a. Top-view of the right wing

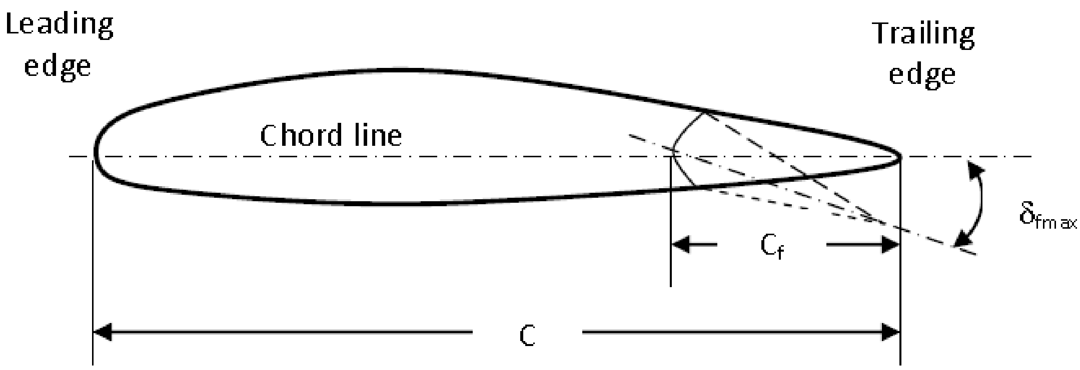

b. The side-view of the inboard wing (flap deflected)

Figure 2.41 High lift device parameters

a. HLD Location

The best location for high lift device is the inboard portion of both left and right of the wing sections. When high lift device is applied symmetrically on the left and right-wing sections, it will prevent any rolling moment; hence the aircraft will remain laterally trimmed. The deflection of high lift device will increase the lift on both inboard sections, but since they are generated symmetrically, both lift increments will cancel each other's rolling moments.
There are two reasons for the selection of inboard section. First of all, it produces a lower bending moment on the wing root. This makes the wing structure lighter and causes less fatigue on the wing in the long run. The second reason is that it

allows the aileron to have a large arm, which is employed on the outboard wing trailing edge. The larger arm for the aileron, when installed on the outboard panels, means the higher lateral control and a faster roll.

b. Type of High Lift Device

The options for the high lift device are introduced in Section 2.12.2. Several design requirements will affect the decision on the type of high lift device. They include, but not limited to:

1. Performance requirements (i.e. the required lift coefficient (ΔC_L) increment during take-off and landing);
2. Cost considerations;
3. Manufacturing limitations;
4. Operational requirements;
5. Safety considerations;
6. Control requirements. The following guideline will help the designer to make the right decision.

The final decision is the outcome of a compromise among all options using a table including the weighted design requirements. For a homebuilt aircraft designer, the low cost is the number one priority, while for a fighter aircraft designer the performance is the first priority. A large transport passenger aircraft designer, believe that the airworthiness must be on the top of the list of priorities.

The following are several guidelines that relate the high lift device options to the design requirements:

1. A more powerful high lift device (higher ΔC_L) is usually more expensive. For instance, a double slotted flap is more expensive than a split flap.

2. A more powerful high lift device (higher ΔC_L) is usually more complex to build. For example, a triple slotted flap is more complex in manufacturing than a single slotted flap.

3. A more powerful high lift device (higher ΔC_L) is usually heavier. For instance, a double slotted flap is heavier than a single slotted flap.

4. The more powerful high lift device (higher ΔC_L), results in a smaller wing area.

5. The more powerful high lift device (higher ΔC_L), results in a slower stall speed, which consequently means a safer flight.

6. A heavier aircraft requires a more powerful high lift device (higher ΔC_L).

7. A more powerful high lift device results in a shorter runway length during take-off and landing.

8. A more powerful high lift device (higher ΔC_L) allows a more powerful aileron.

9. A simple high lift device requires a simpler mechanism to operate (deflect or retract) compared with a more complex high lift device such as a triple slotted flap.

All large aircraft use some forms of slotted flap. The drag and lift of slotted flaps depend on the shape and dimensions of the vanes and flaps, their relative position,

and the slot geometry. Mounting hinges and structure may seriously degrade flap performance if not carefully designed to minimize flow separation. Typical examples are McDonnell Douglas DC-8 original flap hinges and the McDonnell Douglas DC-9 original slat design, both of which were redesigned during the flight test stage to obtain the required C_{Lmx} and low drag.
The triple slotted flap is almost the ultimate in mechanical complexity. For this reason, in the interest of lower design and production cost, some recent aircraft designs have returned to simpler mechanism. For example, the Boeing 767 has single slotted outboard flap and double slotted inboard flap.
Leading edge high lift devices such as slats functions very differently compared with trailing edge high lift devices. The lift coefficient at a given angle of attack is increased very little, but the stall angle is greatly increased. One disadvantage of slats is that the aircraft must be designed to fly at a high angle of attack for take-off and landing to utilize the high available lift increment. This clearly affects the design of the windshield, because of the pilot visibility requirements. Despite disadvantages of slats, they are so powerful in high lift that high speed transport aircraft designed since about 1964 use some form of slats in addition to trailing edge flaps. If leading edge devices serve simply to shorten take-off and/or landing runway lengths below the required values and wing area cannot be reduced (say because of fuel tank requirement), the weight and complexity due to the application of leading edge device ate not justified.
Leading edge devices intended to substantially raise the C_{Lmax} must extend along the entire leading edge except for a small cutout near the fuselage to trigger the inboard stall. Some designs utilize a less powerful device, such as Kruger flap, on the inboard part of the wing to ensure inboard initial stall. Table 5.16 illustrates the type of the high lift device for several aircraft.

c. HLD Span

The spanwise extent of high lift devices depends on the amount of span required for ailerons. In general, the outer limit of the flap is at the spanwise station where the aileron begins. The exact span needed for aileron depend on aircraft lateral controllability requirements. Low speed GA aircraft utilize about 30 percent of the total semi-span for aileron. This means that flaps can start at the side of the fuselage and extent to the 70 percent semi-span station. In large transport aircraft, a small inboard aileron is often provided for gentle maneuver at high speeds, and this serves to reduce the effective span of the flaps. However, in fighter aircraft which are highly maneuverable, aileron requires all wing span stations, so there is theoretically no space for flap. This leads to the idea of flaperon that serves as an aileron as well as a flap. The high lift device span is usually introduced as the ratio to the wing span (i.e. b_f/b). In some references, bf/b refers to the ratio between flap span to net wing span (i.e. from root to tip, not from center line to tip).

Table 2.9 illustrates the ratio of the high lift device span to the wing span for several aircraft. As an initial value, it is recommended to allocate 70 percent of the wing span to the high lift device. The exact value must be determined through the calculation of lift increment due to this span (b_f) for high lift device. There are several aerodynamic tools to accomplish this

When the low cost is the number one priority, select the least expensive high lift device that is the plain flap. If the performance is the number one priority, select the high lift device that satisfies the performance requirements. If only one high lift device such as a single slotted flap does not satisfy the performance requirements, add another high lift device such as leading-edge flap to meet the design requirements. The other option is to combine two high lift devices into one new high lift device. For instance, the business jet Gulfstream IV and Dassault Falcon 900 employ single slotted Fowler flap that is a combination of the single slotted flap and the Fowler flap analysis. An aerodynamic technique called *lift line theory* will be introduced in Section 2.13. Such technique can be employed to calculate the lift increment for each high lift device span. You can then adjust the HLD span (b_f) to achieve the required lift increment. An example at the end of this chapter will illustrate the application.

d. HLD Chord

Since the high lift device is employed temporarily in a regular flight mission that is during the take-off and landing, the lease amount of wing chord must be intended for a high lift device. The wing structural integrity must be considered when allocating part of the wing chord to a high lift device. The chord of the high lift device is often introduced as the ratio to the wing chord (i.e. C_f/C). It is important to note that the deflection of a high lift device will increase the wing drag. Hence, the high lift device chord must not be that much high that the drag increment; due to its deflection; nullifies its advantages. On the other hand, as the high lift device chord is increased, the power required to deflect the device is increased. If the pilot is using the manual power to move the high lift device, the longer high lift device chord requires more pilot power. Therefore, the shorter high lift device is better in many aspects.

Another consideration about the high lift device chord is that the designer can extend the chord up to the rear spar of the wing. Since in most aircraft, rear spar is an important in the wing structural integrity, do not try to cut the rear spar in order to extend the high lift device chord. The high lift device chord and span can be interchanged in some extent. If you have to reduce the span of the high lift device, due to aileron requirements, you can increase the high lift device chord instead. The opposite is also true. If you have to reduce the chord of the high lift device, due to structural considerations, you can increase the high lift device span instead. If the wing is tapered, you may taper the flap as well. So the high lift device chord does not have a constant chord.

Table 2.9 illustrates the ratio of the high lift device chord to the wing chord (C_f/C) for several aircraft. As an initial value, it is recommended to allocate 20% of the wing chord to the high lift device. The exact value must be determined through the calculation of lift increment due to this chord for high lift device. There are several aerodynamic tools to accomplish this analysis. Such aerodynamic technique as *lift line theory* can be employed to calculate the lift increment for each high lift device chord. You can then adjust the HLD chord (C_f) to achieve the required lift increment. An example at the end of this chapter will illustrate the application.

e. HLD Maximum Deflection

Another parameter that must be determined in the design of high lift device is the amount of its deflection (δ_{fmax}). The exact value of the deflection must be determined through the calculation of lift increment due to the high lift device deflection. Table 2.9 illustrates the high lift device deflection (δ_{fmax}) for several aircraft. As an initial value, it is recommended to consider the deflection of 20 degrees during a take-off and 50 degrees for the landing. There are several aerodynamic tools to accomplish this analysis. Such aerodynamic technique as *lift line theory* can be employed to calculate the lift increment for each high lift device deflection. You can then adjust the HLD chord (Cf) to achieve the required lift increment. An example at the end of this chapter will illustrate the application.

Table 2.9 Characteristics of high lift devices for several aircraft

No	Aircraft	Engine	HLD	C_f/C	b_f/b	δ_{fma}	
						TO	Landing
1	Cessna 172	Piston	Single slotted	0.33	0.46	20	40
2	Piper Cherokee	Piston	Single slotted	0.17	0.57	25	50
3	Lake LA-250	Piston	Single slotted	0.22	0.57	25	40
4	Short Sky van 3	Turboprop	Double slotted	0.3	0.69	18	45
5	Fokker 27	Turboprop	Single slotted	0.313	0.69	16	40
6	Lockheed L-100	Turboprop	Fowler	0.3	0.7	18	36
7	Jetstream 41	Turboprop	Double slotted	0.35	0.55	24	45
8	Boeing 727	Turbofan	Triple slotted + LE flap	0.3	0.74	25	40
9	Airbus A-300	Turbofan	Double slotted + LE flap	0.32	0.82	15	35
10	Learjet 25	Turbofan	Single slotted	0.28	0.61	20	40
11	Gulfstream II	Turbofan	Fowler	0.3	0.73	20	40
12	McDonnell DC-9	Turbofan	Double slotted	0.36	0.67	15	50

13	Antonov 74	Turbofan	Double slotted + triple slotted + LE flap	0.24	0.7 25	25	40
14	McDonnell F-15E Eagle	Turbofan	Plain flap	0.25	0.3	-	-
15	Mikoyan MIG-29	Turbofan	Plain flap + LE flap	0.35	0.3 + 1	-	-
16	X-38	Rocket	Split flap	Lifting body		NA	30

In using aerodynamic techniques to calculate incremental lift due the extension of trailing edge flap, it is necessary to determine the increment in wing zero-lift angle of attack ($\Delta\alpha_o$). The following is an empirical equation that allows for such approximation:

$$\Delta\alpha_o \approx -1.15 \cdot \frac{c_f}{c} \delta_f \qquad 2.29$$

This equation provides the section's incremental zero-lift angle of attack ($\Delta\alpha_o$) as a function of flap-to-wing-chord ratio and flap deflection.

2.12.4 Aileron:

Aileron is very similar to a trailing edge plain flap except is deflected both up and down. Aileron is located at the outboard portion of the left and right sections of wing. Unlike flap, ailerons are deflected differentially, left up and right down; or left down and right up. The lateral control is applied on an aircraft through the differential motions of ailerons. Aileron design is part of wing design, but because of the importance and great amount of materials that needs to be covered on aileron design, it will be discussed in a separate chapter later.

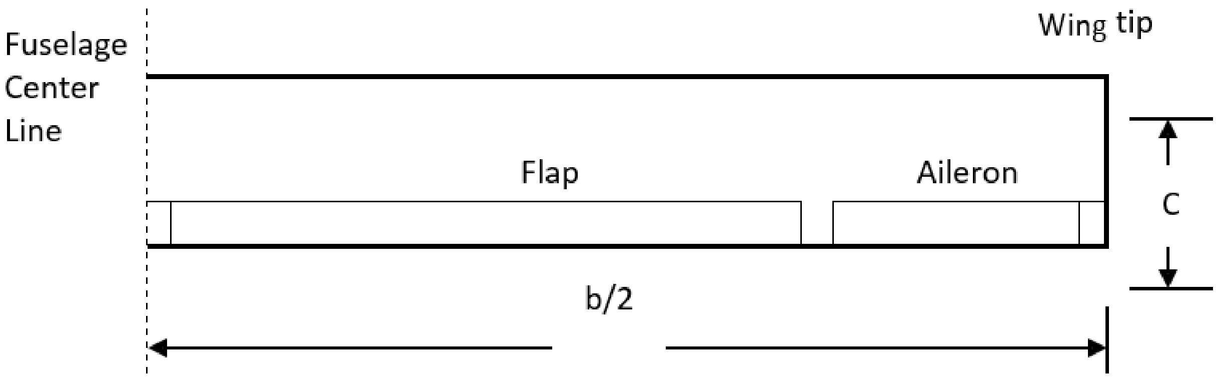

Figure 2.42: Typical location of the aileron on the wing

In this section, it is mainly emphasized that do not consume all wing trailing edge for flap and leave about 30 percent of the wing outboard for ailerons. Figure 2.42 illustrates the typical location of the aileron on the wing. Three major parameters that need to be determined in aileron design process are: aileron chord, aileron span, and aileron deflection (up and down). The primary design requirements in aileron design originate from roll controllability of the aircraft. The full discussion on aileron design and aileron design technique will be covered later.

2.13. Lifting Line Theory:

In section 2.7, it is explained that in the wing design process, the designer must calculate the lift force that a wing is generating. Then, by changing wing parameters one can finalize wing parameters to achieve the design goals while satisfying all design requirements. The technique is essentially coming from the area of Aerodynamics, however, in order to complete the discussion on the wing design, a rather straight forward, but at the same time relatively accurate technique is introduced. A wing designer must have a solid background on the topic of Aerodynamics; so, this section plays the role of a review for you. For this reason, materials in this section are covered without proof. For more and detailed information, you are referred to the.

The technique introduced in this section, allows the reader to determine the amount the lift that is generated by a wing without using sophisticated CFD software. You need to have all wing data in hand such as wing area, airfoil section and its features, aspect ratio, taper ratio, wing incidence, and high lift device type and data. By solving several aerodynamic equations simultaneously, one can determine the amount of lift that a wing is producing. Furthermore, the technique will generate the lift distribution along the span, hence one can make sure that if the lift distribution is elliptical or not.

The technique is initially introduced by Ludwig Prandtl and is called "*lifting-line theory*" in 1918. Almost every *Aerodynamics* textbook has the details of this simple and remarkably accurate technique. The major weakness of this classical technique is that it is a linear theory; thus, it does not predict stall. Therefore, if you know the airfoil section's stall angle, do not employ this approach beyond the airfoil's stall angle. The technique can be applied for a wing with both flap up and flap down (i.e. deflected). In the following, the steps to calculate the lift distribution along the span plus total wing lift coefficient will be presented. Since a wing has a symmetric geometry, we only need to consider one half of the wing. The technique can later be extended to both left and right wing-half. The application of the technique will be demonstrated at the end of this chapter.

Figure 2.43 Dividing a wing into several sections

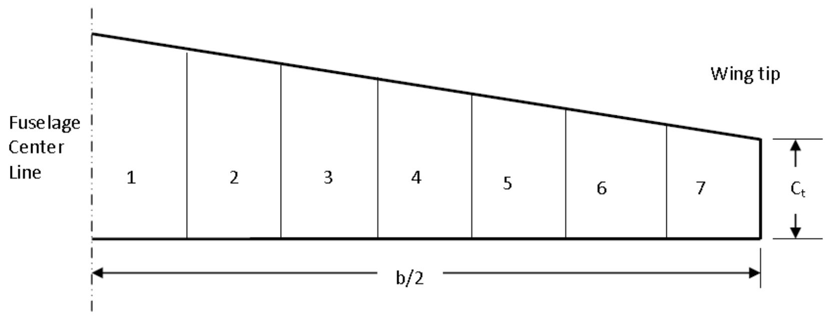

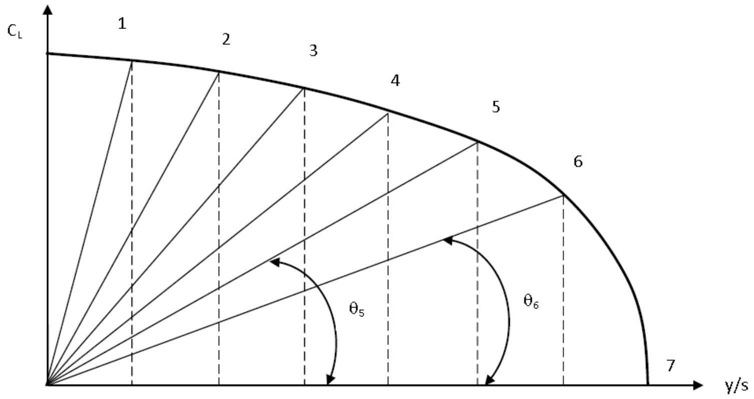

Figure 2.44 Angles corresponding to each segment in lifting-line theory

Step 1. Divide one half of the wing (semi-span) into several (say N) segments. The segments along the semi-span could have equal span, but it is recommended to have smaller segments in the regions closer to the wing tip. The higher number of segments (N) is desired, since it yields a higher accuracy. As an example, in figure 2.43, a wing is shown that is divided into seven equal segments. As noted each segment has a unique chord and may have a unique span. You have the option to consider a unique airfoil section for each segment as well (recall the aerodynamic twist). Then, identify the geometry (e.g. chord and span) and aerodynamic properties (e.g. α, αo, C*l*α) of each segment for future application.

Step 2. Calculate the corresponding angle (θ) to each section. These angles are functions of lift distribution along the semi-span as depicted in figure 2.44. Each angle (θ) is defined as the angle between the horizontal axis and the intersection between lift distribution curve and the segment line. In fact, we originally assume that the lift distribution along the semi-span is elliptical. This assumption will be corrected later.

The angle θ varies between 0 for the last segment; to a number close to 90 degrees for the first segment. The value of angle θ for other segments may be determined from corresponding triangle as shown in figure 2.44. For instance, in figure 2.44, the angle θ6 is the angle corresponding to the segment 6.

Step 3. Solve the following group of equations to find A_1 to A_n:

$$\mu(\alpha_o - \alpha) = \sum_{n=1}^{N} A_n \sin(n\theta)\left(1 + \frac{\mu n}{\sin(\theta)}\right) \quad 2.30$$

This equation is the heart of the theory and is referred to as the *lifting-line* equation or *monoplane* equation. The equation initially developed by Prandtl. In this equation, N denotes number of segments; α segment's angle of attack; α_o segment's zero-lift angle of attack; and coefficients A_n are the intermediate unknowns. The parameter μ is defined as follows:

$$\mu = \frac{\bar{C}_i \cdot C_{l\alpha}}{4b} \quad 2.31$$

where denotes the segment's mean geometric chord, $C_{l\alpha}$ segment's lift curve slope in 1/rad; and "b" is the wing span. If the wing has a twist (α_t)., the twist angle must be applied to all segments linearly. Thus, the angle of attack for each segment is reduced by deducting the corresponding twist angle from wing setting angle. If the theory is applied to a wing in a take-off operation, where flap is deflected, the inboard segments have larger zero-lift angle of attack (α_o) than outboard segments.

Step 4. Determine each segment's lift coefficient using the following equation:

$$C_{Li} = \frac{4b}{C_i}\sum A_n \sin(n\theta) \qquad 2.32$$

Now you can plot the variation of segment's lift coefficient (C_L) versus semi-span (i.e. lift distribution).

Step 5. Determine wing total lift coefficient using the following equation:

$$C_{Lw} = \pi \cdot AR \cdot A_1 \qquad 2.33$$

where AR is the wing aspect ratio.

2.14. Wings Accessories:

Depending upon the aircraft type and flight conditions, the wing may have a few accessories to improve the flow over the wing. The accessories such as wingtip, fence, vortex generator, stall stripes, and strake are employed to increase the wing efficiency. In this section, few practical considerations will be introduced.

2.14.1. Strake

A strake (also known as a leading edge extension) is an aerodynamic surface generally mounted on the fuselage of an aircraft to fine-tune the airflow and to control the vortex over the wing. In order to increase lift and improve directional stability and maneuverability at high angles of attack, highly swept strakes along fuselage forebody may be employed to join the wing sections. Aircraft designers choose the location, angle and shape of the strake to produce the desired interaction figure 2.45.

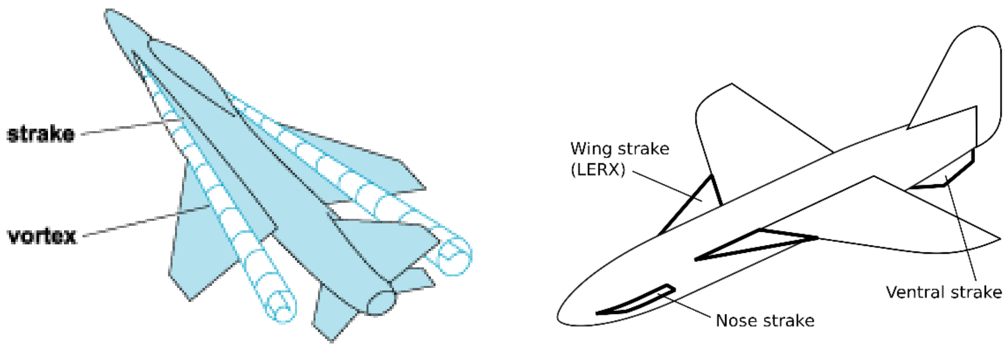

Figure 2.45. Example of aircraft strakes

Fighter aircraft F-16 and F-18 have employed strakes to improve the wing efficiency at high angles of attack. In addition, the provision of strakes on the fuselage, in front of the tail, will increase the fuselage damping which consequently improves the spin recovery characteristics of the aircraft. The design of the strake needs a high fidelity CFD software package.

2.14.2. Fence

Stall fences are used in swept wings to prevent the boundary layer drifting outboard toward the wing tips. Boundary layers on swept wings tend to drift because of the spanwise pressure gradient of a swept wing. Swept wing often has a leading-edge fence of some sort, usually at about 35 percent of the span from fuselage centerline as shown in figure 2.46. The cross-flow creates a side lift on the fence that produces a strong trailing vortex. This vortex is carried over the top surface of the wing, mixing fresh air into the boundary layer and sweeping the boundary layer off the wing and into the outside flow. The result is a reduction in the amount of boundary layer air flowing outboard at the rear of the wing. This improves the outer panel maximum lift coefficient.

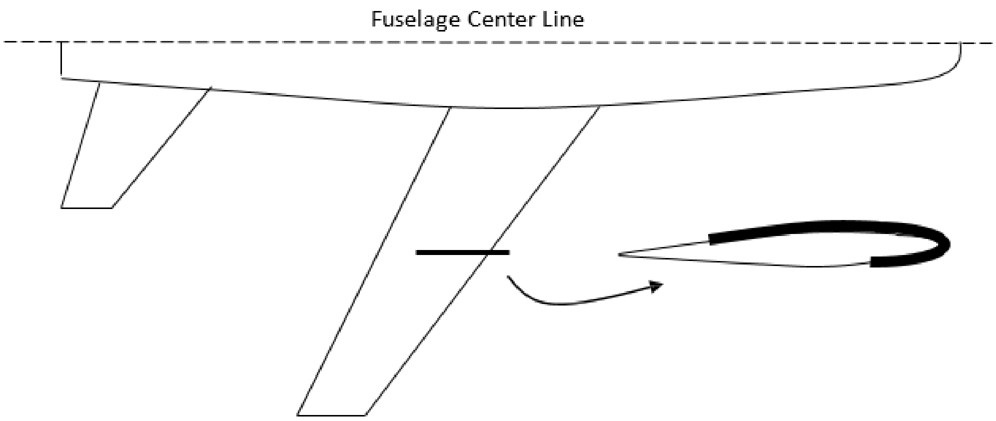

a. Fence over the wing

b. Fence over the wing of General Dynamics F-16XL

Figure 2.46. Example of a stall fence

Similar results can be achieved with a leading-edge snag. Such snags tend to create a vortex which acts like a boundary layer fence. The ideal device is the under-wing fence, referred to as *vortilon*. Pylons supporting the engines under the wing, in practice, serve the purpose of the leading-edge fences. Several high subsonic transport aircraft such as McDonnell Douglas DC-9 and Beech Starship have utilized fence on their swept lifting surfaces. The design of the fence needs a high fidelity CFD software.

2.14.3. Vortex generator

Vortex generators are very small, low aspect ratio wings placed vertically at some local angle of attack on the wing, fuselage or tail surfaces of aircraft. The span of the vortex generator is typically selected such that they are just outside the local edge of the boundary layer. Since they are some types of lifting surfaces, they will produce lift and therefore tip vortices near the edge of the boundary layer. Then these vortices will mix with the high energy air to raise the kinetic energy level of the flow inside the boundary layer. Hence, this process allows the boundary layer to advance further into an adverse pressure gradient before separating. Vortex generators are employed in many different sizes and shapes figure 2.47.

Most of today's high subsonic jet transport aircraft have large number of vortex generators on wings, tails and even nacelles. Even though vortex generators are beneficial in delaying local wing stall, but they can generate considerable increase in aircraft drag. The precise number and orientation of vortex generators are often determined in a series of sequential flight tests. For this reason, they are sometimes referred to as "aerodynamic afterthoughts". Vortex generators are usually added to an aircraft after test has indicated certain flow separations. In Northrop Grumman B-2A Spirit strategic penetration bomber utilizes small drop-down spoiler panels ahead of weapon bay doors to generate vortexes to ensure clean weapon release.

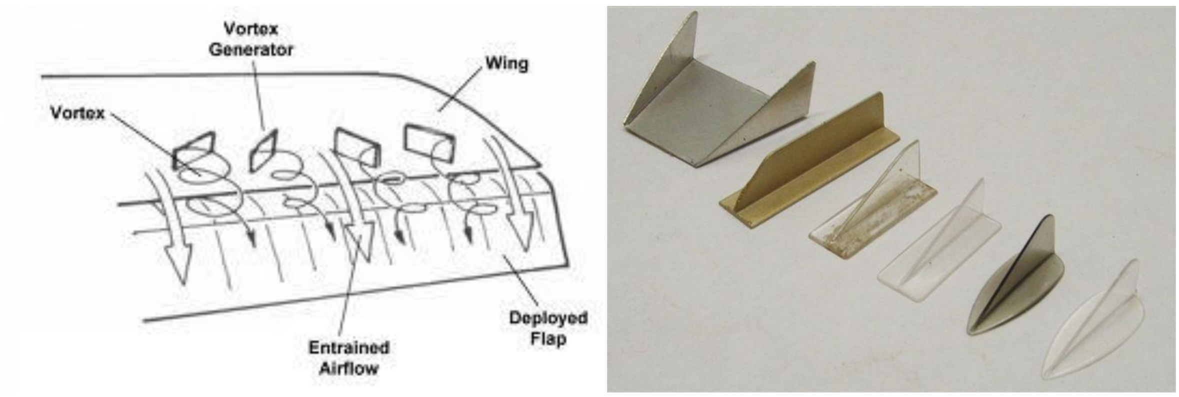

Figure 2.47. Example of aircraft vortex

2.14.4. Winglet

Since there is a considerable pressure difference between lower and upper surfaces of a wing, tip vortices are produced at the wingtips. These tip vortices will then roll up and get around the local edges of a wing. This phenomenon will reduce the lift at the wingtip station, so they can be represented as a reduction in effective wing span. Experiments have shown that wings with square or sharp edges have the widest effective span. To compensate this loss, three solutions are tip-tank; extra wing span; and winglet. Winglets are small, nearly vertical lifting surfaces, mounted rearward and/or downward relative to the wing tips figure 2.48.

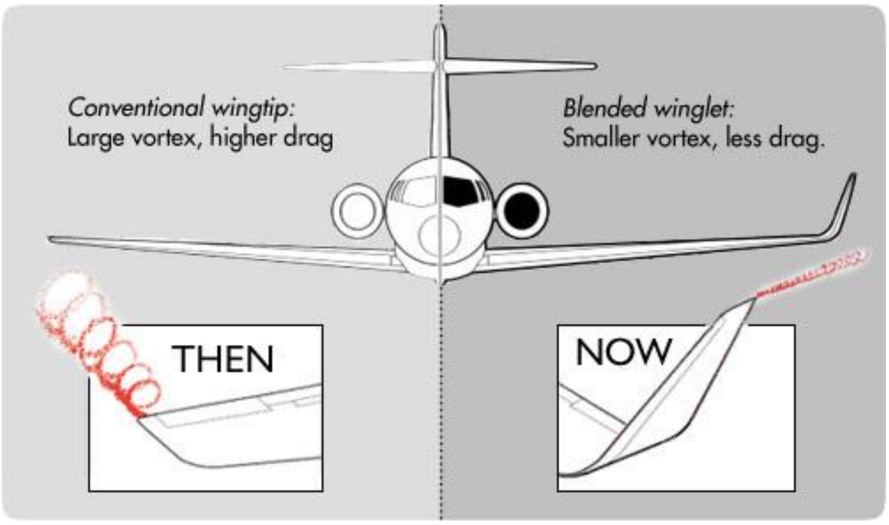

Figure 2.48. Effects of applying winglets on aircraft

The aerodynamic analysis of a winglet (e.g. lift, drag, local flow circulation) may be performed by classical aerodynamic techniques. The necessity of wingtips depends on the mission and the configuration of an aircraft, since they will add to the aircraft weight see figure 2.49.

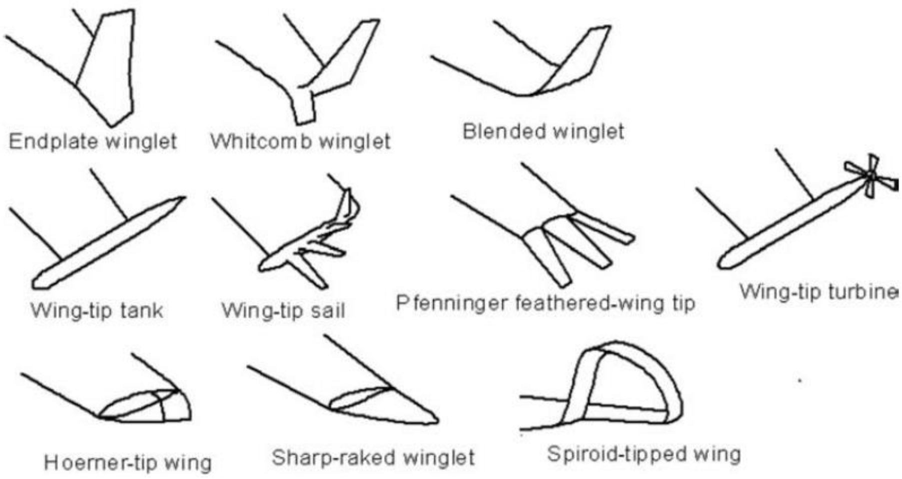

Figure 2.49. Types of winglets on aircraft from NASA

2.15. Wings Lug Design:

Installing wings in the aircraft fuselage is extremally important so there are many types of luging wings, figure 2.50.

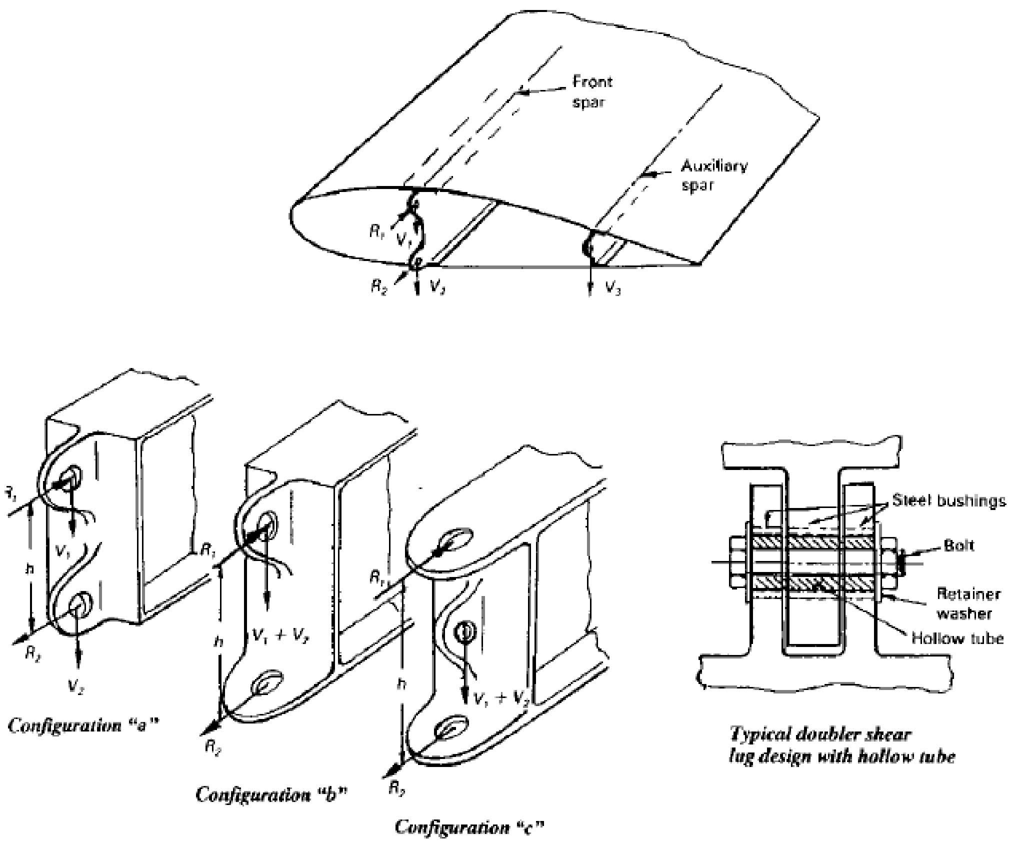

Configuration		Advantages	Disadvantages
"a"	Upper and lower lugs take axial load and vertical load shared by these two lugs	Stronger fittings Less machining cost	Smallest moment arm (h) and produce the highest lug axial loads Difficult to install due to its close tolerance holes requirement Vertical load distribution is difficult to predict
"b"	Upper and lower lugs take axial load and vertical load taken by upper lug only	Easy to install Load distribution is clear Longer moment arm (h) and then produce moderate lug load	Not enough space to install lower lug, if beam depth is too shallow
"c"	Upper and lower lugs take axial load and vertical load taken by center lug only	Easy to install Load distribution is clear Longest moment arm (h) and then produce small lug load	Heavy weight because of the third lug Highest machining cost Not enough space for the center lug, if beam depth is too shallow
Note: Always use double shear design with steel bushings to ensure fatigue life.			

Figure 2.50: Wings Lug Design and Comparison

5.16. Wing Design Steps

The practical steps in a wing design process are introduced as follows:

Primary function: Generation of the lift

1. Select number of wings (e.g. monoplane, bi-plane). See section.
2. Select wing vertical location (e.g. high, mid, low). See section.
3. Select wing configuration (e.g. straight, swept, tapered, delta).
4. Calculate average aircraft weight at cruise:

$$W_{avg} = \frac{1}{2}\left(W_i + W_f\right)$$

where (Wi) is the aircraft at the beginning of cruise and (Wf) is the aircraft at the end of cruising flight.

5. Calculate required aircraft cruise lift coefficient (with average weight):

$$C_{Lc} = \frac{2W_{avg}}{\rho V_c^2 S}$$

6. Calculate the required aircraft take-off lift coefficient:

$$C_{L_{TO}} = 0.85\frac{2W_{TO}}{\rho V_{TO}^2 S}$$

The coefficient 0.85 originates from the fact that during a take-off, the aircraft has the take- off angle (say about 10 degrees). Thus, about 15 percent of the lift is maintained by the vertical component (sin (10)) of the engine thrust.

7. Select the high lift device (HLD) type and its location on the wing.
8. Determine high lift device geometry (span, chord, and maximum deflection).
9. Select/Design airfoil (you can select different airfoil for tip and root).
10. Determine wing incidence or setting angle (i_w). It is corresponding to airfoil ideal lift coefficient; C_{li} (where airfoil drag coefficient is at minimum).
11. Select sweep angle ($\Lambda_{0.5C}$) and dihedral angles (Γ).
12. Select other wing parameter such as aspect ratio (AR), taper ratio (λ) and wing twist angle (α_{twist}).
13. Calculate lift distribution at cruise (without flap, or flap up). Use tools such as lifting line theory, and Computational Fluid Dynamics.
14. Check the lift distribution at cruise that must be elliptic. Otherwise, return to step 13 and change few parameters.
15. Calculate the wing lift at cruise (C_{Lw}). Recall that HLDs are not employed at cruise.
16. The wing lift coefficient at cruise (C_{Lw}) must be equal to the required cruise

lift coefficient (step 5). If not, return to step 10 and change wing setting angle.

17. Calculate wing lift coefficient at take-off ($C_{L\_w\_TO}$). Employ flap at take-off with the deflection of δ_f and wing angle of attack of: $\alpha_w = \alpha_{sTO} - 1$. Note that α_s at take-off is usually smaller than α_s at cruise. Please note that the minus one (-1) is for safety.

18. The wing lift coefficient at take-off ($C_{L\_w\_TO}$) must be equal to take-off lift coefficient (step 6). If not, first, play with flap deflection (δ_f), and geometry (C_f ,b_f); otherwise, return to step 7 and select another HLD. You can have more than one for more safety.

19. Calculate wing drag (D_W).

20. Play with wing parameters to minimize the wing drag.

21. Calculate wing pitching moment (M_{OW}). This moment will be used in the tail design process.

22. Optimize the wing to minimize wing drag and wing pitching moment

Example 2.3

Design a wing for a normal category (General Aviation) aircraft with the following features: $S = 18.1\ m^2$, m = 1,800 kg, V_C = 130 knot (sea level), V_S = 60 knot

Assume the aircraft has a monoplane high wing and employs the split flap.

Solution:

The number of wings and wing vertical position are stated by the problem statement, so we do not need to investigate these two parameters.

1. **Dihedral angle**

   Since the aircraft is a high wing, low subsonic, mono-wing aircraft, based on Table 2.6, a "-5" degrees of Anhedral is selected. This value will be revised and optimized when other aircraft components are designed during lateral stability analysis.

2. **Sweep angle**

   The aircraft is a low subsonic prop-driven normal category aircraft. To keep the cost low in the manufacturing process, we select no sweep angle at 50 percent of wing chord. However, we may need to taper the wing; hence the leading edge and trailing edge may have sweep angles.

3. Airfoil

To be fast in the wing design, we select an airfoil from NACA selections. The selection process of an airfoil for the wing requires some calculations as follows:

$$C_{Lc} = \frac{2W_{avg}}{\rho V_c^2 S} = \frac{2 \times 1800 \times 9.81}{1.225 \times (130 \times 0.514)^2 \times 18.1} = 0.356$$

$$C_{L_{C_w}} = \frac{C_{Lc}}{0.95} = \frac{0.356}{0.95} = 0.375$$

$$C_{li} = \frac{C_{L_{C_w}}}{0.9} = \frac{0.375}{0.9} = 0.416$$

$$C_{Lmax} = \frac{2W_{To}}{\rho_o V_s^2 S} = \frac{2 \times 1800 \times 9.81}{1.225 \times (60 \times 0.514)^2 \times 18.1} = 1.672$$

$$C_{L_{max_w}} = \frac{C_{Lmax}}{0.95} = \frac{1.672}{0.95} = 1.76$$

$$C_{l_{max_{gross}}} = \frac{C_{L_{max_w}}}{0.9} = \frac{1.76}{0.9} = 1.95$$

The aircraft has a split flap, and the split flap generates an ΔC_L of 0.45 when deflected 30^o degrees. Thus:

$$C_{l_{max}} = C_{l_{max_{gross}}} - \Delta C_{l_{mzx\,HLD}} = 1.95 - 0.45 = 1.5$$

Thus, we need to look for NACA airfoil sections that yield an ideal lift coefficient of 0.4 and a net maximum lift coefficient of 1.5.

$$C_{l_i} = 0.416 \approx 0.4$$

$C_{lmax} = 1.95$ (Flaps down)

$C_{lmax} = 1.5$ (Flaps up)

By referring to figure 1.17, we find the following seven airfoil sections whose characteristics match with or is close to our design requirements (all have $C_{li} = 0.4$, $C_{lmax} \approx 1.5$):

63_1-412, 63_2-415, 64_1-412, 64_2-415, 66_2-415, 4412, 4418

Now we need to compare these airfoil sections to see which one is the best. The Table 2.10 compares the characteristics of the seven candidates. The best airfoil is the airfoil whose C_{mo} is the lowest, the $C_{d_{min}}$ is the lowest, the α_s is the highest, the $(C_l/C_d)_{max}$ is the highest, and the stall quality is docile. By comparing the numbers in the above table, we can conclude the followings:

1- The NACA airfoil section 66_2-415 yields the highest maximum speed, since it has the lowest Cd_{min} (i.e. 0.0044).
2- The NACA airfoil section 64_2-415 yields the lowest stall speed, since it has the highest maximum lift coefficient (i.e. 2.1).
3- The NACA airfoil section 66_2-415 yields the highest endurance, since it has the highest $(C_l/C_d)_{max}$ (i.e. 150).
4- The NACA 63_2-415 and 64_2-415 yield the safest flight, due to its docile stall quality.
5- The NACA airfoil section 64_2-415 delivers the lowest longitudinal control effort in flight, due to the lowest Cmo (i.e. -0.056).

Table 2.10. A comparison between seven airfoil candidates for the wings selected

No	NACA	C_{dmin}	C_{mo}	α_s (deg) Flap up	α_o (deg) $\delta_f = 60^o$	$(C_l/C_d)_{max}$	C_l	C_{lmax} $\delta_f = 30^o$	Stall quality
1	63_1-412	0.0049	-0.075	11	-13.8	120	0.4	2	Moderate
2	63_2-415	0.0049	-0.063	12	-13.8	120	0.4	1.8	Docile
3	64_1-412	0.005	-0.074	12	-14	111	0.4	1.8	Sharp
4	64_2-415	0.005	-0.056	12	-13.9	120	0.4	2.1	Docile
5	66_2-415	0.0044	-0.068	17.6	-9	150	0.4	1.9	Moderate
6	4412	0.006	-0.1	14	-15	133	0.4	2	Moderate
7	4418	0.007	-0.085	14	-16	100	0.4	2	Moderate

Since the aircraft is a non-maneuverable GA aircraft, the stall quality cannot be sharp; hence NACA 64_1-412 is not acceptable. If the safety is the highest requirement, the best airfoil is NACA 64_2-415 due to its high C_{lmax}. When the maximum endurance is the highest priority, NACA airfoil section 66_2-415 is the best, due to its high $(C_l/C_d)_{max}$. On the other hand, if the low cost is the most important requirement, NACA 66_2-415 with the lowest C_{dmin} is the best. However, if the aircraft stall speed, stall quality and lowest longitudinal control power are of greatest important design requirement, the NACA airfoil section 64_2-415 is the best. This may be performed by using a comparison table incorporating the weighted design requirements.

Since NACA airfoil section 64_2-415 is the best in terms of three criteria, we select it as the most suitable airfoil section for this wing. Figure 2.51 illustrates the characteristics graphs of this airfoil.

4. Wing setting angle

Wing setting angle is initially determined to be the corresponding angle to the airfoil ideal lift coefficient. Since the airfoil ideal lift coefficient is 0.416, figure 2.51 (left figure) reads the corresponding angle to be 2 degrees. The value (i_w = 2 deg) may need to be revised based on the calculation to satisfy the design requirements later.

5. **Aspect ratio, Taper ratio, and Twist angle**

Three parameters of aspect ratio, taper ratio, and twist angle are determined concurrently, since they are all influential for the lift distribution. Several combinations of these three parameters might yield the desirable lift distribution which is elliptical. Based on the table 2.3, the aspect ratio is selected to be 7 (AR = 7). No twist is assumed (α_t = 0) at this time to keep the manufacturing cost low and easier to build. The taper ratio is tentatively considered 0.3 (λ= 3). Now we need to find out:

a. if the lift distribution is elliptical.

b. if the lift created by this wing at cruise is equal to the aircraft weight.

The lifting line theory is employed to determine lift distribution and wing lift coefficient.

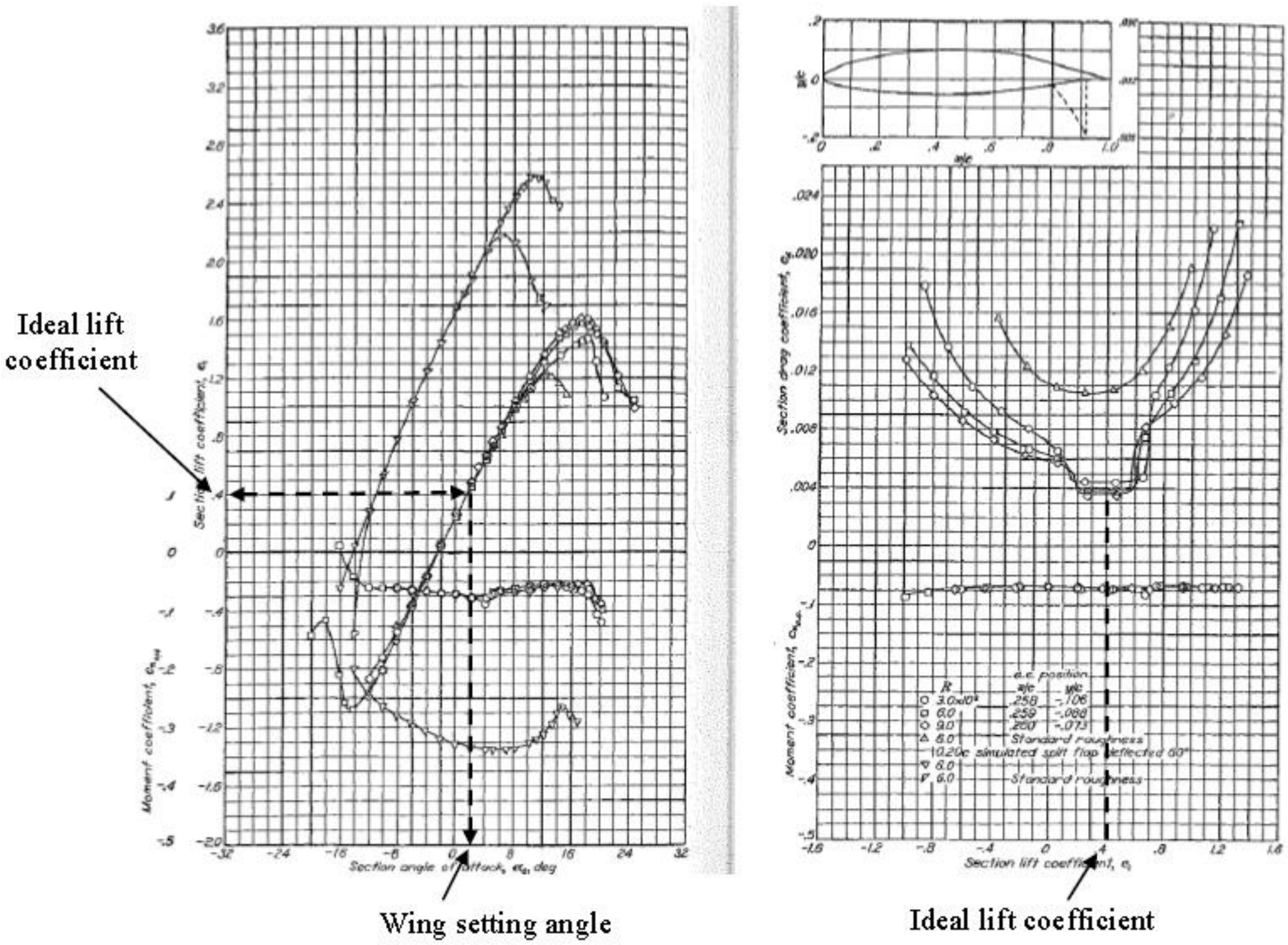

Figure 2.51. Airfoil section NACA 66$_2$-415

6. Other Wing Parameters

To determine other wing parameters (i.e. wing span (b), root chord (C_r), tip chord (C_t), and Mean Aerodynamic Chord (MAC), we must solve the following four equations simultaneously:

$$\boldsymbol{S = b.\bar{C}}$$

$$\boldsymbol{AR = \frac{b^2}{S}}$$

$$\boldsymbol{\lambda = \frac{C_t}{C_r}}$$

$$\boldsymbol{\bar{C} = \frac{2}{3} C_r \left(\frac{1 + \lambda + \lambda^2}{1 + \lambda} \right)}$$

Solution of these equations simultaneously yields the following results:

b = 11.265 m, *MAC* = 1.608 m, C_r = 1.78 m, C_t = 1.42 m

Consequently, other flap parameters are determined as follows:

$$\frac{b_f}{b} = 0.6 \rightarrow b_f = 6.75\, m$$

$$\frac{C_f}{C} = 0.2 \rightarrow C_f = 0.32\, m$$

Figure 2.52 illustrates the right half wing with the wing and flap parameters of example 2.3. The next step in the wing design process is to optimize the wing parameters such that the wing drag and pitching moment are minimized. This step is not shown in this chapter and will be discussed later.

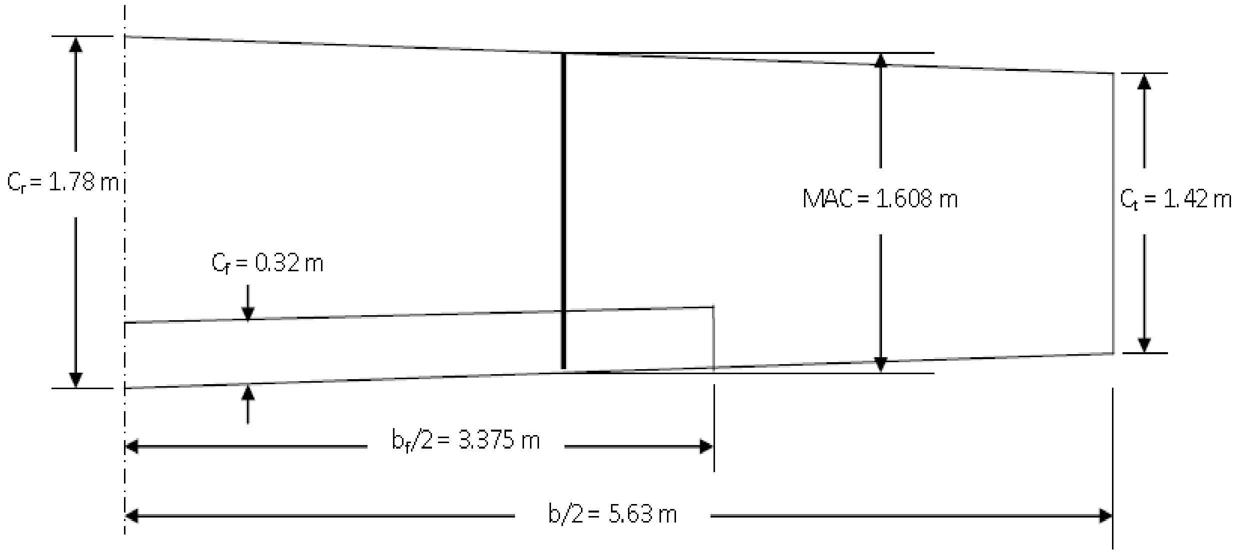

a . Top view of the right half wing

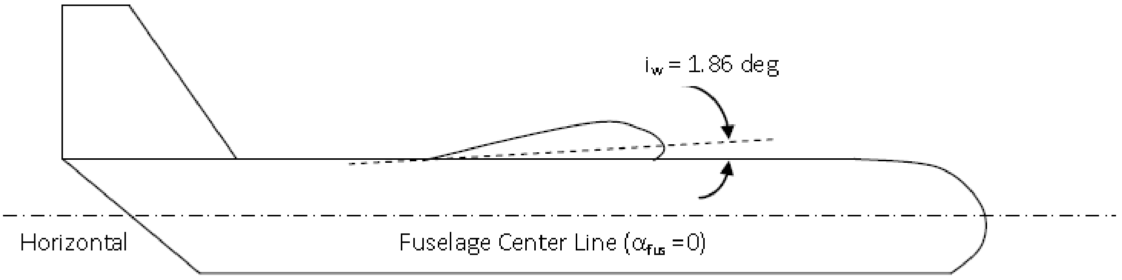

b. Side view of the aircraft in cruising flight

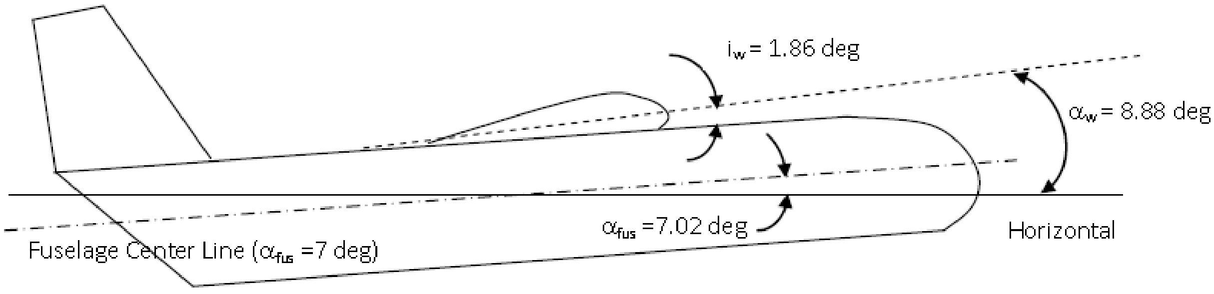

c. Side view of the aircraft in take-off

Figure 2.52. Wing parameters of Example 2.3